Spectrum Sensing Based on Sequential Testing

Xiao Ma

A thesis submitted in partial fulfilment
of the requirements for the degree of
Master of Engineering
in
Electrical and Electronic Engineering
at the
University of Canterbury,
Christchurch, New Zealand.

December 2009

ABSTRACT

Recently, interest has been shown in cognitive radio (CR) systems since they can opportunistically access unused spectrum bands thereby increasing usable communication capacity. Spectrum sensing has been identified as a key function to ensure that CR can detect spectrum holes. In a CR network, a fast and accurate spectrum sensing scheme is important.

Spectrum sensing can be viewed as a signal detection problem. Most of the existing spectrum sensing schemes are based on fixed sample size detectors which means that their sensing time is preset and fixed. However, the work of Wald [27] showed that a detector based on sequential detection requires less average sensing time than a fixed sample size detector.

In this thesis, we have applied the method of sequential detection to reduce the average sensing time. Simulation results have shown that, compared to the fixed sample size energy detector, a sequential detector can reduce sensing time by up to 85% in the AWGN channel for the same detection performance. In order to limit sensing time, especially in a fading environment, a truncated sequential detector is developed. The simulation results show that the truncated sequential detector requires less sensing time than the sequential detector, but the performance degrades due to truncation. Finally, a cooperative spectrum sensing scheme is used where each individual sensor uses a sequential detector. The combining rule used at the fusion center is a selection combining rule. Simulation results show that the proposed cooperative spectrum sensing scheme can reduce the sensing time compared to the individual spectrum sensing scheme.

ACKNOWLEDGMENTS

First and foremost, I would like to thank my supervisor, Professor Desmond Taylor and co-supervisor Dr. Philippa Martin, whose patient guidance and encouragement has made this thesis possible.

Also, I would like to thank my parents for their endless support over the years.

Finally, thanks must go to my friends and the members of Comms lab for their assistance and friendship.

CONTENTS

LIST OF FIGURES

Chapter 1

INTRODUCTION

1.1 GENERAL INTRODUCTION

A wireless communication system was first demonstrated in 1895 by G.Marconi. He discovered that it was possible to send signals using electromagnetic waves. From that time, new communication systems and services have been developed by researchers all around the world.

Signals that carry speech and video are inherently analog. Thus, analog communication systems were developed at an early stage. For example, the amplitude modulation (AM) wireless communication system was first used by American police in 1934 for public safety. In 1939, frequency modulation (FM) was introduced by Edwin Armstrong [10]. It offered more robust and higher quality transmission.

Although most current broadcasting systems convey information to drive analog applications, such as TV or radio, it is important to notice that with the advent of computers and digital information, digital communication systems have been developed to improve service quality. Owing to the application of source coding and channel error control coding, digital communication systems are less subject to distortion and interference than analog systems. Furthermore, digital communication systems are more reliable than analog systems and the cost of digital communication systems is less than that of analog systems [10]. For example, an emerging standard DRM (Digital Radio Mondiale) can offer long-range robust audio transmissions as an alternative to low frequency AM transmissions [2].

It is not only audio broadcast service that have been revolutionized by digital technology. GSM (Global System for Mobile Telephony) is a global digital standard for wireless telephony [8]. It offers higher channel efficiency and security than previous analog technology. Also, digital television (DTV) is slowly replacing analog transmissions. analog video

signals of 6MHz bandwidth can now be compressed to 2Mbit/s streams which require much less channel bandwidth.

It is easy to see that most wireless services of the future will be encoded in the digital domain [10]. This will require digital baseband processing at both transmitter and receiver, and as digital services generally consume less bandwidth than analog services, there are likely to be many more digital services and standards to manage.

The rate of introduction of new services is increasing very quickly. Technical evolution and increasing pressure to minimize service bandwidth has meant that many services have a rapid degree of obsolescence. Future technologies should therefore conform to the idea of reconfigurable equipment [16].

Software radio is a kind of reconfigurable equipment. It is a new class of radio architecture which was developed in the 1990s [25]. The functions of software radio are implemented by programs running on a processor. Based on the same hardware, different transmitter and receiver algorithms are implemented in software. Software radio is a technology which can take wireless equipment design away from fixed traditional implementations and introduce elements of reconfigurability.

There are three advantages of reconfigurable equipment [16]. The first is that the reconfigurable equipment can be multi-functional. It means that a single terminal can be used for operation with more than one transmission standard. The second is that the reconfigurable equipment can evolve. As new standards emerge, software patches can be sent to upgrade terminals. There is no need to alter any terminal hardware. The last is that filtering and mixing can be performed in software. There is less significantly hardware adjustment to be performed.

No matter what kind of wireless communication is employed, it requires spectrum to operate, but there will be some interference if different systems simultaneously operate in the same band. Thus, spectrum is a limited resource. Furthermore, it is currently allocated exclusively to different systems by rules meaning other systems can not use this spectrum at any time and location. However, this form of spectrum allocation leads to the underuse of spectrum [1].

Dynamic spectrum access is a new approach to spectrum management. By using dynamic spectrum access, secondary users (users with no right to use a certain bandwidth) may detect and use the spectrum "holes" for transmission without interfering with primary

users (users with a proprietary right to use a certain bandwidth). This results in a more efficient use of spectrum resource. Cognitive radio (CR) can be viewed as a platform for the realization of dynamic spectrum access [1].

CR was proposed by J.Mitola in 2000 [22]. A CR can be implemented on a hardware radio platform and its radio parameters (e.g. frequency, power, modulation and bandwidth) can be changed depending on the environment. CR will become commercially feasible within the next 5 to 10 years [17] and it can improve the efficiency of spectrum usage.

Some examples of on-going research on CR include the next generation (XG) program [18], [47]. The IEEE 802.22 workshop on wireless regional area networks develops CR technology in the television bands [19]. This research on CR draws upon many communication engineering areas such as signal detection, sensor networks, cooperative communications and others.

In this thesis, we focus on detecting the presence or absence of a primary signal in a noisy environment. This is also called spectrum sensing in a CR system. Actually, signal detection theory has a wide range of applications including communications engineering. Reference [20] is one of the papers which emphasizes the importance of signal detection in communications while [21] provides a good survey of signal detection theory.

Individual sensing is the first step in spectrum sensing [47]. In an individual sensing scheme, different kinds of detectors are proposed for various types of signal. For example, matched filters may be used to detect the signal given suitable prior information. On the other hand, energy detectors are often used to detect random signal or signals of unknown form. Feature detectors can detect not only the presence of the signal but also the modulation type. The important distinction between energy detection, feature detection and matched filter is that energy detector is fully blind. For the future unlicensed spectrum or "public park" spectrum, blind methods are the only option.

A cooperative sensing network is proposed in [47] to improve detection accuracy, reduce sensing time and combat the so-called hidden terminal problem. A cooperative sensing network determines spectrum occupancy through joint detection by several CRs, as opposed to it being determined by an individual CR.

As noted in [47], the development of spectrum sensing technology introduces many challenges. For example, how does one detect the primary signal in a low SNR environ-

ment? How can we improve the probability of detection ? Furthermore, one of the main requirements of CR networks is the detection of the primary signal in a very short time. Hence, spectrum sensing algorithms need to be developed so that the sensing time needed to detect the primary signal can be minimized with a given probability of missed detection.

The goal of this thesis is to develop and evaluate two individual detectors and a cooperative scheme through both mathematical description and computer simulation. The proposed detectors and the cooperative scheme both focus on how to reduce sensing time. The fundamental theory is based on sequential testing which was proposed by Wald in 1947 [27].

The remainder of this chapter is organized as follows. First, it describes how the proposed detection schemes will be performed in the time domain. Second, the representation of signals in this thesis is described. Third, the wireless channel including its characteristics and simulation method are illustrated. Finally, the scope and the contribution of the thesis is summarized.

1.2 TIME DOMAIN DETECTION AND FREQUENCY DOMAIN DETECTION

In this thesis, all the single and cooperative detection schemes are performed in the time domain. Following the work of [14], a bandpass filter is applied at the front end of each CR. The CR only needs to measure the signal in this particular frequency band in the time domain. The CR may transmit when there is no primary signal in this frequency region.

Two questions may arise from the proposed schemes. Is this narrow band idle time detection scheme reasonable? Why not apply wideband spectrum sensing? The answers to these two questions are given below.

Idle time sensing schemes are a reasonable solution over a narrow band. For CR systems which are based on the IEEE 802.22 protocol [5], the primary signal is a 6MHz bandwidth DTV signal. Thus, in practice, the CR knows the bandwidth of the primary signal and, therefore, can employ an appropriate bandpass filter at its front-end. It is only required to detect whether this frequency region is used at a certain time.

A tough problem occurs when the bandwidth W to be sensed is large (wideband spectrum sensing). Suppose we need to sense 1000 channels, each of 10 KHz (meaning, W=10MHz). Continuous analog sensing is not feasible, since it needs as many as 1000

analog filters. Thus, digital signal processing techniques have to be employed [15]. For example, the entire band may be sampled at a high rate and a FFT used to obtain the components of energy over a range of frequencies.

It is often impractical for a CR to sense all the channels simultaneously [1], [3] due to hardware limitations and the energy cost of spectrum monitoring. For example, designing a 1 GHz A/D converter with 12 bits resolution is infeasible owing to comparator ambiguity and clock jitter impairments [4].

The authors of [3] proposed several optimal and suboptimal protocols to avoid wideband sensing and to maximize the overall network throughput. These protocols are based on narrow band sensing and their main contribution is on deciding which single channel is chosen for sensing at each time slot.

However, wideband spectrum sensing is not an impossible mission. A novel wideband spectrum sensing technique is proposed in [63]. This technique jointly detects the signal energy level over several frequency bands rather than only one band at a time.

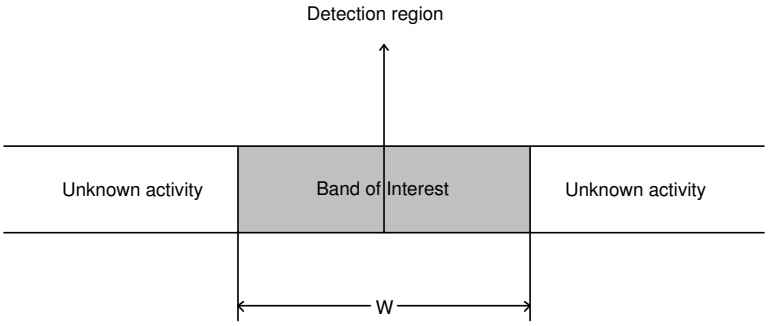

Figure 1.1 Sub-channel detection.

In summary, as shown in Fig. 1.1, the objective of spectrum sensing in this thesis is to sense only one sub-channel and identify whether it is in use at a certain time. Wideband frequency domain sensing is not considered.

1.3 SIGNAL REPRESENTATION

The proposed schemes will be implemented in the time domain to detect the presence of primary signals. In this section, we develop representations of the primary signals in a mathematical form to analyze the systems in the time domain. Thus, we summarize two different signal representations that are to be used in this thesis.

1.3.1 Complex Baseband Signal Representation

In this thesis, I assume that the channel is a wireless channel and the primary signal is a bandpass signal which can be represented as

$$x_c(t) = x_A(t)\cos(2\pi f_c t + x_p(t)) \tag{1.1}$$

where $x_A(t)$ is amplitude, $x_p(t)$ is phase and f_c is the carrier frequency.

However, the carrier frequency f_c is different for various wireless systems. For example, f_c of an AM radio system is in the range 530-1600KHz while f_c of a VHF TV system is in the range 178-216MHz [8]. Obviously, it is impractical to design various communication strategies to different carrier frequencies. Furthermore, this carrier frequency does not convey any information. Only the amplitude $x_A(t)$ and the phase $x_p(t)$ convey information. Any quantity with two independent components can be represented by a complex number and this provides a very useful technique for analyzing bandpass modulation.

After some trigonometric calculations, we have [7]

$$\begin{aligned} x_c(t) &= x_A(t)\cos(2\pi f_c t + x_p(t)) \\ &= x_I(t)\cos(2\pi f_c t) - x_Q(t)\sin(2\pi f_c t) \end{aligned} \tag{1.2}$$

The carrier signal is usually a cosine term. The signal $x_I(t)$ in (1.2) is in-phase with the carrier, and therefore, it is referred to as the in-phase component of the bandpass signal. The sine term is 90° out-of-phase with the carrier term, and hence the signal $x_Q(t)$ is referred to as the quadrature component of the bandpass signal. The transformation between the two representations is given by

$$x_A(t) = \sqrt{x_I(t)^2 + x_Q(t)^2} \qquad x_p(t) = \tan^{-1}[x_Q(t)/x_I(t)] \tag{1.3}$$

and

$$x_I(t) = x_A(t)\cos(x_p(t)) \qquad x_Q(t) = x_A(t)\sin(x_p(t)) \tag{1.4}$$

Thus, a single bandpass signal can be represented by two baseband signals. To make the notation compact we can think of $x_z(t)$ as a complex signal defined as

$$x_z(t) = x_I(t) + jx_Q(t) \tag{1.5}$$

The original bandpass signal can be obtained from the complex envelope by

$$x_c(t) = \sqrt{2}\Re[x_z(t)\exp(j2\pi f_c t)] \tag{1.6}$$

This allows us to represent bandpass signals as complex baseband signals and hence simulate detection systems at baseband.

1.3.2 Vector Representation of Signals

In this thesis, most of the work is based on probability and random process theory which are predicated on the concept of a finite sequence of random variables. However, primary transmitters do not produce random variables at the input to the CR. In contrast, it produces a continuous signal as a function of time at the input to the CR.

We use two approaches to achieve a random vector from a continuous function of time in this thesis. The first one is orthogonal representation of the signal. Consider that a signal $x_i(t)$ of duration T is from any set of M finite energy signals $\{x_i(t)\}$. It can be represented as below [7]:

$$x_i(t) = \sum_{j}^{N} x_{ij}(t)\phi_j(t), \qquad \begin{cases} 0 \le t \le T \\ i = 1, 2, \ldots M \end{cases} \tag{1.7}$$

where the $x_{ij}(t)$ are defined by

$$x_{ij}(t) = \int_0^T x_i(t)\phi_j(t)dt \qquad \begin{cases} i = 1, 2, \ldots M \\ j = 1, 2, \ldots N \end{cases} \tag{1.8}$$

The functions $\phi_1(t), \phi_2(t), \ldots \phi_N(t)$ are called orthonormal basis functions,which means

$$\int_0^T \phi_i(t)\phi_j(t)dt = \delta_{ij} = \begin{cases} 1 & \text{if } i = j \\ 0 & \text{if } i \ne j \end{cases} \tag{1.9}$$

The vector representation of the signal over the duration of T seconds is then given by

$$x_i = [x_{i1}, x_{i1}, \ldots, x_{iN}], \qquad i = 1, 2, \ldots, M \tag{1.10}$$

The second approach is sampling theory. It tell us if a signal $x(t)$ has no frequency higher than W, it can be reconstructed from a series of sample which are $\frac{1}{2W}$ seconds apart. It can be represented as

$$x_i = [x(t_0), x(t_1), \ldots, x(t_N)] \tag{1.11}$$

The time interval between t_N and t_{N-1} is $\frac{1}{2W}$ seconds. Thus over a duration of T s we can obtain complete representation of the signal using 2WT samples. By applying either of the above two approaches, we can represent the waveform signal $x(t)$ in vector form.

1.4 FADING CHANNEL

Selection of an adequate mathematical model to represent the physical channel is one of the crucial things in the design of a communication system [95]. We must collect the physical parameters of the channel and then formulate a model for it on which system design can be based.

1.4.1 Physical Description of the Channel

In a real environment, there are often many reflectors such as buildings and trees between the transmitter and receiver. In this situation, a signal can travel from transmitter to receiver over several paths, and therefore, several distorted and delayed copies of signals are received at the receiver. This phenomenon causes fluctuations in the received signal's amplitude and phase. In this way, the received signal is either amplified or attenuated. This is known as multipath fading and can be modeled as in Fig. 1.2.

There are usually two types of fading effects in practice [8]: large-scale fading and small scale fading. Large-scale fading represents the average signal power attenuation due to obstacles and large scale reflection and refraction. Because the receiver is represented as being "shadowed" by the obstacles, large-scale fading is also called shadowing.

Small-scale fading represents the changes in signal amplitude and phase caused by

small changes in the separation between a receiver and transmitter. These small changes are often on the order of only a half-wavelength of the signal.

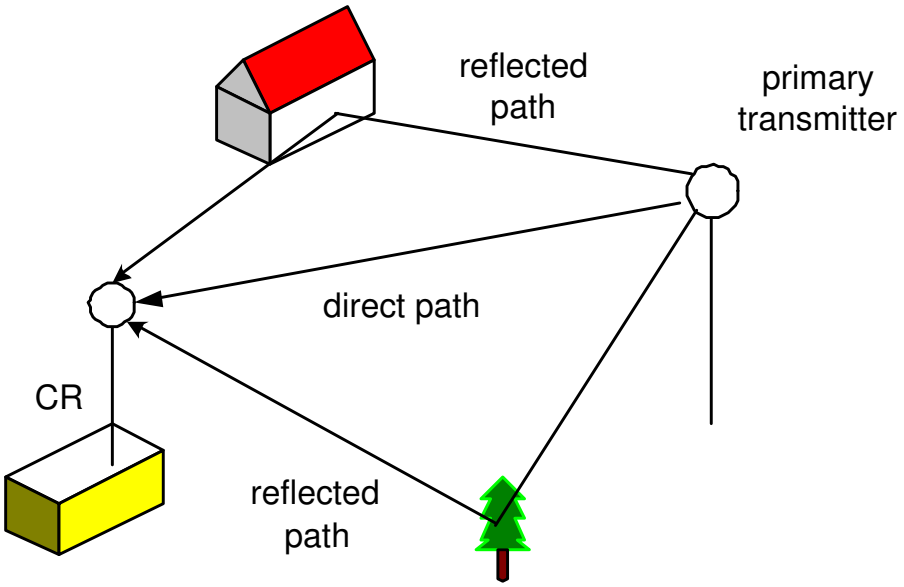

Figure 1.2 Physical model of multipath propagation.

1.4.2 Shadowing

Let us assume that a primary transmitter and a CR are employed with a distance d between them. It is known that the average received signal power at the CR decreases with distance d. It can be represented as a function of distance by using a path loss exponent n [8]

$$PL(d) \propto \frac{d}{d_0}^{n} \tag{1.12}$$

Or in a dB formulation

$$PL(dB) = PL(d_0) + 10n \log_{10}\left(\frac{d}{d_0}\right) \tag{1.13}$$

where n is the path loss exponent which depends on the specific propagation environment and d_0 is a reference distance. In typical wireless environments, n varies between 2 and 6.

However, a question arises from (1.13), namely, what is the situation if the surrounding environmental clutter is different at two different locations which have the same primary transmitter and CR separation? After significant measurement work, it can be found that

at any value of d, the path loss $PL(d)$ at a particular location is random and distributed log-normally about the mean distance-dependent value. The log-normal means normal in dB. Thus, we have [8]

$$PL(dB) = PL(d_0) + 10n\frac{d}{d_0} + X_\sigma \tag{1.14}$$

where the X_σ is a zero-mean Gaussian distributed variable (in dB) with a standard deviation σ (also in dB). The standard deviation is a function of frequency and environment and typical values range from 2dB (mostly line of sight), to 14dB (a heavily shadowed and cluttered environment) [8].

The above definition, assumes that the ratio of transmit and receive power γ has a log-normal distribution for this log-normal shadowing model. The ratio is given by

$$\gamma = \frac{4.34}{\sqrt{2\pi}\sigma\gamma}\exp\left[-\frac{(10\log_{10}^{\gamma} - \mu)^2}{2\sigma^2}\right] \tag{1.15}$$

where μ and σ are the mean and standard deviation of $10log_{10}^{\gamma}$ in dB, respectively. The mean of γ in linear form is then [59]

$$\mu_\gamma = \exp\left[\frac{\mu}{4.34} + \frac{\sigma^2}{2 \times 4.34^2}\right] \tag{1.16}$$

1.4.3 Small-Scale Fading

From section 1.3.1, we have the bandpass transmitted signal as

$$x(t) = \Re[s(t)\exp(j2\pi f_c t)] \tag{1.17}$$

Owing to the effect of multipath propagation, the received signal is usually the sum of many delayed and distorted waves of the transmitted signal. The bandpass received signal may then be written as

$$y(t) = \Re\left\{\sum_{n=1}^{N}\alpha_n(t)s[t-\tau_n(t)]\exp[j(2\pi(f_c t + f_{d,n}(t))(t-\tau_n(t)))]\right\} \tag{1.18}$$

The subscript n indexes the nth wave. The attenuation and propagation delay associated with the nth wave are represented by α_n and τ_n, respectively.

The $f_{d,n}(t)$ in (1.18) represents the Doppler shift of the nth wave due to motion. If we assume the nth wave arrives at the receiver at an angle of $\theta_n(t)$ with respect to the direction of movement, the motion introduces a Doppler shift which is given by

$$f_{d,n}(t) = f_m \cos(\theta_n(t)) \tag{1.19}$$

where $f_m = v/\lambda_c$, λ_c is the wavelength of the arriving wave and v is the speed of the mobile receiver.

If we rearrange (1.18), the received baseband signal is then given by

$$r(t) = \Re\left\{\sum_{n=1}^{N} \alpha_n(t)s[t-\tau_n(t)]\exp[-j2\pi(f_c + f_{d,n}(t))\tau_n(t) - f_{d,n}(t)t]\right\} \tag{1.20}$$

For simplicity, $r(t)$ can be rewritten as

$$r(t) = \Re\left\{\sum_{n=1}^{N} \alpha_n(t)s[t-\tau_n(t)]\exp[-j\phi_n(t)]\right\} \tag{1.21}$$

where

$$\phi_n(t) = 2\pi\{(f_c + f_{d,n}(t))\tau_n(t) - f_{d,n}(t)t\} \tag{1.22}$$

From (1.21) we can see that the channel can be modelled as a time-variant linear filter having the impulse response

$$c(\tau, t) = \sum_{n=1}^{N} \alpha_n(t)\delta[t-\tau_n(t)]\exp[-j\phi_n(t)] \tag{1.23}$$

There are two main criteria used to characterize small scale fading [8]. The first is based on signal time-spreading. As we can see from the above equations, there are n different received components for a single transmitted impulse. We use the time T_m to represent the time between the first and last received component. This is known as the multipath spread of the channel.

The relationship between maximum excess delay time T_m and symbol time T_s can be used to represent two different fading categories, frequency-selective fading and flat fading. A channel is frequency selective if T_m is longer than T_s. This situation happens when the

received multipath components of a symbol lie beyond the symbol's time duration and this introduces intersymbol interference (ISI) distortion [8].

A channel is flat fading if T_m is shorter than T_s. In this situation, all the multipath components of a symbol arrive within a symbol duration. The signal time spreading does not lead to overlap between neighboring received symbols. Hence, there is no longer any channel-induced ISI distortion.

The signal time-spreading criterion describes the time dispersive nature of the channel. However, relative motion between the transmitter and receiver also leads to time variation of the channel. This motion leads to the propagation paths changing, and therefore, the signal's amplitude and phase change at the receiver. Thus, we need another criterion which is called the time variance criterion to describe the fading phenomenon [13].

By using this criterion, we usually use the coherence time T_0 to measure the time duration over which the channel response is essentially invariant. Fast fading is used to describe the channel and is indicated by $T_0 < T_s$. In this situation, the time interval over which the channel is correlated is shorter than the time duration of a symbol. Therefore, the fading character of the channel changes several times during one symbol period and it leads to distortion of the baseband pulse shape, resulting in a loss of SNR [8].

A channel is said to be a slow fading channel if T_0 is longer than T_s. The time duration over which a channel is correlated is then longer than the time duration of a symbol. Hence, the channel does not change during the time in which a symbol is transmitted. The symbols will not be affected by the pulse distortion as described above.

Furthermore, the relationship between Doppler shift and coherence time is

$$T_0 \approx \frac{1}{f_d} \tag{1.24}$$

where f_d or $1/T_0$ is often regarded as the fading rate of the channel. However, in practice, T_0 is defined more precisely as the time duration over which the channel response to a signal has a correlation greater than 0.5. The relationship between T_0 and f_d is then [8]

$$T_0 \approx \frac{9}{16\pi f_d} \tag{1.25}$$

In practice, the fade rate of the channel is only meaningful if it is defined in relation to the symbol duration T_s. Thus, we usually normalize the fade rate of the channel with

respect to T_s or $1/T_s$. It is a slow fading channel if $f_d T_s \ll 1$. Otherwise, it is a fast fading channel [9].

1.4.4 Simulating The Mobile Wireless Channel

The channel is modeled as a slowly varying flat fading channel in this thesis and the simulation model used Jake's model which is based on summing sinusoids [11].

In Jake's model, we assume there are N discrete scatterers surrounding a CR as illustrated in Fig. 1.3 with the nth scatterer at the angle

$$\theta_n = \frac{2\pi n}{N}, n = 1, 2, \ldots, N \tag{1.26}$$

with respect to the direction of motion.

Furthermore, the N waves coming from the N scatterers are of equal strength, and the nth wave experiences a Doppler shift of

$$f_{d,n}(t) = f_m \cos(\theta_n(t)) \tag{1.27}$$

The impulse response of the time-variant multipath fading channel can be modeled as [12]

$$\begin{aligned} c(t) \quad = \quad & \left[\sqrt{\frac{2}{N_1+1}} \sum_{n=1}^{N_1} \sin\left(\frac{\pi n}{N_1}\right) \cos(2\pi f_{d,n}(t)) \cos(\theta_n t) \right. \\ & \left. + \frac{1}{\sqrt{N_1+1}} \cos(2\pi f_{d,n}(t) t) \right] \\ & + j \sqrt{\frac{2}{N_1}} \sum_{n=1}^{N_1} \sin\left(\frac{\pi n}{N_1}\right) \cos(2\pi f_{d,n}(t)) \cos(\theta_n t) \end{aligned} \tag{1.28}$$

where N_1 is

$$N_1 = \frac{1}{2}\left(\frac{N}{2} - 1\right) \tag{1.29}$$

For example, the transmitted signal is assumed to be a QPSK signal in the simulation model. Fig. 1.4 illustrates the time variation of the power of the fading process simulated using Jake's model for $f_d T_s = 6 \times 10^{-4}$ over 10000 symbol periods.

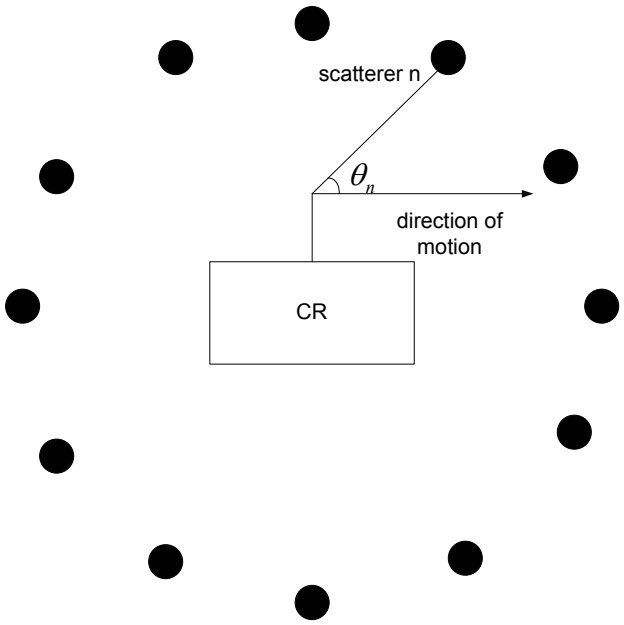

Figure 1.3 Illustrating plane wave arrive.

In a mobile radio channel, the Rayleigh distribution is usually used to describe the time varying nature of the received envelope of a flat fading signal [8]. The received signal envelope r is distributed according to the Rayleigh distribution as [59]

$$p(r) = \frac{r}{\sigma^2} \exp\left(-\frac{r^2}{2\sigma^2}\right) \tag{1.30}$$

where σ is the rms value of the received signal.

Furthermore, the received signal power r^2 is then distributed according to an exponential distribution which is given by

$$p_{r^2}(x) = \frac{1}{2\sigma^2} \exp\left(-\frac{x}{2\sigma^2}\right) \tag{1.31}$$

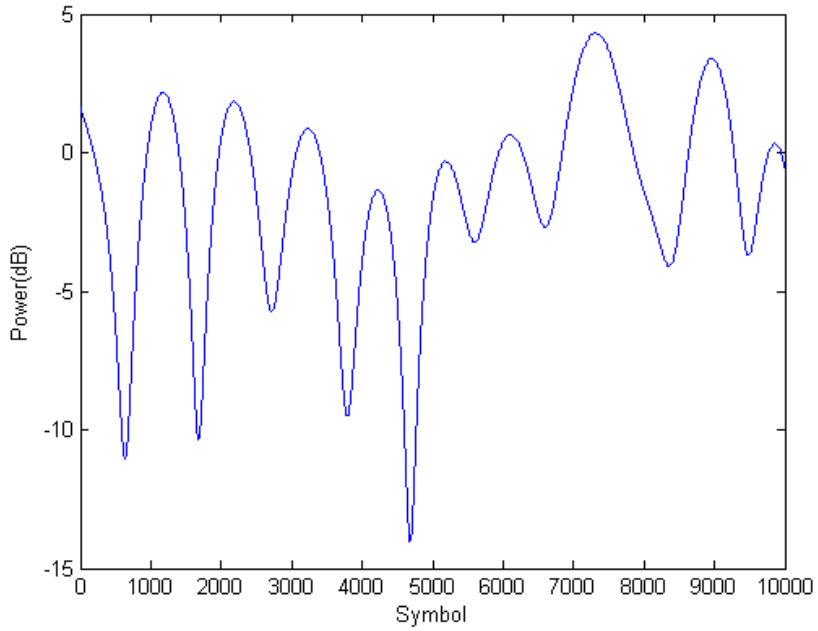

Figure 1.4 Example of fading channel power response simulated using Jake's model.

1.5 SCOPE OF THESIS

Based on my literature review, I found that researchers almost always pay much more attention to how to achieve a higher performance for a spectrum sensing scheme than how to minimize the sensing time. Nevertheless, it is also very important to minimize the sensing time. Thus, a key objective of my research is to minimize the average sensing time.

In the individual detection part of this thesis, the sequential detector is applied in the AWGN channel and in a log-normal shadowing channel. Sequential detection is found to need less sensing time on average than a block based energy detector for a similar level of performance. However, the sensing time of a sequential detector is a random number, and this implies that it sometimes needs an extremely long sensing time. We therefore investigate a truncated sequential detector which always needs less sensing time than an energy detector. However, the truncation also leads to some decrease in detection performance. We evaluate the performance degradation of a truncated sequential detector and demonstrate that in most situations it is modest.

In the cooperative sensing work in chapter 3, a selection rule is applied as the fusion rule to decrease sensing time and to combat the hidden terminal problem. We determine

how much the sensing time can further be reduced using a selection rule. We also investigate how much the overall performance can be increased using a selection rule. From the literature review of cooperative sensing schemes in chapter 2, we find that all the fusion rules in existing schemes are combining rules rather than a selection rule.

Chapter 2

BACKGROUND

2.1 INTRODUCTION

In chapter 1, a general introduction to wireless communication systems is presented. In this chapter, background information on CR, signal detection theory, individual sensing and cooperative sensing will be provided. This chapter is organized as follows. In section 2.2.1, the problem of spectrum shortage is discussed. In section 2.2.2, three approaches to solving this problem are presented. In this thesis, we primarily focus on CR which can be viewed as the platform on which to deploy any one of these three approaches. Thus, an overview of CR is presented in section 2.2.3. Since my work is focused on the spectrum sensing step of CR, which is based on signal detection theory, four fundamental concepts of signal detection theory are presented in sections 2.3. In section 2.4, three different types of individual detectors for spectrum sensing are briefly introduced. However, individual sensing is not reliable enough in practice, and as a result, people often use cooperative sensing which is described in section 2.5.

2.2 COGNITIVE RADIO

2.2.1 Spectrum Scarcity

Researchers are continually designing more advanced transmission schemes. The motivation is to improve the capacity of a communication system. The Shannon capacity formula is given by $C = Blog_2(1 + \frac{S}{N})$ bits/sec, where C is the ergodic capacity of a bandlimited AWGN channel, B is the transmission bandwidth and $\frac{S}{N}$ is the average signal to noise ratio of the channel. From this we can see that if there is more bandwidth available, then the capacity of the system will indeed increase. Bandwidth can be viewed as one of the

most important parameters of communications. Therefore, we may ask if there is more bandwidth we can use?

Today, wireless communication is used in many applications [8], such as military communications, TV broadcast, mobile phones, Bluetooth microphones, WiFi systems and so on. Since spectrum resources are limited, almost all wireless systems are licensed to use only a fixed assigned bandwidth. In other words, today's wireless networks are each based on a fixed spectrum assignment. Governments allocate different frequency bands to different licence holders or services. For example, European governments assign the frequency band 890 MHz-960 MHz to the GSM cellular radio system [8]. In this situation, no one else can use this band at any time. But we can easily find that a specific frequency band is not used all the time. Fig. 2.1 shows that the actual utilization in the 3-4GHz band is 0.5% and drops to 0.3% in the 4-5GHz band [23], [24], [48]. It has also been found that less than 14% of the radio spectrum is truly busy at any given time [23], [24], [48]. Thus, we may ask why don't secondary users use licensed frequency bands when they are not being used by the licensed or primary users?

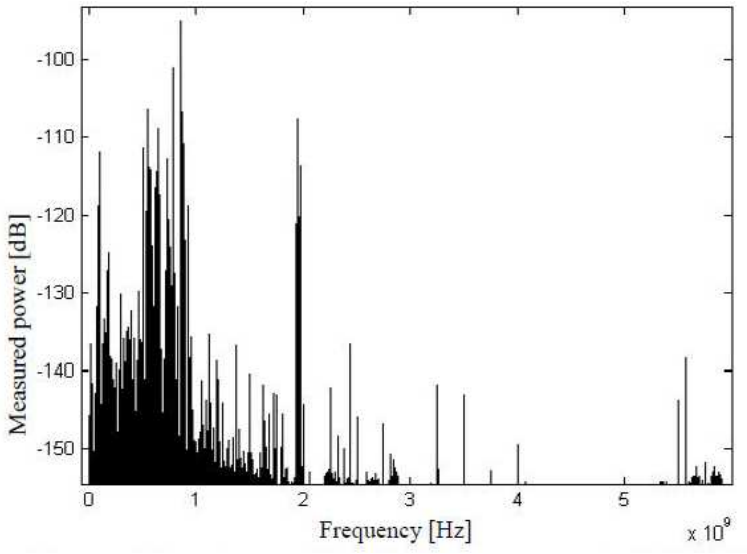

Figure 2.1 A snapshot of the spectrum utilization up to 6GHz in an urban area [23].

2.2.2 Dynamic Spectrum Access

To solve the problem of spectrum scarcity and to increase the efficiency of its use, researchers have proposed an intelligent approach to using the spectrum, known as dynamic spectrum access. This idea was first presented at the first IEEE symposium on new fron-

tiers in dynamic spectrum access networks [24]. Dynamic spectrum access approaches can be considered in terms of three sub models as shown in Fig. 2.2.

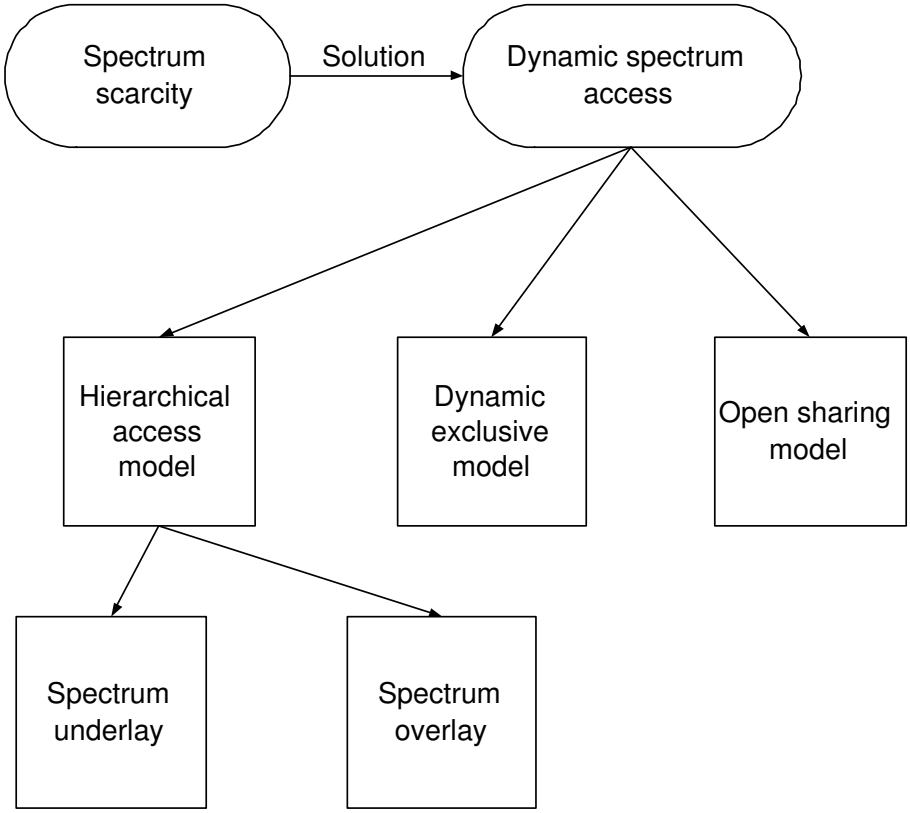

Figure 2.2 The dynamic spectrum access.

The first one is the so-called dynamic exclusive use model [24]. The aim of it is to improve spectrum efficiency. This model still claims that spectrum is licensed for exclusive use. The main idea is to introduce flexibility to improve spectrum efficiency. For example, the licensees can sell and trade spectrum and choose the technology as they wish. In this situation, the market will play a more important role in using the spectrum. Furthermore, the regulatory agencies may allocate the spectrum to different services based on the usage factor of different services.

The second model is the open sharing model, which is also known as spectrum commons [24]. Here, a spectral region is common for all users. However, the commons is not an unregulated free for all and protocols have been proposed to manage the"commons". Detailed information on this model can be found in [41], [52], [53], [54], [55], [56].

The third approach is the hierarchical access model. The basic idea of this model is to allow the secondary user to use licensed spectrum only when its interference to the primary

user is limited. There are two different approaches in this model: spectrum underlay and spectrum overlay.

In the underlay approach, the average transmission power of the secondary user is below the noise floor of the primary user. In this situation, the secondary user can transmit all the time. It does not rely on the detection of white space in the spectrum. As Ultra wideband radio (UWB) spreads the transmission power over a very wide frequency band, it can be viewed as a suitable technology for this approach [24].

The second approach is spectrum overlay which is also called the opportunistic spectrum access [24]. In this approach, there is no restriction on the transmission power of the secondary user. Instead, the secondary user needs to know when and where they may transmit. Thus, a detection scheme to identify the white or vacant space in the spectrum is needed. CR can be applied for this approach.

In summary, dynamic spectrum access is one of the solutions to the spectrum scarcity problem. There are three basic models for dynamic spectrum access. In this thesis, we primarily focus on the spectrum overlay approach of the hierarchical access model. This approach is an important application of CR which was first proposed by Mitola [22] in 2001. Thus, an overview of CR will be provided in the next section.

2.2.3 Software-Defined Radio and Cognitive Radio

CR is based on software defined radio (SDR) [25], [49], [50], [51], [16]. Thus we begin by introducing SDR. It is a relatively new class of radio architecture, which was first developed in the 1990's. A SDR is often described as: "a radio that includes a transmitter in which the operating parameters of frequency range, modulation type or maximum output power, or the circumstance under which the transmitter operates in accordance with commission rules, can be altered by making a change in software without any changes to the hardware components that affect the radio frequency emissions" [25]. Similar and complementary software is used to define the receiver in an SDR. Fig. 2.3 shows a generic SDR receiver architecture. The amplified signal from an antenna is fed directly into a high speed analog-digital convert (ADC). As the converted signal is merely binary data, digital components and techniques can be used to process it. Indeed, most implementations are based on digital signal processing (DSP). A DSP platform can be dynamically reconfigured, leading to a generic hardware platform, which can be made to transmit and receive a wide variety

of signals just by reprogramming it.

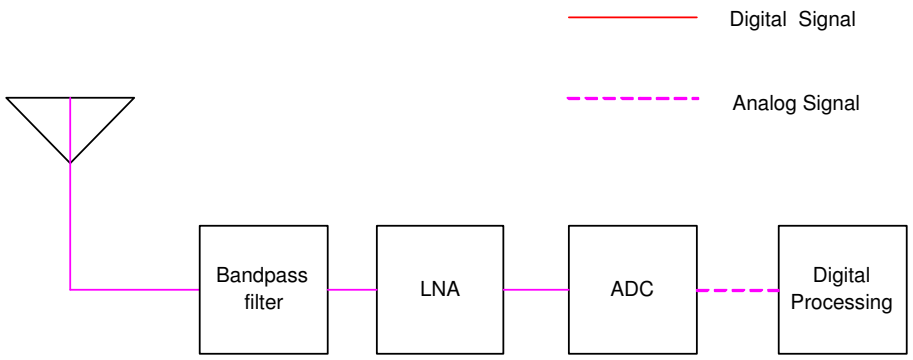

Figure 2.3 Generic software radio receiver architecture.

CR is recognized as an advanced form of SDR with the additional ability to sense its surrounding environment, track potential spectrum changes, and then adapt or react to its findings. We want to apply CR using the hierarchical access model of dynamic spectrum access to identify the white space in the spectrum. There are three steps needed to achieve this objective. These are often represented as a cognition cycle. The steps of the cognition cycle are spectrum sensing, spectrum analysis, and spectrum decision [22]. The relationship among these three steps is shown in Fig. 2.4.

1. In the spectrum sensing step, a CR monitors the spectral bands under consideration, obtains their information and detects spectral holes.

2. In the spectrum analysis step, the characteristics of the spectrum holes that are detected through step 1 are estimated and analyzed.

3. In the spectrum decision step, a CR determines the parameters of transmission such as data rate, transmission mode, and bandwidth available for transmission based on the estimated and analyzed results of step 2. The appropriate spectral band is then chosen according to the user requirements and the radio reconfigured as necessary.

After an operational spectral band is determined by the cognition cycle, communications can be performed using this spectral band. However, the radio environment changes dynamically in both time and space, thus the CR should continue monitoring to detect changes in the surrounding radio environment and the possible emergence of the primary or licensed user of the band.

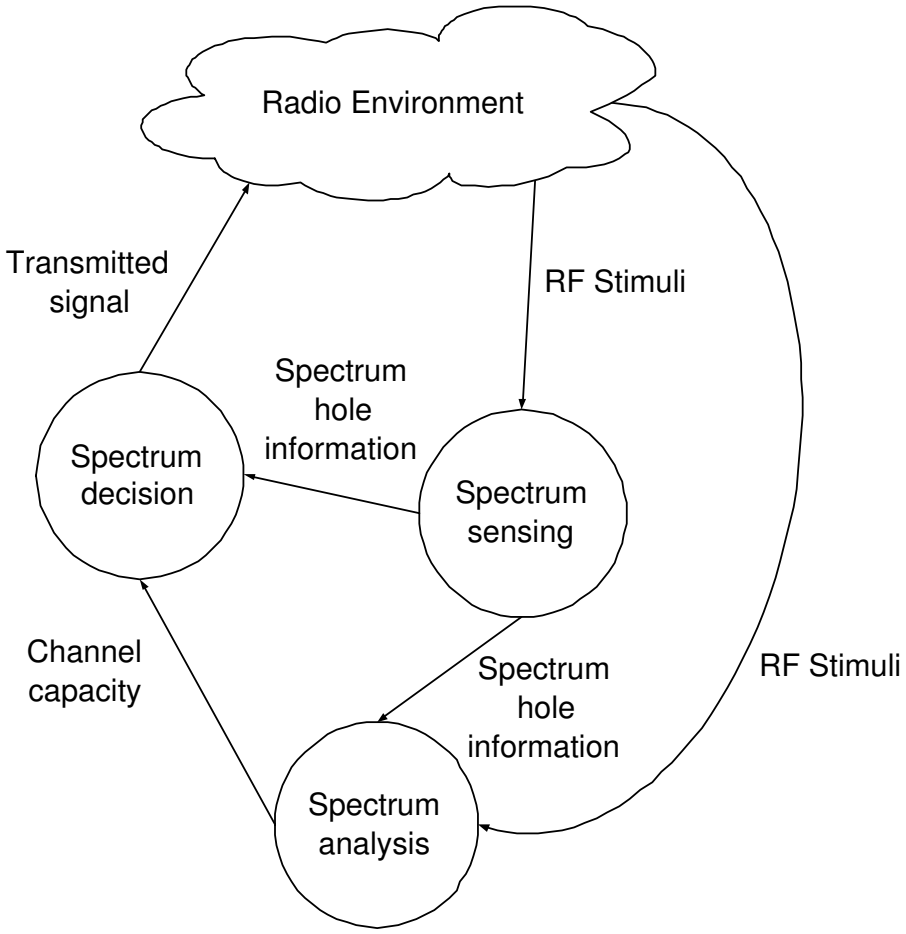

Figure 2.4 Cognition cycle.

2.3 FUNDAMENTALS OF DETECTION THEORY

In this thesis, the work is primarily focused on the spectrum sensing step which is based on signal detection theory. Thus, the basic concepts of signal detection theory are summarized in this section. The work contained in the following chapters will then utilize these concepts.

2.3.1 Probability Density Function

Probability density functions (PDFs) are used frequently in this thesis, so we briefly introduce them in this section.

In practice, signals are usually corrupted by additive noise. Noise is a phenomenon produced by the superposition of many randomly occurring events and it is not possible to specify its instantaneous amplitude at a given time. We can only determine the probability

that it will exceed a given value or lie within a specified range.

Suppose that x is a random variable which is used to represent the instant amplitude of noise at a certain time. We want to know the probability of x falling within the range of amplitudes between v_1 and v_2. We then have

$$P[v_1 \leq x \leq v_2] = \int_{v_1}^{v_2} p_X(x)dx \tag{2.1}$$

where $p_X(x)$ is the PDF of the noise signal. It describes the density of probability at each point in the sample space. The probability of a random variable falling within a given set is given by the integral of its density over the specified interval. In this thesis, the noise is modelled as white gaussian noise having the PDF

$$p_X(x) = \frac{1}{\sqrt{2\pi}\sigma_n} \exp \frac{-(x-\mu_n)^2}{2\sigma_n^2} \tag{2.2}$$

where μ_n is the mean and σ_n is the standard deviation.

2.3.2 Hypothesis Testing

Signal detection is often modeled as hypothesis testing [26], [36], [57]. The simplest case occurs when there are only two hypothesis concerning the received signal:

1. Signal not present
2. Signal present

We often denote the hypothesis "signal not present" by H_0, and the hypothesis "signal present" by H_1. H_0 is often called the null hypothesis while H_1 is often called the alternate hypothesis.

We observe the N samples $x_1 \ldots x_N$, and our objective is to decide which hypothesis is true on the basis of this observation. The choice of N is based on system requirements [26]. In other words, we need to determine whether the sample vector X belongs to the distribution $p(X|H_0)$ or the distribution $p(X|H_1)$. $p(X|H_i)$ is the joint conditional PDF of x_N under hypothesis H_i. For independent x_n, we have

$$p(X|H_i) = \prod_{n=1}^{N-1} p(x_n|H_i) \qquad i = 0, 1 \tag{2.3}$$

We need a test procedure for making one of two decisions "accept H_1" or "reject H_1". This test procedure is called a decision rule.

Before we determine the optimum decision rule, we first denote two kinds of errors. If we reject H_0 when it is true, we have an error of the first kind. If we accept H_0 when H_1 is true, we have an error of the second kind. We can define the probability of error of the first kind as [36]

$$\alpha = \int_{X:L(X)>\gamma} p(X|H_0)dX \tag{2.4}$$

where $L(X)$ is known as a likelihood ratio.

The probability of error of the first kind is also denoted as the probability of false alarm (P_{FA}). The probability of error of the second kind is defined as

$$\beta = \int_{X:L(X)<\gamma} p(X|H_1)dX \tag{2.5}$$

where γ is the threshold to distinguish two hypotheses. The probability of error of the second kind is also denoted as probability of missed detection (P_M).

2.3.3 Fixed Sample-Size Test

Ideally, we should choose a decision rule that minimizes both kinds of errors. However, for a given sample size or number of observations, we can not make both α and β arbitrarily small.

In practice, the Neyman-Pearson theorem [26] is used to find the optimum decision rule. This theorem is defined as: To minimize β for a given α, decide H_1 if

$$L(X) = \frac{p(X|H_1)}{p(X|H_0)} > \gamma \tag{2.6}$$

where the threshold γ is found from

$$\alpha = Pr(L(X) > \gamma|H_0) = \int_{X:L(X)>\gamma} p(X|H_0)dX \tag{2.7}$$

where $X = (x_1, x_2, ..., x_N)$ is the vector of observations or samples.

2.3.4 Sequential Test

An important feature of the Neyman-Pearson theorem is that the sample size N is fixed. Based on predetermined values of α and N, we choose the threshold that minimizes β. Thus, systems employing the Neyman-Pearson theorem are often called fixed sample-size systems. In a fixed sample-size system, the most important consideration is how small can we make β based on the predetermined α and N.

However,there is an alternative approach called a sequential test [27]. The approach in this case is to fix α and β, and then to choose a test that can achieve these values with the minimum number of data samples N. In a sequential test system, the most important aspect is how many samples N we need to achieve the predetermined α and β.

The procedure of a sequential test is shown below: First, we set fixed values, $\alpha = \alpha_0$ and $\beta = \beta_0$. Second, a single sample x_1 is observed. Third, one of three different decisions is made based on this sample. The three possible decisions are shown below:

1. Hypothesis H_1 is accepted.
2. Hypothesis H_1 is rejected.
3. We can not make a decision based on this sample and we need to take more data.

If decision 1 or 2 is made, the test stops. If decision 3 is made, a second sample x_2 is acquired. Based on the combined observation (x_1, x_2) one of the three decisions needs to be made. If decision 1 or 2 is made, the test stops. If decision 3 is made, a third sample x_3 is acquired. This sequence is repeated until the test stops.

Although the number of samples required is a random variable and it is occasionally extremely large before termination of the test, the optimum sequential test needs many fewer samples on average than a traditional fixed sample-size test to achieve the same α and β. Generally speaking, it only needs 10-60 percent on average as many samples as a fixed sample-size test [27], [36], [58].

2.4 INDIVIDUAL DETECTORS

In this section, we will briefly describe three individual detectors which may be applied in a CR system for spectrum sensing. Here, we define an individual detector to be one at a single site.

The aim of spectrum sensing is to detect whether there is a primary signal present in a specific frequency band [47]. A CR has to detect a weak signal due to a primary user in a noisy environment through local observation. There are only two different possible states of a given frequency band: occupied by a primary user or not. We use H_0 to denote the case of no primary signal in a given spectrum band (not occupied) and H_1 can be used to specify the presence of a primary signal (occupied).

2.4.1 Matched Filter

We begin our study of optimal detection approaches by considering the problem of detecting a known deterministic signal in AWGN channel [26]. Here we consider a complex base band equivalent discrete time signal model in noise. In a sampled form detector tests the following two hypotheses

$$\begin{aligned} H_0: \quad & R[n] = W[n] \\ H_1: \quad & R[n] = S[n] + W[n] \end{aligned} \tag{2.8}$$

where $S[n]$ is a known signal, $W[n]$ is white Gaussian noise, $n = 1 \dots N$, and $R[n]$ is the received signal at the secondary user. N is the number of samples in the observation interval. It is chosen based on system requirements, such as the performance to be achieved or the maximum allowable sensing time.

By using the Neyman-Pearson criterion, we finally obtain the test statistic V as (details can be found in [26])

$$V = \sum_{n=1}^{N-1} R[n]S^*[n] \tag{2.9}$$

where $*$ represents the complex conjugate.

The test statistic V is then compared with the threshold γ_m to form the decision

$$\begin{aligned} V &> \gamma_m \quad \text{Decide signal present} \\ V &< \gamma_m \quad \text{Decide signal not present} \end{aligned} \tag{2.10}$$

The threshold γ_m of the matched filter can be found in [26].

The matched filter is the optimal detector for known $S[n]$. A matched filter is identical to a correlator [26], and thus many authors also call this optimal detector a correlator or replica-correlator in some papers. The matched filter requires the primary signal and its sampled values to be completely known a priori to the receiver. Otherwise, if a priori information is not very accurate, then the matched filter performance is very poor.

2.4.2 Energy Detector

We now discuss the optimal detection approaches for detecting a random signal in AWGN. The detector again tests the two hypotheses in sampled form as,

$$\begin{aligned} H_0: \quad R[n] &= W[n] \\ H_1: \quad R[n] &= S[n] + W[n] \end{aligned} \tag{2.11}$$

where $n = 1 \ldots N$ and N is the observation interval or number of samples. $S[n]$ is the unknown transmitted signal. $R[n]$ is the received signal at the secondary user. By using the Neyman-Pearson theorem again, we decide H_1 if

$$V = \sum_{n=1}^{N-1} |R[n]|^2 > \gamma \tag{2.12}$$

This detector thus computes the energy in the received signal and compares it to a threshold γ. Hence, it is known as an energy detector. The derivation of γ will be shown in the next chapter to require knowledge of AWGN variance.

Energy detection can be performed in either the time domain or the frequency domain. To measure the signal in a particular frequency band in the time domain, a bandpass filter is applied to the signal and the power of the output signal samples is measured. To measure the signal power in the frequency domain, the signal is fast Fourier transformed and the signal energy is measured in all frequency bins in the target frequency region.

Most researchers investigate energy detection in the time domain. However, a pre-filter matched to the bandwidth to be searched is used. In practice, this is quite inflexible, especially in the case of narrowband signals and sine waves. Thus, some researchers [37],

[38], [39], [40] apply energy detection in the frequency domain by using the FFT instead of a pre-filter.

Performance of an energy detector is very poor in a noise uncertain environment [2]. Noise in most communications systems is an aggregation of various independent sources including not only thermal noise at the receiver, but also interference due to nearby unintended emissions. By using the central limit theorem (CLT), it is often assumed the noise at a receiver is Gaussian. However the actual noise process is only approximately Gaussian [31]. This is called noise uncertainty. We know that the receiver tries to estimate the noise variance by taking a large number of samples. But, there will be some residual uncertainty in this estimation. Owing to this noise uncertainty, there exists a SNR threshold at the receiver, which we can call SNR_{wall}. If the received SNR at the receiver is smaller than SNR_{wall}, then accurate detection is impossible [31].

Energy detection makes a decision using only one parameter of the received signal – *energy*. It can make a decision quickly with high accuracy when the received SNR is high enough. In contrast, it makes errors if the received SNR is low, because it does not know whether the received energy is noise or signal energy.

2.4.3 Feature Detector

In this situation, we need more parameters to distinguish the two hypotheses. Various forms of feature detector are proposed in the frequency domain for this purpose. The idea of such alternative detectors can be found in [28], [29], [30]. The modulated signals are then considered as cyclostationary since their mean and autocorrelation exhibit periodicity. These features are detected by analyzing a spectral correlation function (SCF). The noise is a wide-sense stationary signal without correlation, while the modulated signals are cyclostationary with spectral correlation. Thus, the spectral correlation function can differentiate the noise energy from the modulated signal energy. For this reason, the cyclostationary feature detector can perform better than the energy detector in a noise uncertainty environment. Furthermore, it can also show us the type of modulated signal. However, a cyclostationary feature detector is quite limited at low SNR, has higher computational complexity and requires long observation times. This reduces the throughput of a CR system.

2.4.4 Summary of Individual Detector

In summary, a matched filter can be applied only when the signal waveform of the primary user's signal is known. Energy detection can be easily applied but performs relatively poorly when using a short sensing time. A feature detector can provide good performance given sufficiently long sensing time.

The above three detectors are the most popular detectors in practice. There are also various other detectors proposed. For example, the author of [32] proposed an energy-feature based detector. The energy detector is used to determine the presence of signal energy in the band of interest, and is followed by feature detection to determine if indeed the signal energy is due to the presence of a primary user when the received SNR is low. Kim et. al. [42] use a hidden markov model (HMM) to classify the signal features due to its robust pattern matching capability. The results show that this scheme can detect and classify signals over a range of low SNRs. Wild et. al. [43] detect the primary signals based on detecting local oscillator leakage power. By using this method, we can not only detect the presence of primary signals but also can find their locations. Tian et. al. [44] proposed a wavelet based approach for wideband spectrum sensing in a CR system. Pandhripande et. al. [45] applied energy detection in a multiple-antenna system and analyzed the detection performance. Neihart et. al. [46] proposed a parallel multi-resolution spectrum sensing approach in a multiple-antenna system. It is found that this method requires less sensing time than in the case of the single antenna systems.

Severally other detectors have been proposed in an attempt to provide better performance than the three popular detectors described above. The alternatives improve various aspects, such as detecting the primary signal in a low SNR region, improving overall detection performance, reducing sensing time or scanning a larger bandwidth. Our goal is to reduce average sensing time.

2.5 COOPERATIVE DETECTION

The above detectors are non-cooperative which means a CR detects transmitted primary signals purely by local observation. However, such an approach does not deal with the problem of "hidden terminals" [33] which arises when the CR is shadowed or in multipath fading. Fig. 2.5 illustrates one of the CRs being shadowed by a tree which obstructs the signal path between the primary transmitter and CR. In this situation, a CR may not

reliably detect the primary transmitter and may try to use the channel when there is still a primary signal present.

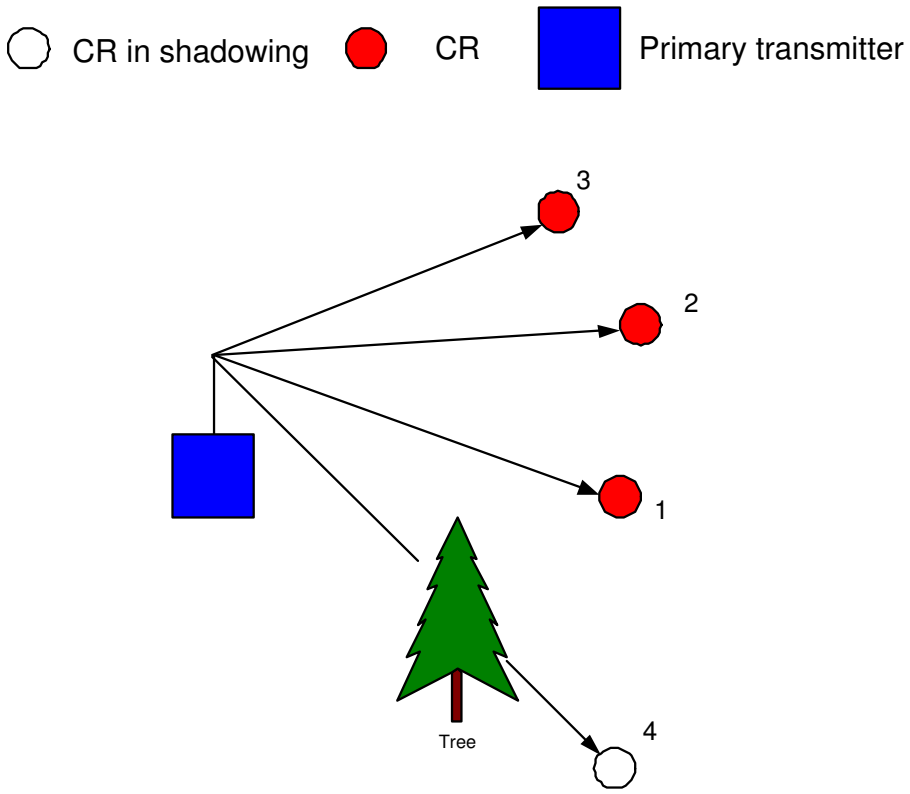

Figure 2.5 Hidden terminal problem in cognitive radio system.

An approach to combatting this problem and increasing the spectral estimation reliability is cooperative spectrum sensing. In cooperative spectrum sensing, the spectrum occupancy is determined by the joint work of several CRs, as opposed to it being determined by an individual CR.

There are typically two parts of a cooperative sensing network; namely the individual sensors and the fusion center. Individual sensors can be any of the detectors which are presented in section 2.4. Each sensor collects information on the primary signal if it is present, such as energy, log-likelihood ratio and it can even make a local decision based on this information. It sends this information or local decision to the other sensors and ultimately to the central processor which is known as the fusion center. The fusion center makes a final decision based on the received information or local decisions.

In this section, a short literature review of existing cooperative sensing schemes is presented, and then two different kinds of cooperative detection structure are introduced.

2.5.1 Literature Review of Existing Cooperative Sensing Schemes

Some basic ideas of distributed detection which are quite useful for cooperative spectrum sensing are reviewed in [88], [89]. The fundamentals of cooperative spectrum sensing in CR can be found in [78]. Based on our literature review of cooperative sensing in CR system, we have found that researchers generally want to achieve three different objectives by using cooperative sensing as detailed below.

Most researchers focus on how to achieve good detection performance. Their proposed cooperative schemes are often fixed sensing time schemes and their aim is to achieve high performance during this fixed sensing time. Plenty of schemes are applied to achieve this aim. The most popular one is to use weighting [63], [64], [65], [74], [75] which may relate to local SNR, distance between primary and secondary user, local P_D and so on. All of these weights represent in some sense the reliability of each local decision. At the fusion center, the weighted local decisions are combined. In this way, the reliable local decisions contribute more to the final decision and, therefore, better performance can be achieved.

In addition, there are also several different schemes to achieve high performance, such as a double threshold energy detector [66], [67], hierarchy rules in the fusion center [68], adaptive rules in the fusion center [86], a linear quadratic rule in the fusion center [83], cluster networks [69], setting a more accurate threshold at the fusion center [73] and increasing sensing time to achieve a higher performance [79]. Some researchers even separate the spectrum sensing task from the secondary users. They use sensing devices to detect primary users and propose a handshake technique between a sensing device and a secondary user [70]. Furthermore, the writers of [84], [85] calculate the optimal number of individual sensors in a cooperative network for the best detection performance.

The second objective of cooperative spectrum sensing is to transmit local decisions to the fusion center using a small bandwidth. This problem is crucial in a soft decision scheme [87]. Thus, how to efficiently quantize the soft information is a hot research area [76], [77]. Furthermore, censoring schemes are also popular [61], [62]. In order to minimize the probability of error, sensors are assumed to censor their observations and only transmit the local likelihood ratio values which do not fall in a certain interval.

The last objective is to reduce sensing time. There are two approaches to minimize sensing time. The first approach is called the “change detection” algorithm [71]. This algorithm refers to the detection of abrupt changes in the distribution of observed signals as

quickly as possible. The detector based on this algorithm is called an event based detector [72]. This detector does not sense the level of energy. It only senses surges in energy level. If there is a surge, they will announce that a primary user has entered the system. Simulation results show that this approach can reduce the sensing time significantly.

The second approach is sequential testing. Some researchers apply the sequential test at an individual sensor only and a traditional combining scheme at a fusion center [81] while others apply a sequential test both at the individual sensors and at the fusion center [80], [82].

2.5.2 Structure of Cooperative Networks

Based on the structures of a cooperative sensor network [34], we can divide the cooperative sensor networks into two categories. The first is a serial structure, which is illustrated in Fig. 2.6.

Each sensor makes a decision based on its own observation and the decision from a previous sensor in a serial structure. In this situation, the accuracy of the final decision is significantly higher than those of the individual sensors [34].

However, there are two drawbacks to the serial network. Firstly, delay accumulates since each sensor has to wait for results from the previous sensor. Thus, it tends to need a long sensing time. Secondly, the performance degrades if the link in the serial stage is broken at one of the intermediate stages. In other words, the reliability of serial structure is relatively low.

The second structure is a parallel structure, as illustrated in Fig. 2.7. In this structure, we assume there are K detectors and the observations at each detector are denoted by $y_i, i = 1, \ldots, K$. Then, the decision rule can be written as

$$\begin{aligned} u_i &= +1 \quad \text{if } H_0 \text{ is declared} \\ u_i &= -1 \quad \text{if } H_1 \text{ is declared} \end{aligned} \tag{2.13}$$

Each detector uses a decision rule $g_i(y_i)$ to make the decision $u_i, i = 1, \ldots, K$, given by (2.13). The individual decision rule $g_i(y_i)$ can be any of various rules based on system requirements, including the Neyman-Pearson rule, sequential testing rule and so on. Data

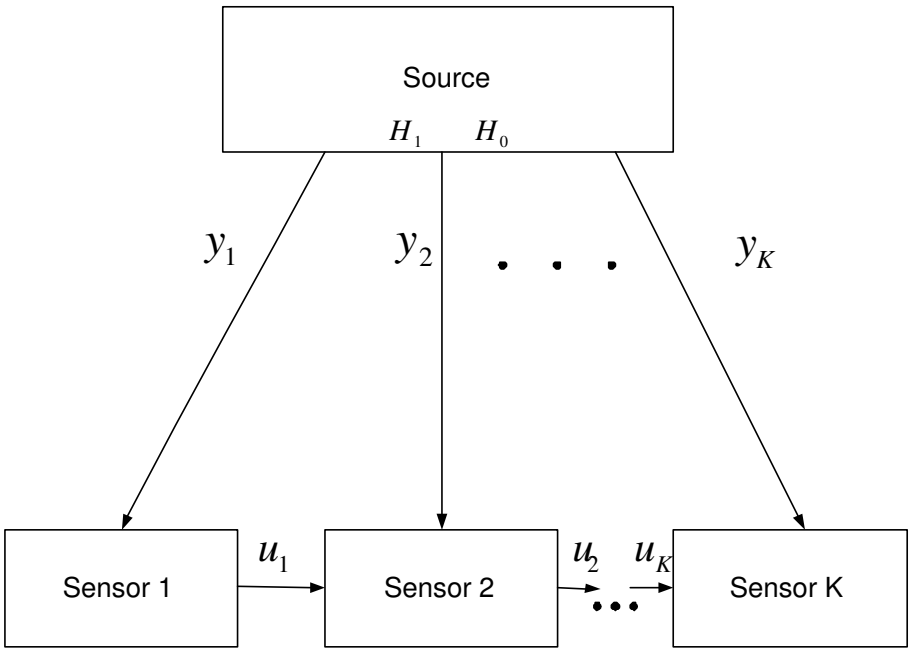

Figure 2.6 Serial structure of cooperative network.

fusion rules at the data fusion center are often implemented as "k out of K" [35] logical fusions. This means that if k or more detectors decide H_1, then the global decision is H_1, which is

$$\begin{aligned} u &= 1 \quad \text{if } u_1 + u_2 + \ldots + u_K > 2k - K \\ u &= -1 \quad \text{otherwise} \end{aligned} \tag{2.14}$$

Logical functions such as AND, OR, are special cases of the "k out of K "rule.

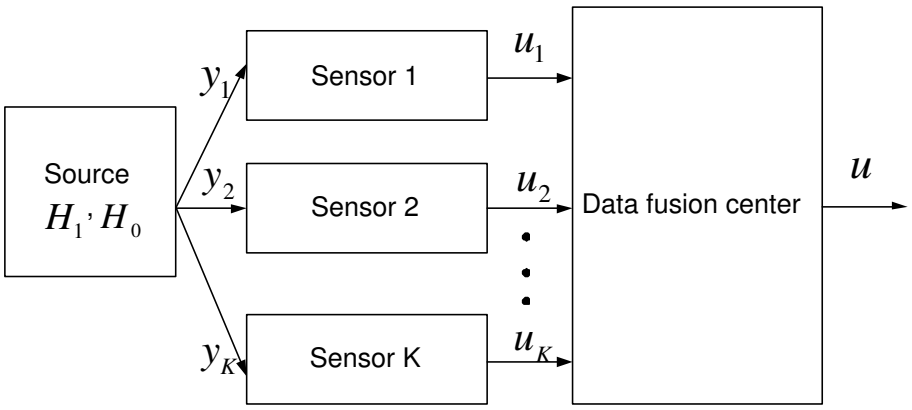

Figure 2.7 Parallel structure of cooperative network.

In the parallel structure, all the individual sensors transmit their local decision to the fusion center simultaneously. They do not wait for other sensors. Under this circumstance, the sensing time is less than that of the serial structure. Furthermore, the parallel structure is more reliable than the serial structure because it is not very sensitive to the problem of broken links. Thus, a parallel structure is employed in the remainder of this thesis.

2.6 SUMMARY

This chapter first provided an overview of spectrum scarcity and dynamic spectrum access. Due to the problem of spectrum scarcity, researchers have proposed an intelligent approach to manage the spectrum, known as dynamic spectrum access. By applying this intelligent approach, we can use the spectrum more efficiently. There are three sub models of dynamic spectrum access. CR can be viewed as the platform of one of these sub model, namely the hierarchical access model. Some detailed information concerning SDR and CR was provided. We also noted that our research is mainly focused on the spectrum sensing step of CR.

Since spectrum sensing is normally modeled as a signal detection problem, some useful mathematic fundamentals of signal detection theory, such as: PDF, Neyman-Pearson theorem and sequential testing theory were introduced. However, apart from the sequential case, the above detectors are all fixed sample-size detectors which means their sensing times are preset and fixed. In the next chapter, a detector with a flexible sensing time based on Wald's sequential test theory is described in detail. The main purpose of applying this detector is to reduce average sensing time, while retaining good detection performance.

Cooperative sensing was introduced in the last part of this chapter. Cooperative sensing schemes aim both to achieve better performance and to reduce the sensing time.

Chapter 3

SPECTRUM SENSING BASED ON SEQUENTIAL TESTING

3.1 INTRODUCTION

The design of spectrum sensing schemes has recently attracted significant research attention. Spectrum sensing is used to detect a primary signal or signals in the presence of noise over a broad bandwidth. Several detectors that can be applied for spectrum sensing are reviewed in chapter 2. All of them are fixed sample size detectors which means that the sensing time or number of observation per test is preset and fixed [47].

If the constraint of fixed sample size is not required, it is possible to construct new hypotheses tests which on average need a smaller number of samples to achieve the same P_D and P_{FA}. These include the sequential test proposed by A.Wald [27]. However, the sequential test has the disadvantage that the sample size required to terminate a certain test is a random variable. Thus, the sequential test sometimes requires an extremely large number of samples before making a decision. In a cognitive radio system, extremely long sensing time can't be tolerated [90]. It is then reasonable to interrupt the procedure before the test reaches a natural termination resulting in a truncated sequential test, albeit with some loss of detection performance.

In order to combat the "hidden terminal" problem and to increase the spectral estimation reliability, cooperative spectrum sensing is often applied in practice. In the cooperative spectrum sensing approach, spectrum occupancy is determined by the joint work of several CRs, as opposed to being determined by an individual CR.

In this chapter, a truncated sequential detector is developed for individual sensing. The sensing time is a random variable, which on average is less than that for the fixed sample detector for the same performance. In addition, cooperative spectrum sensing schemes which are used to improve system performance are reviewed and a new selection

combining rule based on sequential testing is proposed for reducing sensing time.

We begin by considering a block energy detector in a Rayleigh fading channel. This will be used as a reference system. A block diagram of an energy detection system is shown in Fig. 3.1.

This chapter is organized as follows. We will first introduce the structure of the selected primary transmitter in section 2 and then the energy detector in section 3. The proposed truncated sequential detector will be described in section 4. In the section 5, we will describe the proposed cooperative scheme.

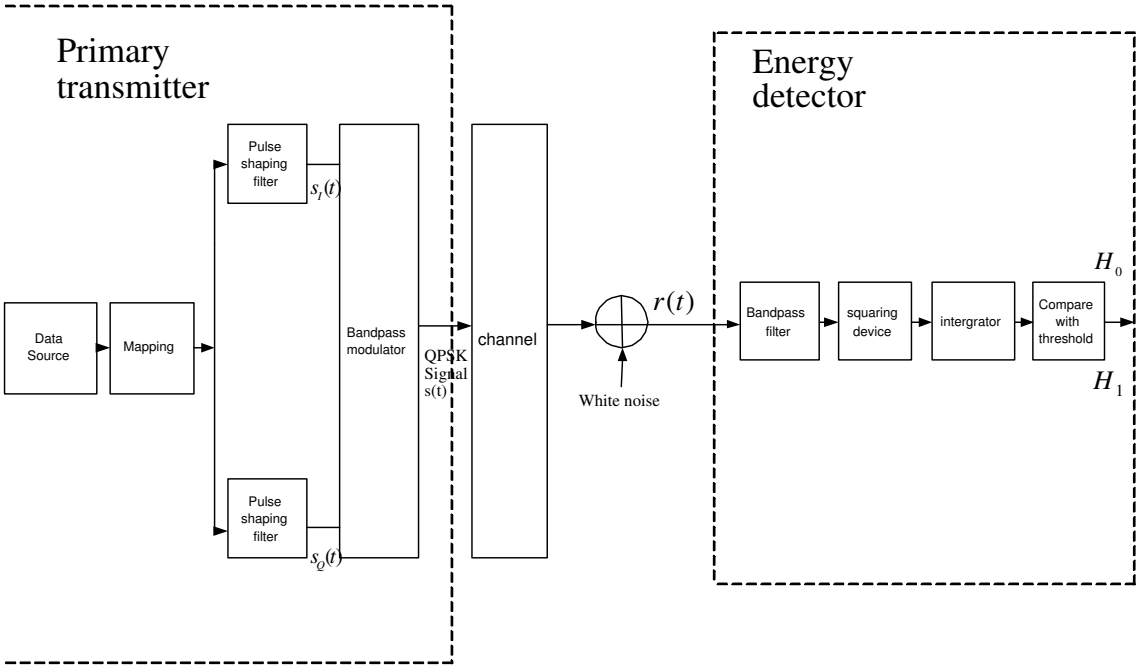

Figure 3.1 Block diagram of an energy detection scheme.

3.2 PRIMARY TRANSMITTER

The modulation type of the primary transmitter can be various. For example, in [87], the author assumed the primary signal is OFDM modulated while the author of [92] assumed the primary signal is BPSK modulated. In my thesis, all the detectors are based on energy detection. In this situation, the actual modulation type is not crucial. Because the detector only detects the presence of a primary signal by measuring the received signal energy and does not need to detect the modulation type. Thus, we choose quadrature phase-shift keying (QPSK) modulation for convenience.

We assume the primary transmitter has the scheme shown in Fig. 3.2. The input information source is converted to binary digits (bits). The bits are then grouped to form digital message symbols. Each symbol m_n can be viewed as a member of a finite alphabet set containing M members. Pulse shaping is the process which transforms message symbols to waveforms. We assume the primary user transmits a QPSK signal. In this situation, two baseband waveforms $s_I(t)$ and $s_Q(t)$ transmit in parallel. They can be represented by

$$s_I(t) = \sum_{n=0}^{N} s_I^n v(t - nT_s) \tag{3.1}$$

$$s_Q(t) = \sum_{n=0}^{N} s_Q^n v(t - nT_s) \tag{3.2}$$

where s_I^n and s_Q^n are message symbols, $v(t)$ is the basic pulse and T_s is the symbol time.

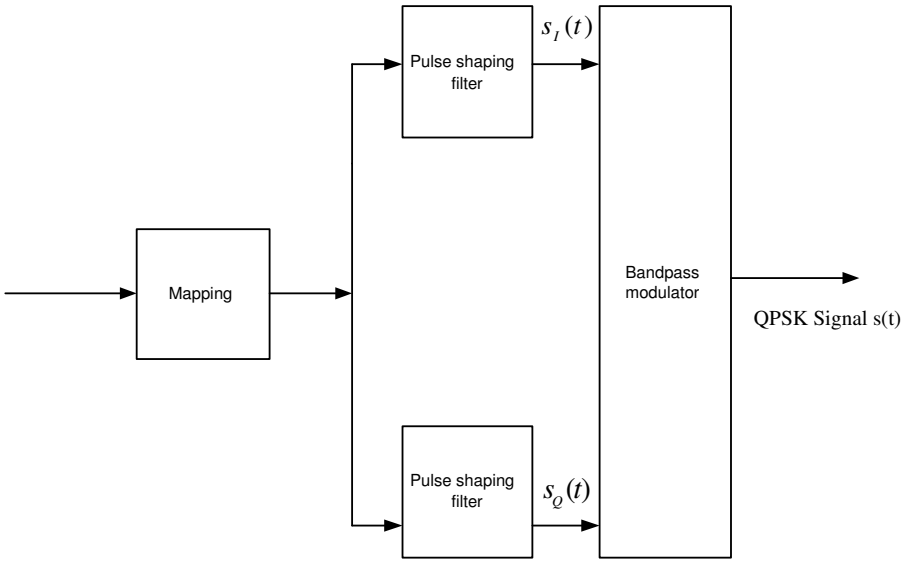

Figure 3.2 Block diagram of primary transmitter.

For a wireless application, the baseband signal modulates an RF carrier to form a bandpass signal. The bandpass waveform of a QPSK signal can be represented as

$$s_k(t) = s_I(t)\cos(w_c t) + s_Q(t)\sin(w_c t) \tag{3.3}$$

where w_c is the carrier frequency. It has the energy per symbol given by [7]

$$E_s = \int_0^{T_s} s_k^2(t)dt \qquad k = 1, \ldots, M. \tag{3.4}$$

Based on the group of symbols $s_I(t)$ and $s_Q(t)$, the phase of the carrier takes one of four equally spaced values, namely $\pi/4$, $3\pi/4$, $5\pi/4$ and $7\pi/4$. The resulting QPSK signal can also be defined as [7]

$$s_k(t) = \sqrt{\frac{2E_s}{T_s}} \cos\left[2\pi f_c t + (2k-1)\frac{\pi}{4}\right], 0 \le t \le T_s, \qquad k = 1, 2, 3, 4 \tag{3.5}$$

or equivalently

$$s_k(t) = \sqrt{\frac{2E_s}{T_s}} \cos\left[(2k-1)\frac{\pi}{4}\right] \cos(2\pi f_c t) - \sqrt{\frac{2E_s}{T_s}} \sin\left[(2k-1)\frac{\pi}{4}\right] \sin(2\pi f_c t) \tag{3.6}$$

Using the basis functions

$$\phi_1(t) = \sqrt{\frac{2}{T_s}} \cos(2\pi f_c t) \tag{3.7}$$

$$\phi_2(t) = \sqrt{\frac{2}{T_s}} \sin(2\pi f_c t) \tag{3.8}$$

the QPSK signal can be expressed as a set of four signals

$$s_1(t) = \sqrt{\frac{E_s}{2}}\phi_1(t) + \sqrt{\frac{E_s}{2}}\phi_2(t) \tag{3.9}$$

$$s_2(t) = -\sqrt{\frac{E_s}{2}}\phi_1(t) + \sqrt{\frac{E_s}{2}}\phi_2(t) \tag{3.10}$$

$$s_3(t) = -\sqrt{\frac{E_s}{2}}\phi_1(t) - \sqrt{\frac{E_s}{2}}\phi_2(t) \tag{3.11}$$

$$s_4(t) = \sqrt{\frac{E_s}{2}}\phi_1(t) - \sqrt{\frac{E_s}{2}}\phi_2(t) \tag{3.12}$$

which are often represented in a signal constellation diagram as shown in Fig. 3.3.

3.3 PROBLEM FORMULATION

A CR attempts to classify the given channel as either occupied by a primary signal or vacant. This is a binary testing hypothesis problem. The two hypotheses may be summarized as

$$\begin{array}{lllll} H_0 & r[n] & = & w[n] & \text{Channel vacant} \\ H_1 & r[n] & = & hs[n] + w[n] & \text{Channel occupied} \end{array} \tag{3.13}$$

where the primary user's signal, the noise, channel gain and the received signal are denoted by $s[n]$, $w[n]$, h and $r[n]$, respectively.

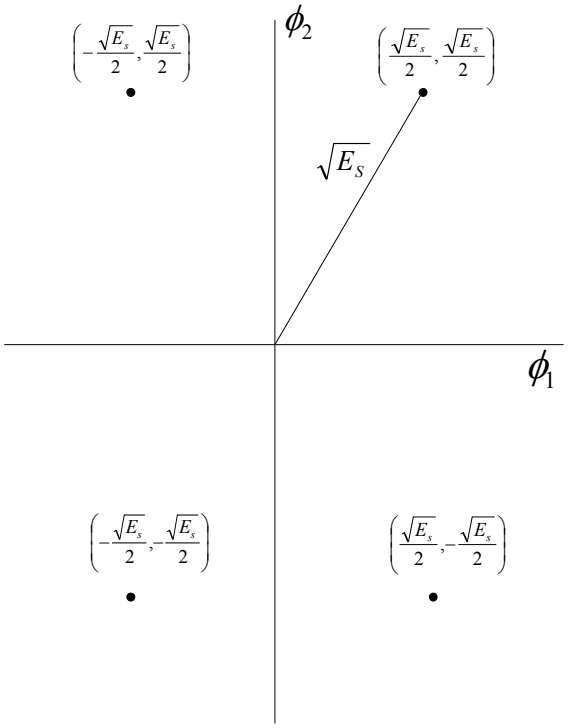

Figure 3.3 Constellation diagram of QPSK.

The detector can make only two decisions, namely,

1. D_0 the channel is vacant
2. D_1 the channel is occupied

As discussed in chapter 2, there are two types of errors when a CR makes a decision. When the channel is vacant the CR can declare that the channel is occupied. This is called a false alarm. The probability of this event is referred to as the probability of false alarm, P_{FA}, and is defined as

$$P_{FA} = P(D_1|H_0) \tag{3.14}$$

A false alarm is called an error of the first kind [36].

When the channel is occupied the CR can declare that the channel is vacant. This is missed detection. The probability of this event is referred to as the probability of missed detection, P_{MD}, and is defined as

$$P_{MD} = P(D_0|H_1) \tag{3.15}$$

A missed detection is called an error of the second kind [36].

The relationship between P_{MD} and probability of correct detection P_D is given by

$$P_D = 1 - P_{MD} \tag{3.16}$$

The errors P_{MD} and P_{FA} are often used to define the system requirements of practical detection systems [90]. Our objective is to develop a detector which can satisfy the system requirements with small sensing time and low computing complexity.

3.4 ENERGY DETECTOR

The energy detector measures the energy of a signal within a certain time and compares it with a threshold. It can be used for any signal type and requires almost no information about the primary signal. Energy detection is often modeled as a hypothesis testing problem and its performance is then evaluated by the probabilities of correct detection and false alarm (P_D, P_{FA}).

In this section, we will first analyze the detection problem mathematically, and then evaluate the choice of detection threshold.

3.4.1 Statistical Analysis

As shown in Fig. 3.4, a bandpass filter of bandwidth W is first employed to limit the noise power. The signal power is confined inside a *priori* known bandwidth W. The energy detector only looks for the presence of a primary signal within the bandwidth W, and the activity outside of this band is unknown.

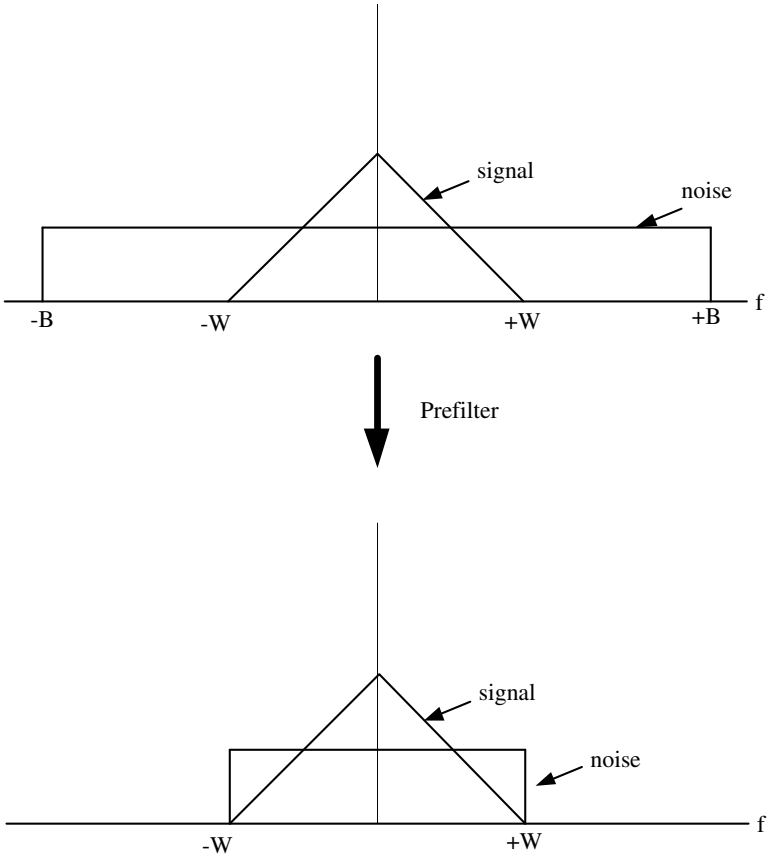

Figure 3.4 Narrowband detection.

A block diagram of an energy detector is shown in Fig. 3.5. The output of the bandpass filter first passes through a squaring device, and is then integrated over a fixed sensing time T to measure the energy of the received signal waveform. The integrator output is compared with a threshold to make a decision between the two hypotheses.

The signal detection problem is based on the theory of random processing. In order to analyze it, we need to transform the received signal waveform into a sequence of random variables. By using the Nyquist sampling theory, we can express each sample of the received signal in the form

$$r_i = r\left(\frac{i}{2W}\right) \qquad i = 1, 2, \ldots, +\infty \tag{3.17}$$

where W is the bandwidth of the signal. Roughly speaking, the bandwidth of a digital signal is $1/T_s$ Hz, where T_s is the symbol duration of the signal [60]. For example, if we transmit a digital signal at a rate of 1 megasymbol/s we will have a bandwidth of approximately 1MHz.

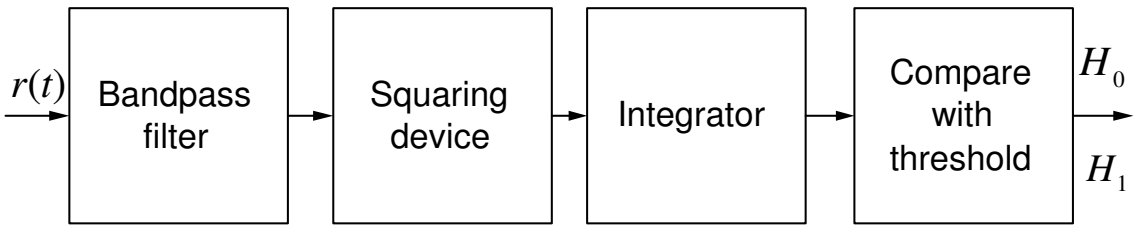

Figure 3.5 Block diagram of an energy detector.

We define the energy per symbol as E_s, but we also need to define the energy per sample, since the samples are summed to form a test statistic. We first define the power of the signal $s(t)$ as the energy per symbol E_s divided by the symbol duration T_s, which can be represented as

$$P_s = E_s/T_s = E_s R \tag{3.18}$$

where R is the symbol rate of the system.

Suppose the transmitted signal is observed over a time duration of T seconds. Then the energy per sample is

$$\frac{P_s T}{2WT} = \frac{P_s}{2W} \tag{3.19}$$

If we use N_0 to represent the two-sided noise power density, the noise power is $2WN_0$ and its energy over the T-second interval is $2N_0WT$. Then the energy per sample of noise signal at the pre-filter output is

$$\frac{2N_0WT}{2WT} = \frac{2N_0W}{2W} = N_0 \tag{3.20}$$

In a sensing duration of T seconds, there will be $2WT$ samples. If there is only a noise signal $n(t)$ present, we can express the energy of the received signal during sensing time T as

$$V = \int_0^T n^2(t)dt = \frac{1}{2W}\sum_{i=1}^{2TW} n_i^2 \tag{3.21}$$

where

$$n_i = n\left(\frac{i}{2W}\right) \tag{3.22}$$

is a Gaussian random variable with zero mean and variance

$$\sigma_i^2 = 2WN_0 \tag{3.23}$$

However, recalling the definition of the chi-square distribution, we know that the chi-squared PDF arises as the PDF of x where [26]

$$x = \sum_{i=1}^{N} x_i^2 \qquad \text{if } x_i \sim N(0,1) \tag{3.24}$$

and the x_i are independent and identically distributed. In the following discussion, we will use the chi-squared PDF to describe the noise signal samples. From (3.24) we find that the variance of n_i must be normalized to 1. Thus, we normalize the random variable n_i as

$$b_i = \frac{n_i}{\sqrt{2WN_0}} \tag{3.25}$$

Moreover, we use $V^{'}$ which is monotonic with V to represent the test statistic as

$$V^{'} = \frac{1}{N_0}V = \frac{1}{N_0}\int_0^T n^2(t)dt \tag{3.26}$$

If there is only noise present we finally have

$$V^{'} = \frac{1}{N_0}\int_0^T n^2(t)dt = \frac{1}{2WN_0}\sum_{i=1}^{2TW} n_i^2 = \sum_{i=1}^{2TW} b_i^2 \tag{3.27}$$

which can be written in the simple form

$$V^{'} = \sum_{i=1}^{2TW} b_i^2 \tag{3.28}$$

We need to investigate the distribution of the test statistic $V^{'}$. Under H_0, $V^{'}$ can be viewed as the sum of the squares of N standard Gaussian variants with zero mean and unit variance. Therefore, $V^{'}$ is said to have a chi-square distribution with N degrees of freedom. N equals approximately $2TW$ which represents the number of samples within each observation period.

The simulation model in this thesis is based on a complex baseband model. By using this model, we can focus on the slowly varying parts of the signal and make the treatment independent of the carrier frequency. From (3.3) and (3.6) we know that the received complex baseband signal at a CR, assuming a signal present, is

$$\widetilde{s(t)} = s_I(t) + j s_Q(t) \tag{3.29}$$

where

$$s_I(t) = \sqrt{\frac{2E_s}{T_s}} \cos\left[(2k-1)\frac{\pi}{4}\right] \qquad k = 0, 1, 2, 3 \tag{3.30}$$

and

$$s_Q(t) = \sqrt{\frac{2E_s}{T_s}} \sin\left[(2k-1)\frac{\pi}{4}\right] \qquad k = 0, 1, 2, 3 \tag{3.31}$$

In this thesis we design sensing schemes to detect the presence of a signal based on energy. Thus, there is no need to distinguish which symbol in the alphabet is transmitted. QPSK is a nominally constant energy modulation, meaning the energy of the waveform $s_i(t)$ for all signals of symbol duration T_s are the same. No matter the value of i, the energy of the complex baseband signal $\widetilde{s(t)}$ in a symbol duration T_s is

$$E_{base} = 2 \times \left\{\sqrt{\frac{E_s}{T_s}}\right\}^2 \times T_s = 2E_s \tag{3.32}$$

From this we also know that the relationship of energy in the same duration, T_s, of transmitted signal $s(t)$ and complex baseband signal $\widetilde{s(t)}$ is

$$E_s = \frac{E_{base}}{2} \tag{3.33}$$

In this situation, we can also express the energy of the transmitted primary signal under H_1 in the observation interval (0,T) as

$$\int_0^T s^2(t)dt = \frac{1}{2}\int_0^T |\widetilde{s(t)}|^2 dt = \frac{1}{2W}\sum_{i=1}^{2TW} \alpha_i^2 \tag{3.34}$$

where α_i is

$$\alpha_i = \pm\sqrt{\frac{E_s}{T_s}} \tag{3.35}$$

The energy of I and Q channel signals in a given time T is the same.

After the normalization as in (3.25), we obtain the test statistic as

$$V^{'} = \frac{1}{N_0}V = \frac{1}{N_0}\int_0^T s^2(t)dt = \sum_{i=1}^{2TW}\beta_i^2 \tag{3.36}$$

where

$$\beta_i = \frac{\alpha_i}{\sqrt{2WN_0}} \tag{3.37}$$

The energy of the received signal $r(t)$ in the interval (0,T) is

$$V = \int_0^T r^2(t)dt = \frac{1}{2W}\sum_{i=1}^{2TW}(\alpha_i + b_i)^2 \tag{3.38}$$

and the test statistic $V^{'}$ is then given by the normalized value

$$V^{'} = \frac{1}{N_0}\int_0^T r^2(t)dt = \sum_{i=1}^{2TW}(\beta_i + b_i)^2 \tag{3.39}$$

where β_i is the normalized primary signal energy and b_i is the normalized noise signal.

We note that the noncentral chi-squared PDF with N degrees of freedom and non-centrality parameter $\gamma = \sum_{i=1}^{N}\mu_i^2$ arises as the PDF of x where we have the random variable

$$x = \sum_{i=1}^{N} x_i^2 \qquad \text{if } x_i \sim N(\mu_i, 1) \tag{3.40}$$

Therefore, when signal is present, $V^{'}$ can be seen to have a noncentral chi-square distribution with N degrees of freedom and a non-centrality parameter γ. From (3.39), we find that the non-central parameter is given by

$$\gamma = \sum_{i=1}^{2TW}\beta_i^2 = \frac{1}{N_0}\int_0^T s^2(t)dt = \frac{E_T}{N_0} \tag{3.41}$$

where E_T is used to represent the signal energy in the sensing interval of duration T. The

non-central parameter γ is defined as the received SNR.

Finally, we may represent the test statistic being drawn from a chi square distribution as

$$V' = \begin{cases} \chi^2_N & H_0 \\ \chi^2_N(\gamma) & H_1 \end{cases} \tag{3.42}$$

where $N = 2TW$ is the number of degrees of freedom. χ^2_N represents the chi-square distribution with N degrees of freedom. $\chi^2_N(\gamma)$ represents the noncentral chi-square distribution with N degrees of freedom and noncentrality γ. The first arises when there is no signal present and the second when a signal is present.

3.4.2 Threshold Derivation

In practice, P_{FA} as defined in (3.14) only depends on the noise variance and N, thus the threshold can be set regardless of the primary user signal level and the effect of fading or shadowing. We will select the threshold to obtain a fixed P_{FA} and then calculate the resulting probability of detection P_D.

Other researchers often approximate the PDF of V' using a Gaussian distribution if N is sufficiently large ($N > 250$) [14]. The threshold λ in a closed form is then given by [14]

$$\lambda = \sigma_n^2(Q^{-1}(P_{FA})\sqrt{2N} + N) \tag{3.43}$$

However, N usually is much smaller than 250 and, therefore this assumption can't be satisfied. We need then to derive the threshold in an alternative way.

The PDF of V' [26] under the two hypotheses is

$$H_0: \quad f_{V'}(x|H_0) = \frac{1}{2^{\frac{N}{2}}\Gamma(\frac{N}{2})} x^{\frac{N}{2}-1} \exp\left(-\frac{1}{2}x\right) \tag{3.44}$$

$$H_1: \quad f_{V'}(x|H_1) = \frac{1}{2}\left(\frac{x}{\gamma}\right)^{\frac{N-2}{4}} \exp\left(-\frac{1}{2}(x+\gamma) I_{\frac{N}{2}-1}(\sqrt{\gamma x})\right) \tag{3.45}$$

where $\Gamma(x)$ is the gamma function, $I(x)$ is a modified Bessel function of the first kind and x is the sample of the received signal.

We may then find the probability of false alarm P_{FA} as

$$P_{FA} = Q_{\chi_N^2}(\lambda) = \int_{\lambda}^{\infty} f_{V'}(x|H_0)dx \tag{3.46}$$

The function $Q_{\chi_N^2}(\lambda)$ can be found from the following equations [26]

$$Q_{\chi_N^2}(\lambda) = \begin{cases} 2Q(\lambda) & \text{if } N = 1 \\ 2Q(\lambda) + \frac{\exp(-\frac{1}{2}\lambda)}{\sqrt{\pi}} \sum_{k=1}^{\frac{N-1}{2}} \frac{(k-1)!(2\lambda)^{k-\frac{1}{2}}}{(2k-1)!} & \text{if } N > 1 \text{ and } N \text{ odd} \\ \exp(-\frac{1}{2}\lambda) \sum_{k=0}^{\frac{N}{2}-1} \frac{(\frac{\lambda}{2})^k}{k!} & \text{if } N \text{ is even} \end{cases} \tag{3.47}$$

We can evaluate the threshold λ using (3.46) and (3.47) for a specified P_{FA} and N. Note that $Q(x)$ is the Gaussian Q function

$$Q(x) = \frac{1}{2\pi\sigma^2} \int_{x}^{\infty} \exp^{\frac{-x^2}{2\sigma^2}} dx \tag{3.48}$$

3.5 ENERGY DETECTOR IN FADING CHANNELS

In this section, we investigate the performance degradation of an energy detector in both a Rayleigh fading channel and a log-normal shadowing channel.

We first set the threshold to meet the specified P_{FA}. P_{FA} is considered for the case of no signal transmission and as such is independent of SNR. The threshold in a fading environment is initially assumed to be the same as in an AWGN channel.

Then, we apply the threshold to the data when the signal is present and compute the average probability of correct detection $\overline{P_D}$. We use average probability of correct detection $\overline{P_D}$ to evaluate system performance because the level of the received signal is no longer a fixed value in a fading environment. It is a random variable. Thus, the P_D for each individual experiment is quite different and we need to have a sufficient number of experiments and take the mean value of the P_D to estimate $\overline{P_D}$. It can also be represented as

$$\overline{P_D} = \int_{x} P_D(\gamma, \lambda) f_{\gamma}(x)dx \tag{3.49}$$

where $f_{\gamma}(x)$ is the PDF of the SNR under fading.

The performance of an energy detector in a fading channel in this thesis is based on

measurement. We apply the Rayleigh fading channel and log-normal channel models in the simulation and then evaluate the overall $\overline{P_D}$. From section 3.4, we know that the performance is related to the received SNR which is often given by (3.41) in the AWGN channel. However, in a fading environment, we must use the average SNR to evaluate the performance. The simulation results will be shown in chapter 4.

3.6 SEQUENTIAL DETECTOR

As we indicated in chapter 2, there are primarily two purposes for proposing a new detector. The first one is to achieve better performance (higher P_D) and the second one is to reduce the sensing time. We also know that a CR must detect the presence of a primary signal in the following two situations [94].

The first is that of sounding the channel before data transmission to decide whether the channel is available. The sensing time should be minimized because while the CR is sensing it can not transmit anything. A long sensing time leads to a decrease in system throughput.

The second is that of sensing the channel periodically during data transmission to identify whether the primary signal is returning. In this situation, the sensing time should also be minimized because the CR must detect the returning primary user rapidly and then abandon the channel. Otherwise, it will interfere with the primary user.

From the above, we see that a relatively short sensing time is needed in both situations. Thus, the proposed sequential detector in this thesis is primarily aimed at reducing sensing time.

The detector proposed here is based on the sequential probability ratio test of Wald [27]. It can reduce the average sensing time significantly. In a fixed block energy detection system, one of two possible decisions is made after a fixed number of samples N. However, in a sequential system, the number of samples needed to make a decision is no longer a fixed value. It is a random variable because a sequential detector stops testing whenever the received sample provides sufficient information to accept or reject a hypothesis at a given performance level.

3.6.1 Sequential Testing and Threshold Derivation

Following the work of [27], let us suppose r_n is a sample at time n and $R_n = [r_1, r_2 \dots r_n]^T$ is the vector of samples up to time n. The likelihood ratio for the nth sample is given by

$$\Lambda(r_n) = \frac{p(r_n|H_1)}{p(r_n|H_0)} \tag{3.50}$$

and for R_n may be written as

$$\begin{aligned} \Lambda(R_n) &= \frac{p(R_n|H_1)}{p(R_n|H_0)} \\ &= \prod_{k=1}^{n} \frac{p(r_k|H_1)}{p(r_k|H_0)} \\ &= \frac{p(r_n|H_1)}{p(r_n|H_0)} \prod_{k=1}^{n-1} \frac{p(r_k|H_1)}{p(r_k|H_0)} \\ &= \Lambda(r_n)\Lambda(R_{n-1}) \end{aligned} \tag{3.51}$$

if we assume each sample is independent.

The sequential test is defined as follows: On the basis of each sample, the likelihood ratio $\Lambda(R_n)$ is computed and compared with two thresholds A and B. If $\Lambda(R_n) > A$, hypothesis H_1 is accepted, and the test is terminated. If $\Lambda(R_n) < B$, hypothesis H_0 is accepted, and the test is terminated. If $B < \Lambda(R_n) < A$, neither hypothesis is acceptable; an additional sample is taken and the procedure repeats.

We now need to specify the values of the thresholds A and B. Suppose we perform a sequential test, and after observing the nth sample, we compute the likelihood ratio

$$\Lambda(R_n) = \frac{p(R_n|H_1)}{p(R_n|H_0)} = A \tag{3.52}$$

where A is the threshold which leads us to the decision "accept H_1". We then have

$$p(R_n|H_1) = Ap(R_n|H_0) \tag{3.53}$$

This equation is equivalent to

$$\int_{\Gamma_1} p(R_n|H_1)dR_n = A \int_{\Gamma_1} p(R_n|H_0)dR_n \tag{3.54}$$

where both integrations are over a region Γ_1 consisting of all values or samples that lead to the acceptance of H_1. We also know that

$$\int_{\Gamma_1} p(R_n|H_1)dR_n = P_D \tag{3.55}$$

$$\int_{\Gamma_1} p(R_n|H_0)dR_n = P_{FA} \tag{3.56}$$

Finally, we have

$$A = P_D/P_{FA} \tag{3.57}$$

We use an analogous method to find the value of B and we conclude that the termination of the sequential test with the acceptance of hypothesis H_0 leads to

$$p(R_n|H_1) = Bp(R_n|H_0) \tag{3.58}$$

The above equation is equivalent to

$$\int_{\Gamma_0} p(R_n|H_1)dR_n = B\int_{\Gamma_0} p(R_n|H_0)dR_n \tag{3.59}$$

where both integrations are over region Γ_0 consisting of all values or samples that lead to the acceptance of H_0. We also know that

$$\int_{\Gamma_0} p(R_n|H_1)dR_n = P_M \tag{3.60}$$

$$\int_{\Gamma_0} p(R_n|H_0)dR_n = 1 - P_{FA} \tag{3.61}$$

Finally, we have from (3.59) that

$$B = P_M/(1 - P_{FA}) \tag{3.62}$$

From above derivation, we find that the thresholds A and B are related to P_M and P_{FA}. In the sequential test, thresholds A and B are preset values determined before testing begins. This also means that the P_M and P_{FA} are also preset values.

3.6.2 Average Number of Samples

Since A, B and $\Lambda(R_n)$ are nonnegative quantities, a convenient monotonic function for this application is the logarithm. For convenience in the following, we first define the following variables

$$L(r_n) = \log \Lambda(r_n) = \log \frac{p(r_n|H_1)}{p(r_n|H_0)} \tag{3.63}$$

$$L(R_n) = \log \Lambda(R_n) = \log \frac{p(r_1, \ldots, r_n|H_1)}{p(r_1, \ldots, r_n|H_0)} \tag{3.64}$$

where $L(r_n)$ represents the log likelihood ratio of the nth samples while $L(R_n)$ represents the joint log likelihood ratio of n samples.

The average number of samples required is often used to evaluate the performance of a sequential detector because the required number of samples is a random variable. Let the random variable n represent the number of samples required to terminate the sequential test. This implies that at the $(n-1)th$ stage, $\log B < L(R_{n-1}) < \log A$; but at the nth stage, either $L(R_n) \leq \log B$ or $L(R_n) \geq \log A$.

We ignore the excess over the boundary $\log A$ and $\log B$ [27], if any, and the random variable $L(R_n)$ can then take one of two values $\log A$ or $\log B$ and the four possible combinations of terminations and hypothesis are

$$L(R_n) = \begin{cases} P_{FA} \log A & \text{when } H_0 \text{ is true} \\ P_D \log A & \text{when } H_1 \text{ is true} \\ (1 - P_{FA}) \log B & \text{when } H_0 \text{ is true} \\ P_M \log B & \text{when } H_1 \text{ is true} \end{cases}$$

We can find the conditional expectation of the random variable $L(R_n)$ as

$$\overline{L(R_n)} = \begin{cases} P_{FA} \log A + (1 - P_{FA}) \log B & \text{when } H_0 \text{ is true} \\ P_D \log A + P_M \log B & \text{when } H_1 \text{ is true} \end{cases} \tag{3.65}$$

We also know that

$$L(r_n) = \log \left[\frac{p(r_n|H_1)}{p(r_n|H_0)} \right] \tag{3.66}$$

Suppose that N samples $r_1, \ldots, r_N$ are taken and that N is set large enough that n never exceeds N which means that the test always terminates before the Nth observation. We then have

$$\begin{aligned}\sum_{n=1}^{N} L(r_n) &= (L(r_1) + L(r_2) + \ldots + L(r_n)) + (L(r_{n+1}) + \ldots + L(r_N)) \\ &= L(R_n) + (L(r_{n+1}) + L(r_{n+2}) + \ldots + L(r_N)) \end{aligned} \tag{3.67}$$

The N samples $r_1, \ldots, r_N$ can be viewed as samples of a random variable r. If we take the expectation of both sides of (3.67) with respect to r, we obtain

$$N\overline{L(r_n)} = \overline{L(R_n)} + \overline{(N-n)L(r_n)} = \overline{L(R_n)} + (N - \bar{n})\overline{L(r_n)} \tag{3.68}$$

By simplifying (3.68), the average number of samples $\bar{n}$ required is then given by

$$\bar{n} = \overline{L(R_n)}/\overline{L(r_n)} \tag{3.69}$$

If we use $\bar{n}(H_i)$ to represent the expectation of n given that hypothesis H_i is true and use $\overline{L(H_i)}$ to represent the expectation of $L(r_n)$ given that hypothesis H_i is true, we finally have under the two hypotheses

$$\bar{n}(H_0) = \frac{P_{FA}\log A + (1 - P_{FA})\log B}{\overline{L(H_0)}} \tag{3.70}$$

$$\bar{n}(H_1) = \frac{P_D \log A + P_M \log B}{\overline{L(H_1)}} \tag{3.71}$$

We also need to work out the term $\overline{L(H_0)}$ and $\overline{L(H_1)}$ in (3.70) and (3.71). If we assume that there is no signal present, the term $\overline{L(H_0)}$ is then obtained by

$$\sum_{n=1}^{N} L(r_n) = N\overline{L(H_0)} \tag{3.72}$$

and

$$\overline{L(H_0)} = \frac{\sum_{n=1}^{N} L(r_n)}{N} \tag{3.73}$$

It means that we add up the log likelihood ratio of N samples and then divide by N to obtain $\overline{L(H_0)}$. The term $\overline{L(H_1)}$ can be obtained in the same way if we assume that there is a signal.

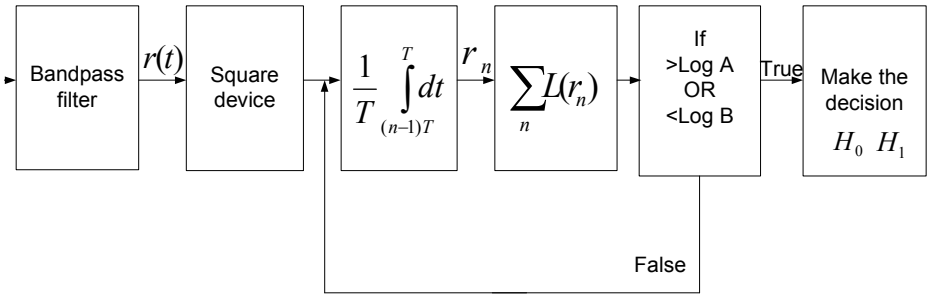

Figure 3.6 Block diagram of sequential detector.

The conditional average percentage saving of the sequential test compared to the fixed number sample system is given by

$$PS_i = (1 - \frac{\bar{n}(H_i)}{N_{fss}}) \times 100\% \qquad i = 0, 1 \tag{3.74}$$

where N_{fss} represents the number of required samples for a fixed sample size detection system at the same performance level.

3.6.3 Structure of Proposed Sequential Detector

The overall structure of the proposed sequential detector is shown in Fig. 3.6. It is an energy based sequential detector. The first and second blocks in Fig. 3.6 are the same as the previous block-based energy detector shown in Fig. 3.5. The following integrator generates a sample r_n every T seconds. Then we calculate likelihood ratios based on r_n.

From (3.42) we know that the PDF of the samples R_n is a chi-square distribution when there is no signal. The PDF of the samples R_n is a noncentral chi-square distribution when there is a signal present. This can be summarized as

$$\begin{aligned} H_0: \quad & R_n \sim \chi^2_N \\ H_1: \quad & R_n \sim \chi^2_N(\gamma) \end{aligned} \tag{3.75}$$

The PDFs of the chi-square and noncentral chi-square distribution as defined in (3.44) and (3.45), are complicated. Thus, calculating the likelihood ratio using them is difficult. In order to reduce system computing complexity, we first need to simplify (3.44)and (3.45). From [26] we know that (3.44) can be significantly simplified when the number of degrees of freedom N is 2, as this implies that

$$N = 2TW = 2 \Longrightarrow T = \frac{1}{W} \tag{3.76}$$

Thus, we choose $\frac{1}{W}$ as the sampling interval and the log likelihood ratio of the nth sample r_n is then given by

$$\begin{aligned} L(r_n) &= \log \frac{p(r_n|H_1)}{p(r_n|H_0)} \\ &= \log \frac{\frac{1}{2}\exp(-\frac{r_n+\gamma}{2})I_0(\sqrt{\gamma r_n})}{\frac{1}{2}\exp(-\frac{r_n}{2})} \\ &= \log \left(\exp\left(-\frac{\gamma}{2}\right) I_0(\sqrt{\gamma r_n})\right) \end{aligned} \tag{3.77}$$

where I_0 is the zero order modified Bessel function of the first kind and γ is the received SNR under H_1.

For the independent sample r_n, $L(r_n)$ is then compared with the two thresholds, $\log A$ and $\log B$, to make a decision. If it can not make a decision, a new sample r_{n+1} is taken and the value of $L(r_n) + L(r_{n+1})$ is compared with the two thresholds. This procedure repeats until a decision can be made.

However, in order to achieve further simplification, we know that a zero-th order modified Bessel function of first kind can be approximately replaced by an exponential

function when the term $\sqrt{\gamma r_n}$ is large [93]. Then (3.77) may be rewritten as

$$\begin{aligned} L(r_n) &\cong \log \frac{\frac{1}{2}\exp(-\frac{r_n+\gamma}{2})\exp(\sqrt{\gamma r_n})}{\frac{1}{2}\exp(-\frac{r_n}{2})} \\ &\cong \log\left(\exp\left(-\frac{\gamma}{2}+\sqrt{\gamma r_n}\right)\right) \end{aligned} \tag{3.78}$$

If we assume that the sequential test terminates at the Nth stage, then the log likelihood ratio is

$$\begin{aligned} \log\Lambda(R_n) &= \log\left(\exp\left(-\frac{\gamma}{2}\right)\exp(\sqrt{\gamma r_1})\right)+\log\left(\exp\left(-\frac{\gamma}{2}\right)\exp(\sqrt{\gamma r_2})\right) \\ &\quad +\ldots+\log\left(\exp\left(-\frac{\gamma}{2}\right)\exp(\sqrt{\gamma r_N})\right) \end{aligned} \tag{3.79}$$

After some simplification, we then have

$$\log\Lambda(R_n) = \left(-\frac{\gamma}{2}\right)N+\sqrt{\gamma r_1}+\sqrt{\gamma r_2}+\ldots+\sqrt{\gamma r_N} \tag{3.80}$$

If we compare the equation with the two thresholds $\log A$ and $\log B$, we have

$$\sqrt{\gamma r_1}+\sqrt{\gamma r_2}+\ldots+\sqrt{\gamma r_N} > \log A+(-\frac{\gamma}{2})N \qquad \text{accept } H_1 \tag{3.81}$$

$$\sqrt{\gamma r_1}+\sqrt{\gamma r_2}+\ldots+\sqrt{\gamma r_N} < \log B+(-\frac{\gamma}{2})N \qquad \text{accept } H_0 \tag{3.82}$$

We finally obtain a simple form of (3.77) as

$$\sum_{n=1}^{N} y_n \geq \frac{\log A+\frac{\gamma}{2}N}{\sqrt{\gamma}} \qquad \text{accept } H_1 \tag{3.83}$$

$$\sum_{n=1}^{N} y_n \leq \frac{\log B+\frac{\gamma}{2}N}{\sqrt{\gamma}} \qquad \text{accept } H_0 \tag{3.84}$$

else take one more sample

where $y_n = \sqrt{r_n}$.

The simulation results for the proposed sequential detector are shown in chapter 4.

From the simulation results we will see that the proposed sequential detector requires less average sensing time than the traditional energy detector for the same performance.

3.6.4 Truncated Sequential Test

The sequential test leads to the average number of samples per test being smaller than that required by the fixed sample system for the same level of performance [36]. However, an individual test may require an extremely large number of samples before termination. We want the sensing time of the proposed detector to always be shorter than that of the block energy detector for a given pair of P_D and P_{FA}. Furthermore, the primary user signal must be sensed periodically within some predetermined time interval. This interval is determined by the primary user system QoS tolerances. For example, each DTV channel must be sensed every 2 seconds [90] which means that the CR must make a decision within 2 seconds. Thus, it is sometimes necessary to interrupt the procedure before the test reaches a natural termination. This resulting of test is known as a truncated sequential test.

The procedure for a truncated sequential test is quite similar to that of the sequential test. We first carry out the sequential test until either hypotheses H_1 or H_0 is accepted, or the preset stage N_s is reached. The test terminates even when neither of the hypotheses has been accepted at the $N_s th$ stage.

A simple rule for the acceptance or rejection of hypotheses H_i at the preset stage N_s is [27]

$$\text{if} \quad \sum_{n=1}^{N_s} L(r_n) \leq 0 \qquad \text{accept } H_0 \tag{3.85}$$

$$\text{if} \quad \sum_{n=1}^{N_s} L(r_n) > 0 \qquad \text{accept } H_1 \tag{3.86}$$

which means that the new threshold is 0 if we take the logarithm of the sample r_n. It is not related to the threshold A and B anymore.

We substitute (3.78) into (3.85) and then we have

$$\text{if} \quad \sum_{n=1}^{N_s} \log\left(\exp\left(-\frac{\gamma}{2}+\sqrt{\gamma r_n}\right)\right) \leq 0 \qquad \text{we accept } H_0 \tag{3.87}$$

$$\text{if} \quad \sum_{n=1}^{N_s} \log\left(\exp\left(-\frac{\gamma}{2}+\sqrt{\gamma r_n}\right)\right) > 0 \qquad \text{we accept } H_1 \tag{3.88}$$

Finally, we have

$$\sum_{n=1}^{N_s} y_n \geq \frac{N_s\sqrt{\gamma}}{2} \qquad \text{accept } H_0 \tag{3.89}$$

$$\sum_{n=1}^{N_s} y_n > \frac{N_s\sqrt{\gamma}}{2} \qquad \text{accept } H_1 \tag{3.90}$$

where $y_n = \sqrt{r_n}$.

This truncated procedure guarantees that the required number of samples will never exceed N_s. However, the resulting P_{MD} and P_{FA} of the truncated sequential test is greater than for the standard sequential test. The degradation of performance will be evaluated in the next chapter using simulation.

3.7 COOPERATIVE SENSING

The above proposed detector is for individual sensing which means the CR detects the transmitted primary signals using only local observations. However, a CR may not detect the primary transmitter owing to the effect of shadowing which is often called the "hidden terminal" problem [47].

An approach to combatting this problem and increasing the spectral estimation reliability is cooperative spectrum sensing. In cooperative spectrum sensing, the spectrum occupancy is detected by the joint work of several CRs, as opposed to being determined by an individual CR.

3.7.1 Motivation for Proposed Cooperative Sensing Scheme

Based on the literature review in chapter 2, we can summarize the objective of cooperative sensing as "achieving high performance within a short sensing time". However, there is

always a tradeoff between performance and sensing time. Although some schemes can achieve high performance with a relatively small sensing time, the computational complexity of these schemes is high.

The proposed scheme in this thesis is mainly focused on how to reduce sensing time for a given level of performance. Sensing time should be minimized because the CR system can't communicate during this time. In addition to reducing sensing time, we also consider performance and system complexity. In summary, the objective of the scheme is to achieve reasonable performance quickly using a simple system structure.

In a wireless communication system, the channel conditions are often determined by multipath fading and shadowing. These effects all lead to some degradation of detector performance which leads to long sensing times and poor performance. Fortunately, these effects differ at different locations and times. Thus, it is reasonable to assume that not all CRs are in the worst channel conditions simultaneously. We can then take advantage of this assumption.

3.7.2 Selection Combining Rule

Previous researchers [63], [66] [68], [86], [73], [79] often assume that the individual sensing results are combined at a fusion center from each sensor simultaneously because a fixed sample system is applied. Then the fusion center makes the final decision based on these results. However, if sequential testing is applied at each individual sensor, the sensing time of each individual sensor is a random variable. Individual decisions will then be received at a fusion center at different times.

In order to model the hidden terminal problem in the preset system, only shadowing is considered. Fig. 3.7 illustrates a cooperative scheme using the sequential test and selection combining rule in a shadowing environment. We first assume that the noise power at each sensor is the same. The received signal energy is different for various sensors due to shadowing and, therefore, the sensing time of each individual sensor would also be different. We also assume that the sensing time of sensor 1 in Fig. 3.7 is the shortest and it transmits its individual decision to the fusion center immediately .

The fusion center does not wait for all the individual results to be collected. It starts testing when the first individual result (sensor 1's decision) is received, and then makes a final decision based on it. Thus, the required sensing time is shorter than the traditional

one which waits for all the individual results. The flowchart of the proposed cooperative scheme is shown in Fig. 3.8.

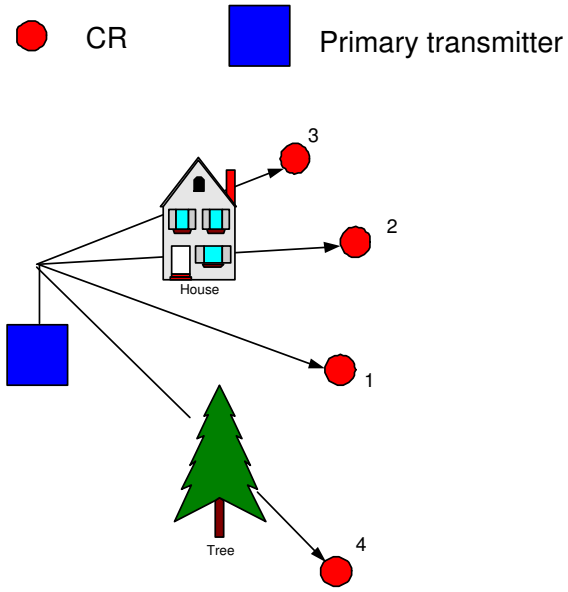

Figure 3.7 Cooperative sensing in shadowing environment.

We can also express this scheme in a mathematical way. The path between transmitter and receiver is often characterized by rapid Rayleigh fluctuations about a slowly varying mean signal strength so that the received signal is given by [91]

$$r(t) = l(t)f(t)s(t) + n(t) \tag{3.91}$$

where $s(t)$ is the transmitted signal, $f(t)$ is the signal fluctuation due to Rayleigh fading, $l(t)$ is caused by the shadowing and $n(t)$ is noise.

In order to model the "hidden terminal" problem, we ignore the effect of Rayleigh fading and then we obtain

$$r(t) = l(t)s(t) + n(t) \tag{3.92}$$

where $l(t)$ is characterized by a log-normal distribution. We can denote the received signal of each of k sensors at time i as

$$r_{i,k} = l_{i,k}s_{i,k} + n_k \tag{3.93}$$

It is also assumed that the noise power n_k at each sensor is the same. However, the received signal power is different for various sensors due to the shadowing $l_{i,k}$. In

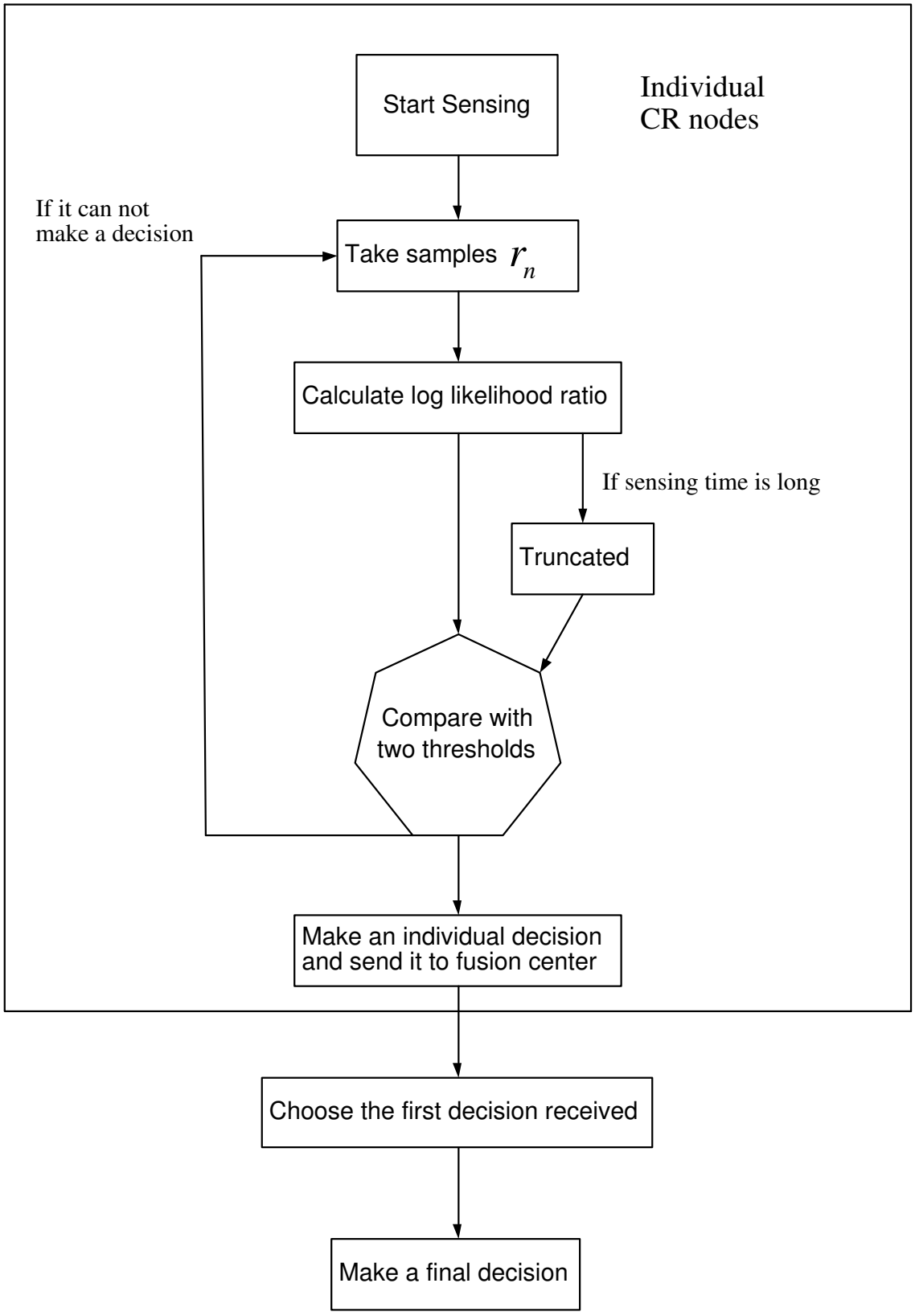

Figure 3.8 Flowchart of the proposed cooperative sensing scheme.

this situation, the sensing time t_k of each individual sensor is also different. The fusion center makes the final decision based on the first incoming individual sensing result and the overall sensing time is represented as

$$t_{overall} = min\{t_k\} \tag{3.94}$$

In conclusion, in order to make the final decision quickly, we ignore the individual results from the sensors which have a relatively long sensing time.

3.7.2.1 Soft Versus Hard Decision Combining

There are two different kinds of combining approaches in a cooperative scheme. The first kind is called soft decision combining. By using this combining approach, each individual sensor forwards some parameters to the fusion center directly. These parameters can be received signal energy, likelihood ratio and so on. The fusion center makes the final decision based on these parameters. The individual sensor does not make any local decision. It only collects parameters and forwards them to the fusion center.

The second one is called hard decision combining. By using this combining approach, each individual sensor makes its own decision and forwards it to the fusion center. The fusion center makes a final decision based on these local decisions. However, the overall performance of hard decision is often worse than that of soft decision combining [63]. For a given P_{FA}, the overall P_D can be improved up to 40% if soft decision combining is applied.

Hard decision combining is applied in my scheme. Let us use u_k to represent the individual decision of the kth sensor as

$$\begin{aligned} u_k &= +1 \quad \text{if } H_1 \text{ is declared} \\ u_k &= -1 \quad \text{if } H_0 \text{ is declared} \end{aligned} \tag{3.95}$$

which means that the kth individual sensor sends a "1" to the fusion center when H_1 is declared,"-1" when H_0 is declared. The fusion center makes the final decision based on one of the k individual results according to selection combining rules.

There are two reasons for applying hard decision combining. The first is that the hard decision combining rule is a low complexity rule which is easy to implement. The second

reason is that forwarding parameters requires more bandwidth than only forwarding local decisions. Forwarding parameters may overload the entire network.

3.7.2.2 Comparison of the New Scheme and Traditional Scheme

The traditional scheme can be viewed as a democratic scheme. Each sensor transmits its decision to the fusion center and the fusion center makes a final decision based on these results. The "AND", "OR" or majority rule is applied in the fusion center.

In contrast, the new scheme is a dictatorial scheme. The fusion center makes a final decision based only on the result from the quickest individual sensor. It ignores the results from the remaining sensors and, therefore, the overall sensing time can be minimized.

The performance of this selection combining rule is based on measurement and it will be presented in the next chapter. From that, we can find out the cost of the new selection combining rule.

3.8 SUMMARY

This chapter has provided detailed information on the proposed detectors and cooperative sensing schemes based on it. It argues that the proposed sequential and truncated sequential detectors can save sensing time compared to an energy detector. Based on research on existing cooperative sensing in CR systems, we developed a cooperative scheme to reduce sensing time with simple computational complexity. Simulation results for the proposed detectors and cooperative sensing scheme will be presented in the next chapter.

Chapter 4

SIMULATION RESULTS

4.1 INTRODUCTION

In this chapter, computer simulation results for the detectors and cooperative scheme proposed in chapter 3 are presented. There are two main purposes of this chapter. The first one is to investigate how much the sensing time can be reduced using the proposed detectors and the cooperative scheme. The second purpose is to investigate the performance (P_D) of the proposed detectors and the cooperative scheme. The simulation environment is introduced in the first section. Then the simulation results for the proposed detectors are presented. Finally, simulation results for the proposed cooperative scheme are presented. The fixed sample size energy detector is simulated as a reference system.

4.2 SIMULATION ENVIRONMENT

4.2.1 AWGN Channel

The primary signal is assumed here to be a QPSK signal. QPSK is used throughout as an example signalling format so as to consider energy detection of signals having a non-zero bandwidth. Almost any other format could equally well be used. In the AWGN channel, the primary signal is only perturbed at the detector by AWGN. We often use the notation E_s/N_0 to define the ratio of primary signal energy to noise energy [59], [7], [60], [8]. The energy per symbol E_s and the noise power spectral density N_0 are defined as

$$E_s = \frac{P_s}{R} \tag{4.1}$$

$$N_0 = \frac{P_n}{R} \tag{4.2}$$

where P_s is the signal power per symbol, R is the symbol rate and P_n is the average noise power.

If we divide (4.1) by (4.2), we have

$$\begin{aligned} E_s/N_0 &= \frac{P_s}{R} \cdot \frac{R}{P_n} \\ &= \frac{P_s}{P_n} \end{aligned} \tag{4.3}$$

and P_n can be written as

$$P_n = \frac{P_s}{E_s/N_0} \tag{4.4}$$

When E_s/N_0 is in dB, (4.4) can be rewritten as

$$P_n = P_s \cdot \frac{1}{10^{\frac{E_s/N_0}{10}}} \tag{4.5}$$

Since the Gaussian noise is equally distributed in the in-phase and quadrature-phase channels, we finally define the average noise power per dimension as

$$attn = \sqrt{\frac{1}{2} P_n} \tag{4.6}$$

However, as discussed in chapter 3, we also need to define the energy per sample because the proposed detector observes samples not symbols.

Suppose the sensing time is T, then the energy per sample, assuming Nyquist rate sampling, is

$$\frac{P_s T}{2WT} = \frac{P_s}{2W} \tag{4.7}$$

The noise power is P_n and its energy in the T seconds interval is $P_n T$. Then the energy per sample of the noise signal is

$$\frac{P_n T}{2WT} = \frac{P_n}{2W} \tag{4.8}$$

If we divide (4.7) by (4.8), we have

$$\frac{\frac{P_s}{2W}}{\frac{P_n}{2W}} = \frac{P_s}{P_n} \tag{4.9}$$

which is exactly the same as (4.3).

4.2.2 Fading Channel

When we consider the fading channel, the received signal's amplitude is attenuated by a fading factor α. After passing through a fading channel, the signal is also perturbed by AWGN. Therefore, we define the instantaneous signal to noise ratio per symbol as [59] [8]

$$\gamma = \frac{\alpha^2 E_s}{N_0} \tag{4.10}$$

The average SNR per symbol is then

$$\bar{\gamma} = \frac{\overline{\alpha^2} E_s}{N_0} \tag{4.11}$$

where $\overline{\alpha^2}$ is the mean-squared value of α.

There are two different kinds of fading channel considered in this thesis. The first is a non-selective Rayleigh fading channel. In this situation, the fade factor assumed is constant over one symbol period, but may change from symbol to symbol.

The second is a log-normal shadowing channel with a standard deviation of 6dB. The standard deviation of a log-normal shadowing channel is typically between 2dB and 14dB [8].

4.3 SIMULATION PARAMETERS

There are two important system parameters considered in this chapter. The first is the average number of samples $\bar{n}$ required to make a decision. The sensing time of a sequential detector is often evaluated by $\bar{n}$ [27], [36]. The average number of samples required is given by

$$\bar{n} = \frac{\text{sum(number of required samples in each simulation loop)}}{\text{number of simulation loops}} \tag{4.12}$$

In each simulation loop, the primary transmitter transmits a certain number of samples. The number of transmitted samples must be larger than the number of samples to make a decision, otherwise the detector does not have enough samples to make a decision. The number of transmitted samples in each simulation loop does not affect the performance of the detector. The decision interval affects the performance of the detector.

The second parameter is the average percentage saving (PS) of a sequential detector compared to the block based energy detector [36]. The PS can be represented as

$$PS = \left(1 - \frac{\bar{n}}{N_{fss}}\right) \times 100\% \tag{4.13}$$

where N_{fss} represents the required number of samples for the block based energy detector to achieve a given performance level.

4.4 INDIVIDUAL SENSING PERFORMANCE

4.4.1 Energy Detection in Fading Channels

In this subsection, we present the performance of an energy detector in a Rayleigh fading channel and in a log-normal shadowing channel with different average received SNR and decision interval. We consider a primary transmitter using QPSK modulation. The block based energy detector compares the received signal energy over the decision interval with the threshold, and then makes a decision. It was explained in chapter 3 that the threshold of an energy detector in a Rayleigh fading channel is the same as in an AWGN channel. After normalization as presented in chapter 3, we find that the threshold is related to the preset P_{FA} and decision interval [14].

A Rayleigh fading channel can be modeled using Jake's model which is discussed in chapter 1. We are interested in describing the performance of a detector by its complementary receiving operating curves (complementary ROC curves) which plot P_M versus P_{FA} for different values of the parameters of interest [26].

We assume that the primary transmitter transmits 100 samples in each simulation loop for the block based case. 100 samples is an arbitrary choice which is larger than the decision interval. The size of the decision interval is set to 10 samples in Fig. 4.1. In this figure, the energy detector takes the first 10 samples and then makes a decision in each

simulation loop. Once a decision is made, a simulation loop ends and the next simulation loop starts.

Fig. 4.1 illustrates the complementary ROC curves for a Rayleigh fading channel for different average received SNR with a constant decision interval. In practice, P_{FA} and the decision interval are used to set the threshold. For a given average received SNR and decision interval, our purpose is to evaluate the achievable value of P_M. In Fig. 4.1, we see that P_M decreases as P_{FA} increases. This is because the value of P_{FA} affects the threshold. A larger P_{FA} results in a smaller threshold and, therefore, a relatively small P_M can be achieved. One can also notice that for a given P_{FA}, the P_M decreases as the average received SNR increases. The reason is that a primary signal with a larger average received SNR leads to a smaller P_M if the threshold is fixed.

Fig. 4.2 and Fig. 4.3 illustrate the complementary ROC curves for a Rayleigh fading channel for different average received SNRs with two different sizes of decision interval. The decision intervals of Fig. 4.2 and Fig. 4.3 are 6 samples and 20 samples, respectively.

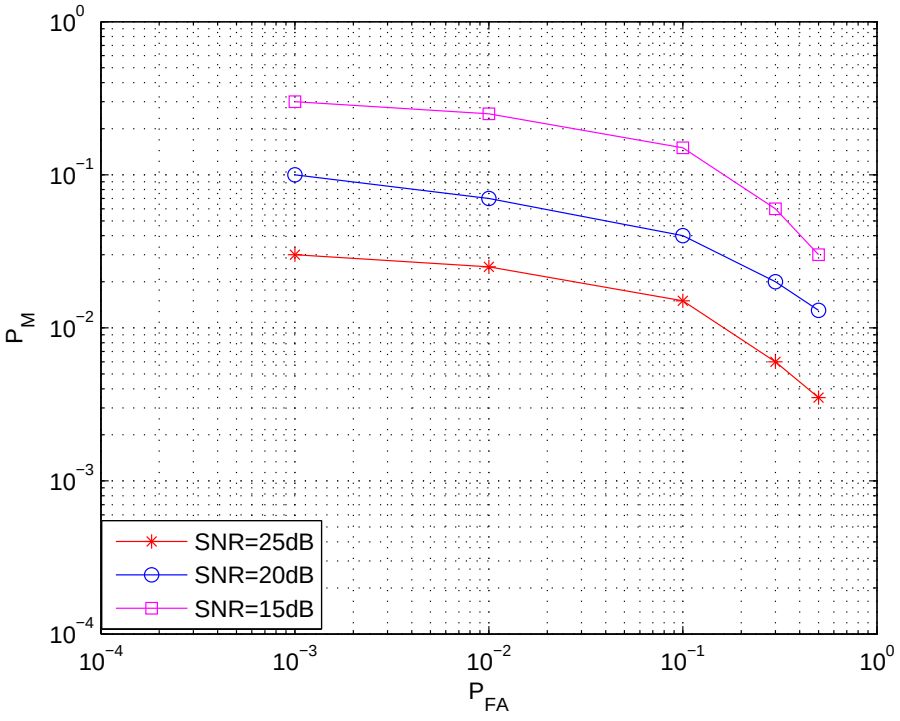

Figure 4.1 Complementary ROC curves for a Rayleigh channel at different average SNR (10 samples per block).

Figs. 4.4, 4.5 and 4.6 illustrate the complementary ROC curves for a log-normal shadowing channel with a standard deviation of 6dB for different average received SNR

and decision interval. The size of the decision intervals in Figs. 4.4, 4.5 and 4.6 are 6, 10 and 20 samples, respectively. From these three figures, we see that P_M decreases as P_{FA} increases and we also notice that for a given P_{FA}, P_M decreases as the average received SNR increases.

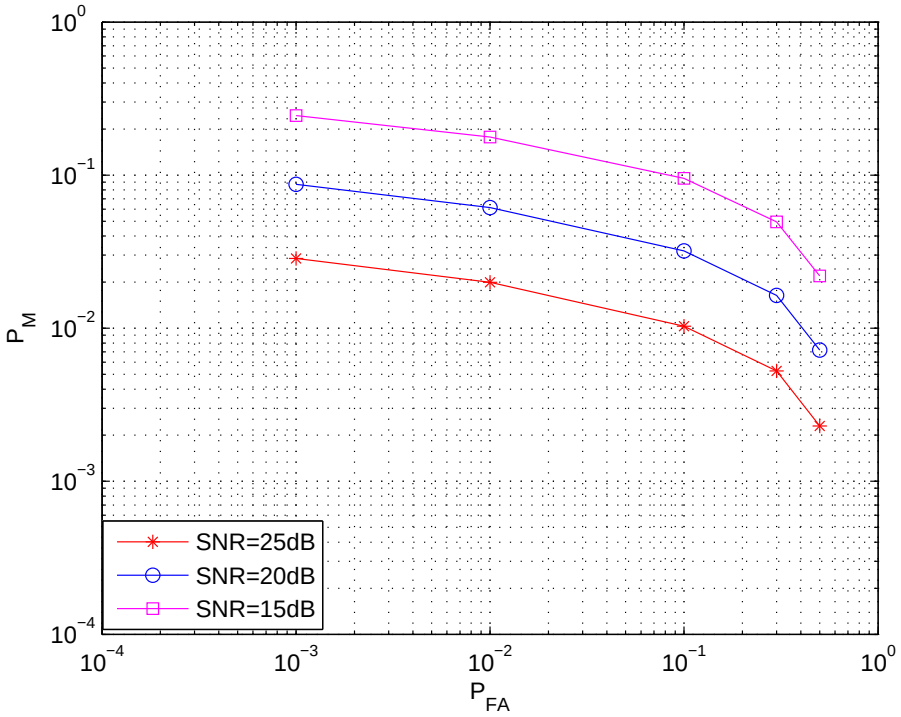

Figure 4.2 Complementary ROC curves for a Rayleigh channel at different average SNR (6 samples per block).

Fig. 4.7 shows the performance of an energy detector over a log-normal shadowing channel for different values of the standard deviation of shadowing. The size of decision interval in Fig. 4.7 is 10 samples and the average received SNR is 10dB. From Fig. 4.7 we can see that P_M increases as the standard deviation (std) of the shadowing increases.

4.4.2 Sequential Detection

In this subsection, we investigate the performance of the proposed sequential detector in terms of the average number of samples required and distribution of the number of required samples. We still consider a primary transmitter using QPSK modulation. The structure of the sequential detector has been presented in chapter 3.

The number of samples required for the sequential detector to make a decision is a random variable and it may take extremely large values. Thus, we initially assume the

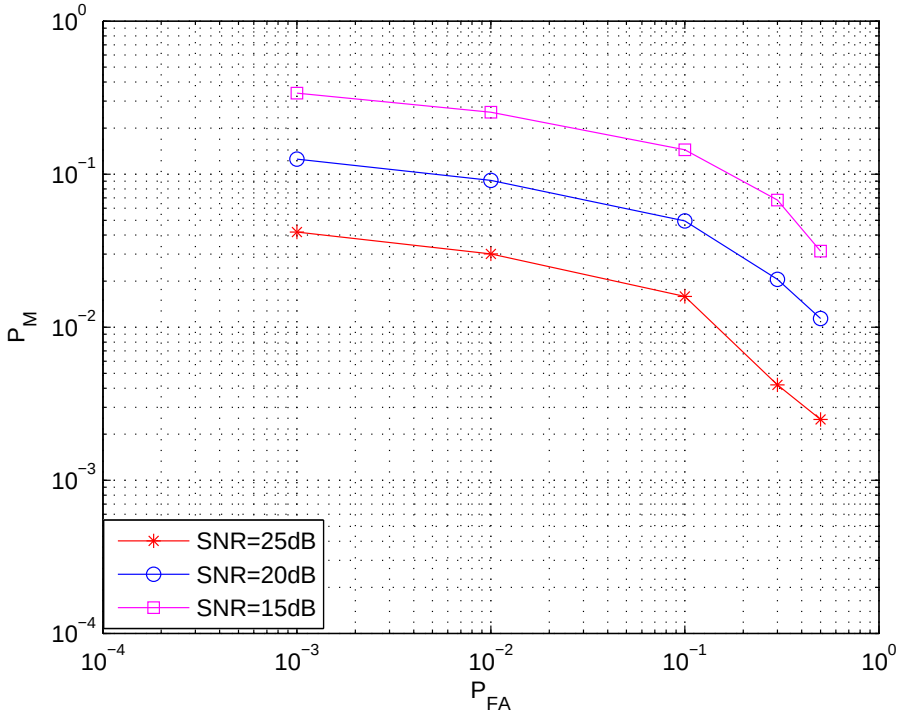

Figure 4.3 Complementary ROC curves for a Rayleigh channel at different average SNR (20 samples per block).

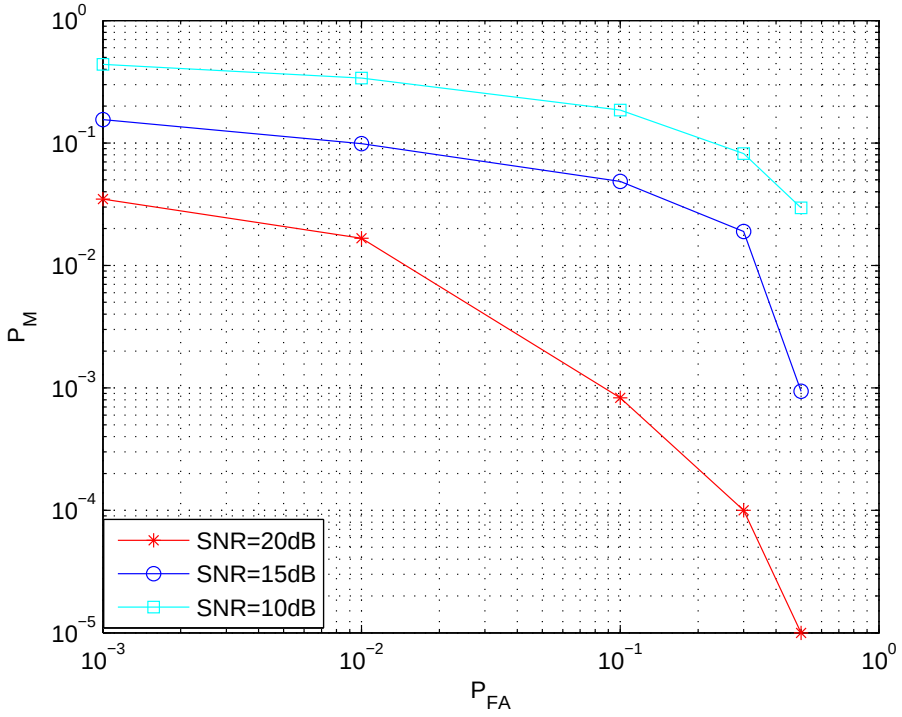

Figure 4.4 Complementary ROC curves for a log-normal shadowing channel at different average SNR (6 samples per block).

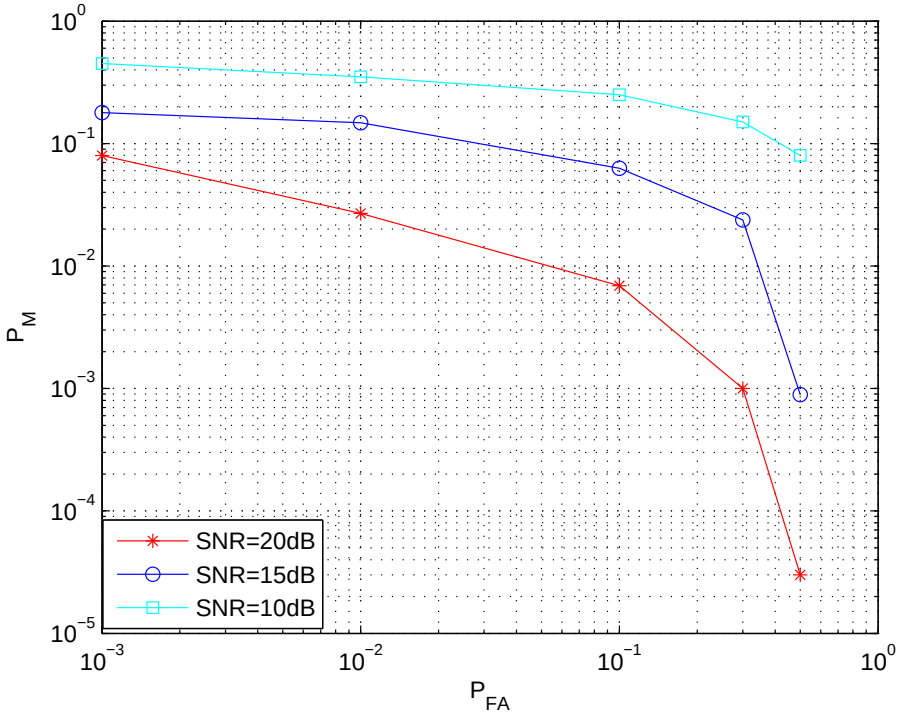

Figure 4.5 Complementary ROC curves for a log-normal shadowing channel at different average SNR (10 samples per block).

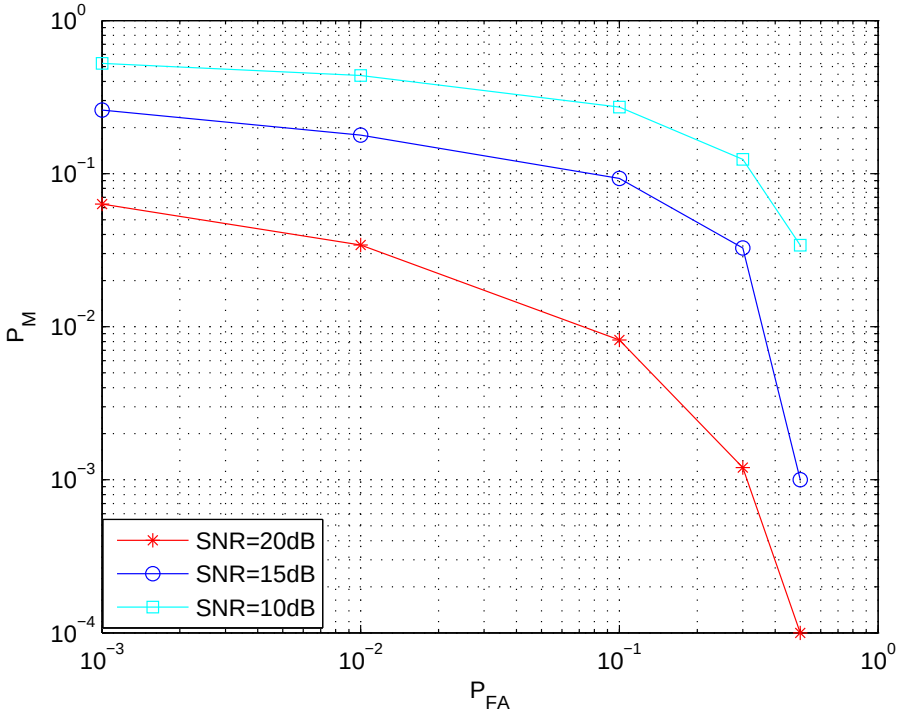

Figure 4.6 Complementary ROC curves for a log-normal shadowing channel at different average SNR (20 samples per block).

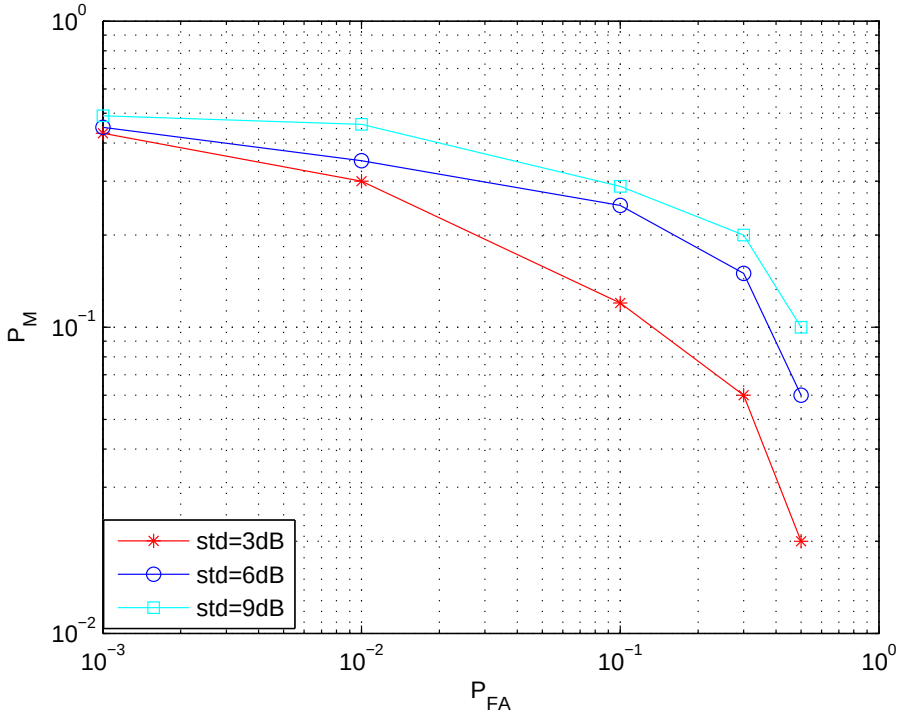

Figure 4.7 Complementary ROC curves for log-normal shadowing channel with different standard deviation values of the shadowing at a received SNR of 10dB (10 samples per block).

primary transmitter transmits 500 samples in each simulation loop for the sequential based case. In each simulation loop, the sequential detector starts at the first received sample and terminates when it makes a decision. The number of samples required is the number needed for the sequential detector to reach a decision.

Fig. 4.8 shows the distribution of the number of samples required for the sequential detector when there is a primary signal in the AWGN channel. The x label represents the number of samples required in a given simulation loop. The y label represents the frequency of a certain number of required samples in 1000 simulation loops. For example, in Fig. 4.8, the sequential detector only needs 5 samples to make a correct decision for 120 times out of 1000 simulation loops. Furthermore, we only plot simulation loops which make a correct decision.

The preset P_D is 0.99 in Fig. 4.8. We only plot the simulation loops which make the correct decision and find that the decisions of 989 simulation loops are correct. It means that P_D is 0.989 which is very close to the preset 0.99. Furthermore, the average number of samples required per decision in this figure is 8.12.

Fig. 4.9 shows the distribution of the number of required samples for the proposed

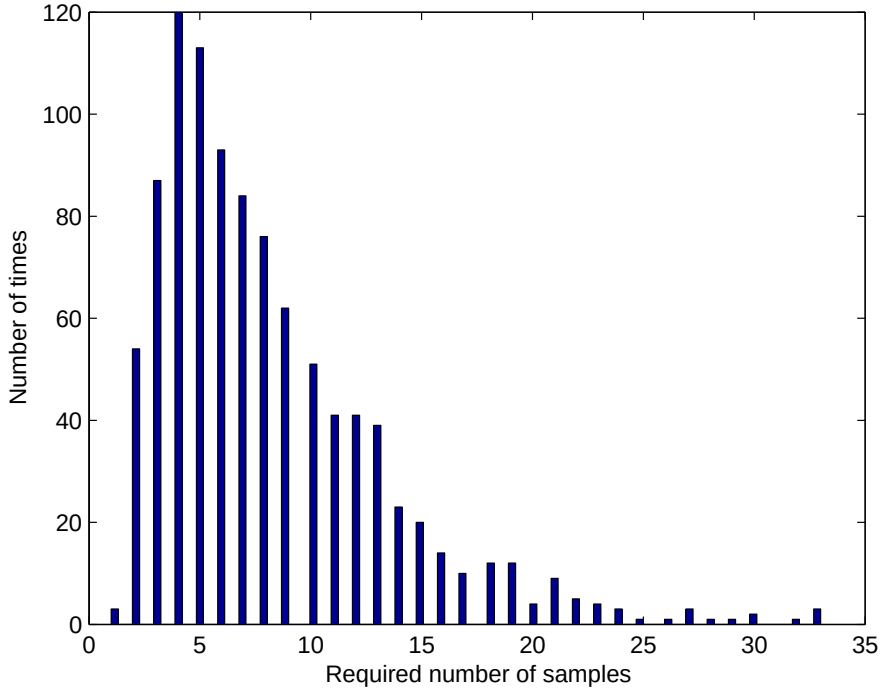

Figure 4.8 Histogram of the required number of samples for a AWGN channel at a received SNR of 5dB ($P_D = 0.99$ and $P_{FA} = 0.01$).

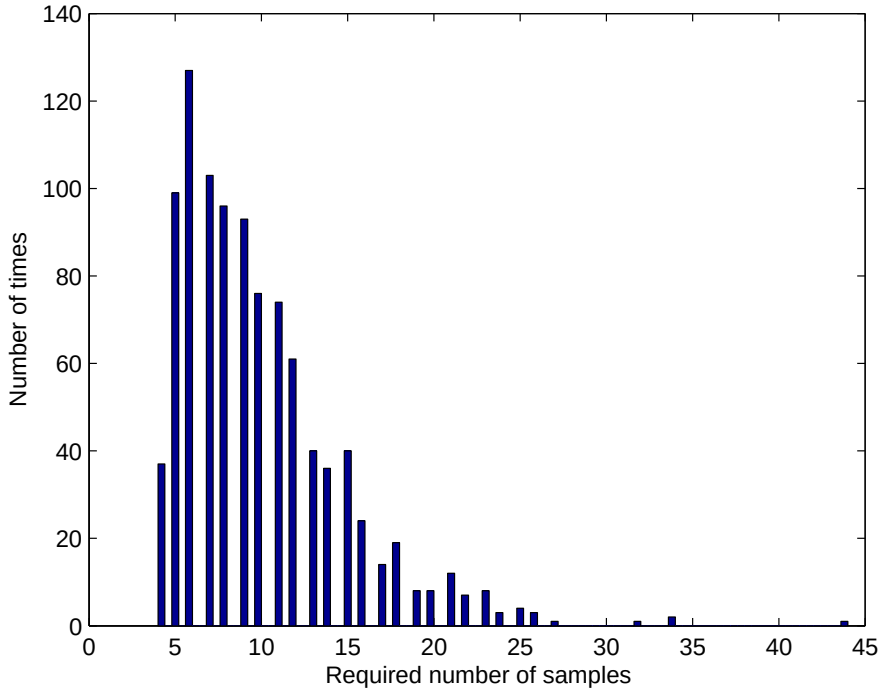

Figure 4.9 Histogram of the required number of samples for a AWGN channel (no signal present, $P_{FA} = 0.01$).

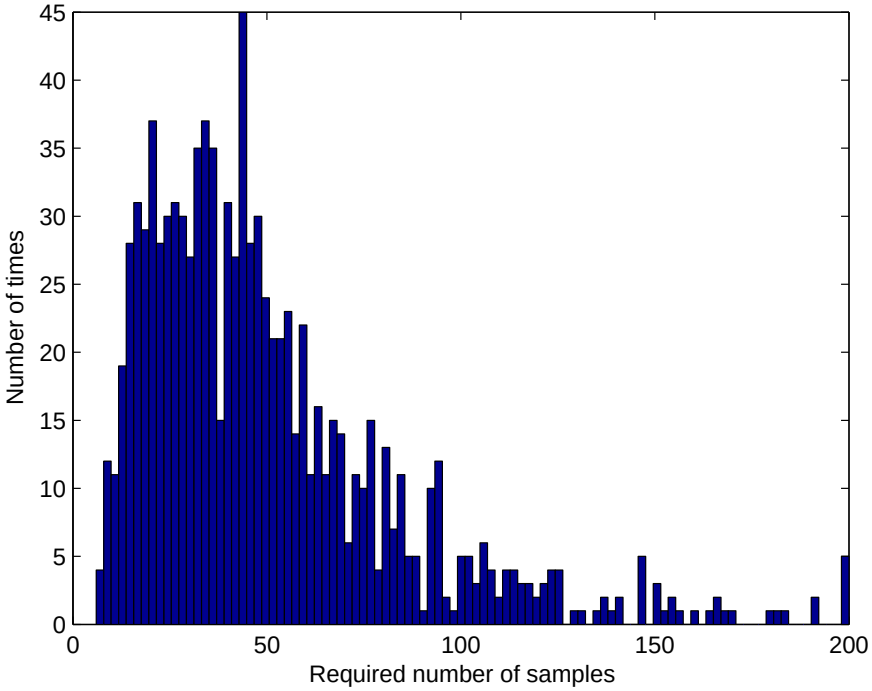

Figure 4.10 Histogram of the required number of samples for a AWGN channel at a received SNR of 0dB ($P_D = 0.99$ and $P_{FA} = 0.01$).

sequential detector in the AWGN channel when there is no primary signal present. The preset P_{FA} is 0.01. We still only plot the simulation loops which make correct decisions and find that 992 simulation loops make the correct decision. It means that P_{FA} is 0.008 which is very close to the preset 0.01. The average number of required samples in this figure is 9.97.

The purpose of plotting Fig. 4.9 is to demonstrate that our proposed sequential detector can achieve both the preset value of P_D and P_{FA}. It implies that the proposed sequential detector works well. In the following sections, we will not plot the distribution of the number of samples required when there is no primary signal. The reason is that we can't determine the effect of shadowing and received SNR if there is no primary signal. This can occur only when the primary signal is present.

Fig. 4.10 and Fig. 4.11 show the distribution of the number of required samples for the proposed sequential detector for different received SNRs in the AWGN channel. The preset P_D is 0.99 and P_{FA} is 0.01. The decisions of 989 simulation loops are right in Fig. 4.10 and 988 are correct in Fig. 4.11. Figs. 4.8, 4.10 and 4.11 confirm that there is no improvement in the number of correct decisions when the received SNR is increased.

However, the average number of required samples for Fig. 4.10 and Fig. 4.11 are 50.28 and 2.04 which means that the average number of required samples is sharply reduced when the received SNR is increased. In conclusion, we can say that a larger SNR leads to making the decision more quickly on average.

At this stage, we want to know what affects P_D and P_{FA} for the sequential detector. Fig. 4.12 and Fig. 4.13 give us the answer. Fig. 4.12 and Fig. 4.13 show the distribution of the number of samples required across different preset P_D and P_{FA} in the AWGN channel. The preset P_D and P_{FA} in Fig. 4.12 are 0.90 and 0.01, respectively. The preset values of P_D and P_{FA} in Fig. 4.13 are 0.80 and 0.01, respectively. The decisions of 901 simulation loops are correct in Fig. 4.12 and 802 simulation loops are correct in Fig. 4.13 . The average received SNR for these two figures are the same and set to 5dB.

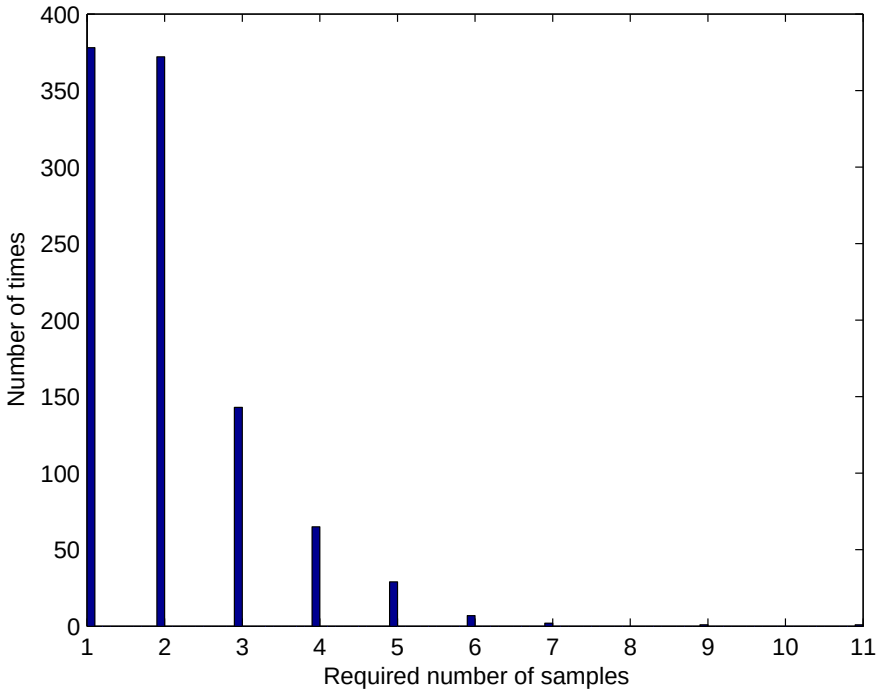

Figure 4.11 Histogram of the required number of samples for a AWGN channel at a received SNR of 10dB ($P_D = 0.99$ and $P_{FA} = 0.01$).

Furthermore, the average number of samples required per decision for Fig. 4.12 and Fig. 4.13 are 7.85 and 6.18, respectively. These two figures prove that if we increase the preset value of P_D, the average number of samples required also increases.

Fig. 4.14 compares the average number of samples required per decision of the proposed sequential detector with the block based energy detector for the same performance

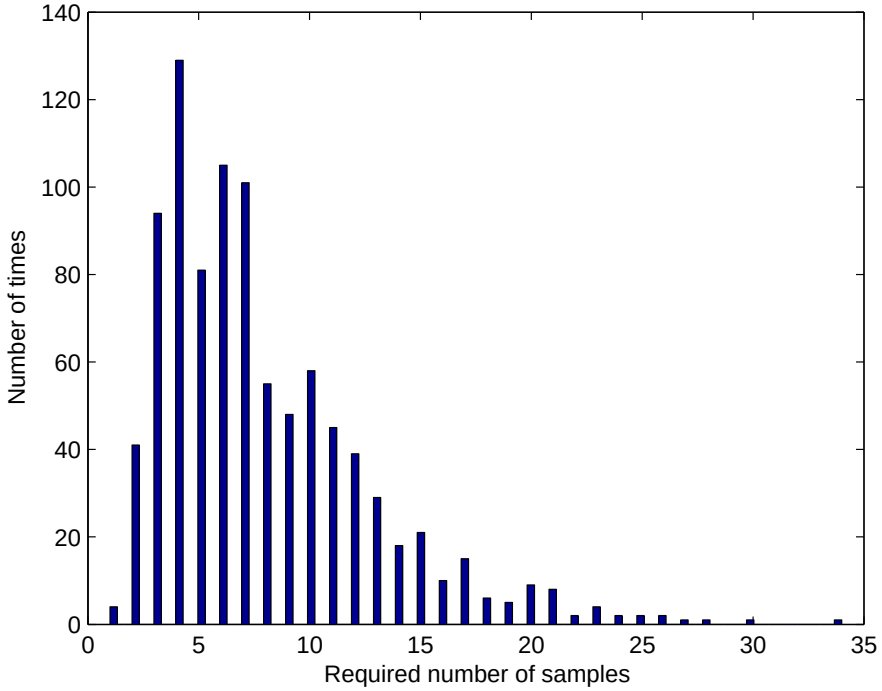

Figure 4.12 Histogram of the required number of samples for a AWGN channel using preset $P_D = 0.9$ and $P_{FA} = 0.01$ (received SNR=5dB).

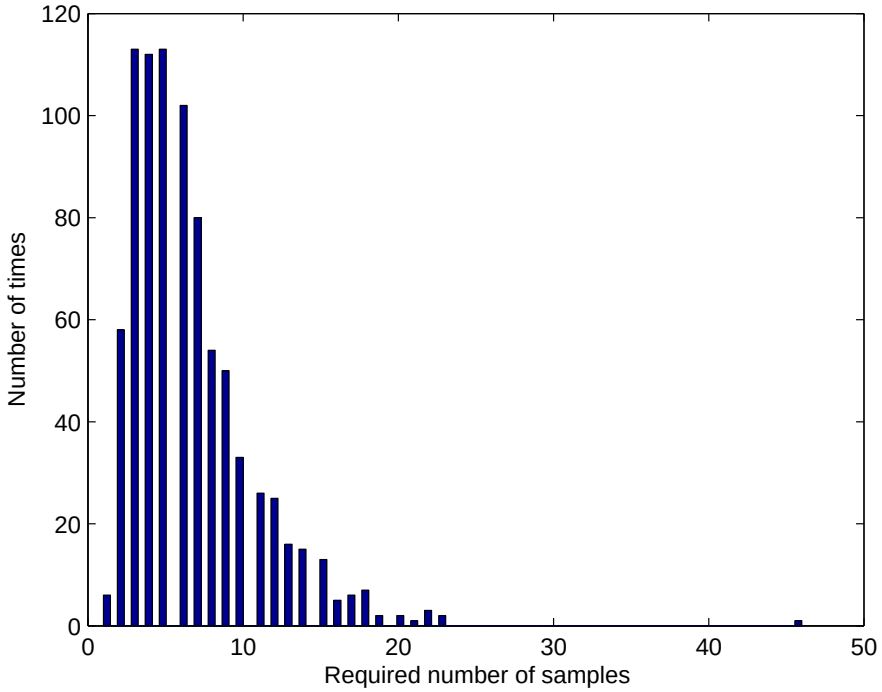

Figure 4.13 Histogram of the required number of samples for a AWGN channel using preset $P_D = 0.8$ and $P_{FA} = 0.01$ (received SNR=5dB).

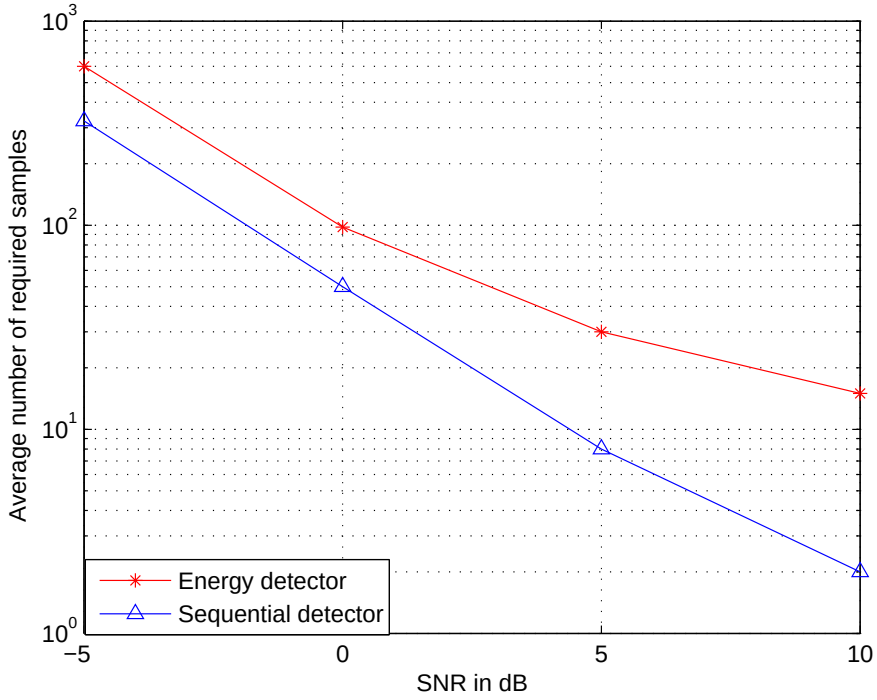

Figure 4.14 Average number of required samples for sequential detector and block based energy detector for a AWGN channel at different received SNR using $P_D = 0.99$ and $P_{FA} = 0.01$.

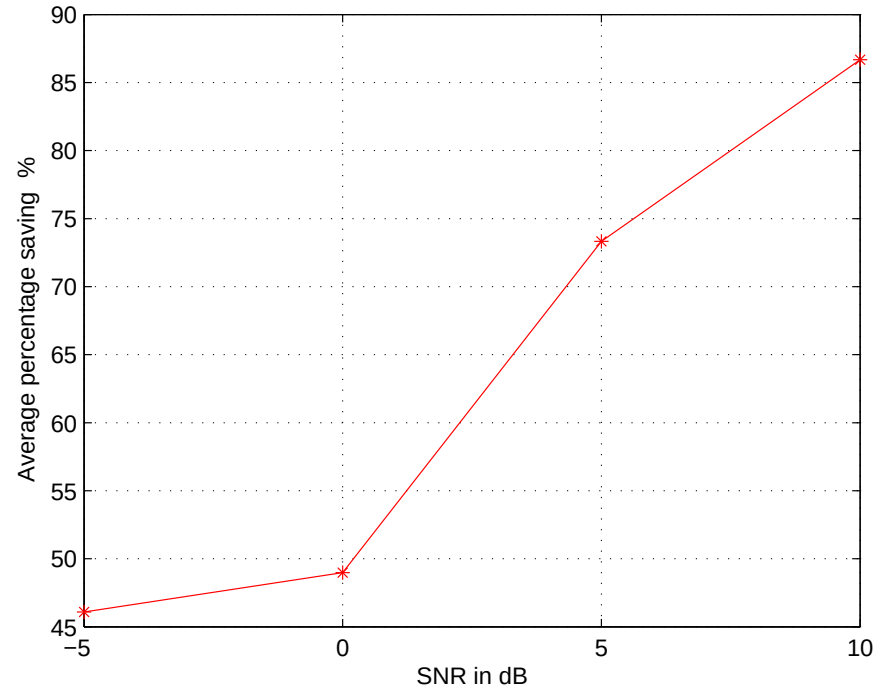

Figure 4.15 Average percentage saving (PS) of sequential detector compared to the block based energy detector for a AWGN channel.

in the AWGN channel. The preset value of P_D and P_{FA} of the sequential detector are 0.99 and 0.01, respectively. The number of required samples for the block based energy detector to achieve the same performance is also plotted at different SNR. From Fig. 4.14 we find that the sequential detector saves $45\% - 85\%$ of the number of required samples compared to the block based energy detector for the same performance. It means that on average, the sequential detector will detect the primary signal more quickly at the same level of detection accuracy.

Fig. 4.15 demonstrates the average percentage saving (PS) of a sequential detector compared to the block based energy detector. From Fig. 4.15 we can see that the average number of samples required using a sequential detector for different received SNR is significantly lower. For example, when the received SNR is 0dB, we can save 48% of the number of required samples by using a sequential detector. Furthermore, we also find that the PS increases gradually from lower SNR to higher SNR.

4.4.3 Truncated Sequential Detector

As we discussed in chapter 3, the number of required samples for each decision should be minimized. Furthermore, the number of samples required for the sequential detector to make a decision is a random variable and it may take extremely large values. Thus we also need to determine or specify the maximum number of required samples in each decision. For the above two purposes, we investigate the truncated sequential detector in terms of the distribution of number of required samples and the degradation of performance due to truncation. By its definition, the average number of required samples for a truncated sequential detector will be lower than for the sequential detector. We also investigate how much the average number of required samples is reduced using the truncated sequential detector.

The decision rule at the truncation point was presented in chapter 3. The truncation point is the number of required samples for a block based energy detector to achieve the same performance. In this situation, the truncated sequential detector always requires fewer samples than the block based energy detector.

Figs. 4.16, 4.17 and 4.18 show the distribution of the number of samples used by a truncated sequential detector for different received SNR in the AWGN channel. We still only plot the correct decisions. The preset values P_D and P_{FA} are 0.99 and 0.01,

respectively. The truncation point is 97 in Fig. 4.16, meaning simulation loops are forced to make a decision after 97 samples. This is why we find the rightmost bar in Fig. 4.16 is relatively large. Clearly at this low value of SNR, a significant number of decisions require 97 or more samples to make a decision. The truncation points in Figs. 4.17 and 4.18 are 29 and 14, respectively.

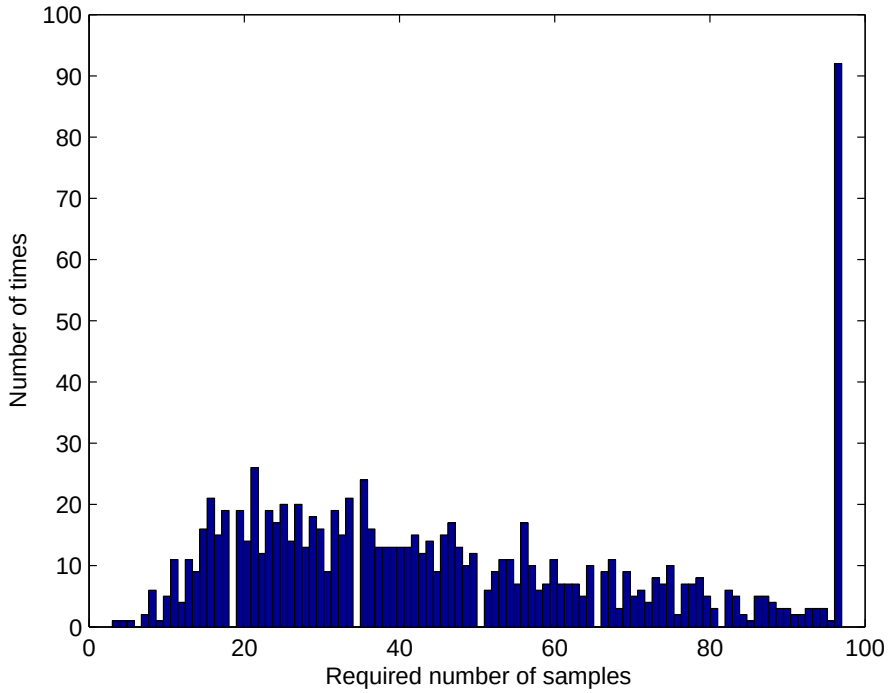

Figure 4.16 Histogram of the required number of samples for the truncated sequential detector for a AWGN channel at a received SNR of 0dB (truncation point=97, preset $P_D = 0.99$ and preset $P_{FA} = 0.01$).

The average number of required samples in Figs. 4.16, 4.17 and 4.18 are 46.89, 8.02 and 2.01, respectively. We find that the average number of required samples of a truncated sequential detector is smaller than for the sequential detector as the maximum number of samples is bounded. However, we also find that the reduction in average number of required samples is small when the received SNR is relatively large. This phenomenon is shown in Fig. 4.19.

From chapter 3, we know that the performance of the truncated sequential detector is worse than the sequential detector due to truncation. Based on the truncation points given above, the achieved P_D is shown in Fig. 4.20 for various received SNR. This figure demonstrates the degradation of P_D with respect to the preset P_D. The preset P_D is 0.99 in Fig. 4.20 which is the design value for a sequential detector.

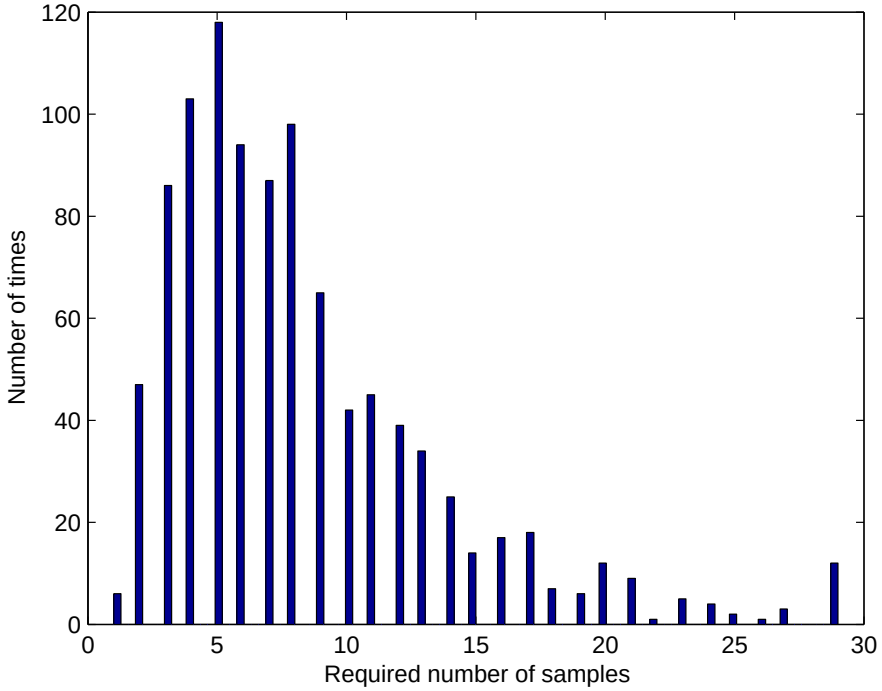

Figure 4.17 Histogram of the required number of samples for the truncated sequential detector for a AWGN channel at a received SNR of 5dB (truncation point=29, preset $P_D = 0.99$ and preset $P_{FA} = 0.01$).

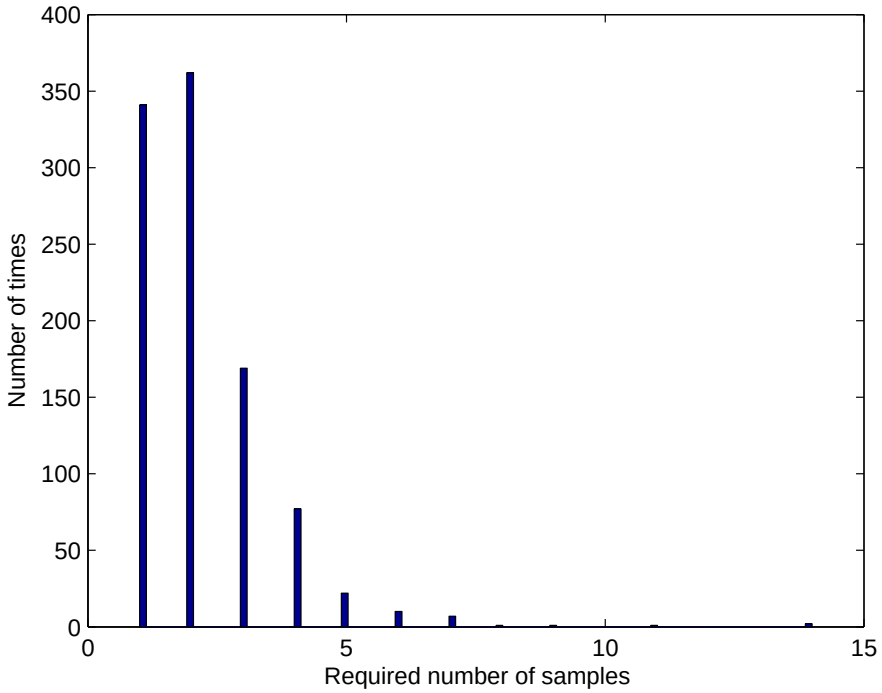

Figure 4.18 Histogram of the required number of samples for the truncated sequential detector for a AWGN channel at a received SNR of 10dB (truncation point=14, preset $P_D = 0.99$ and preset $P_{FA} = 0.01$).

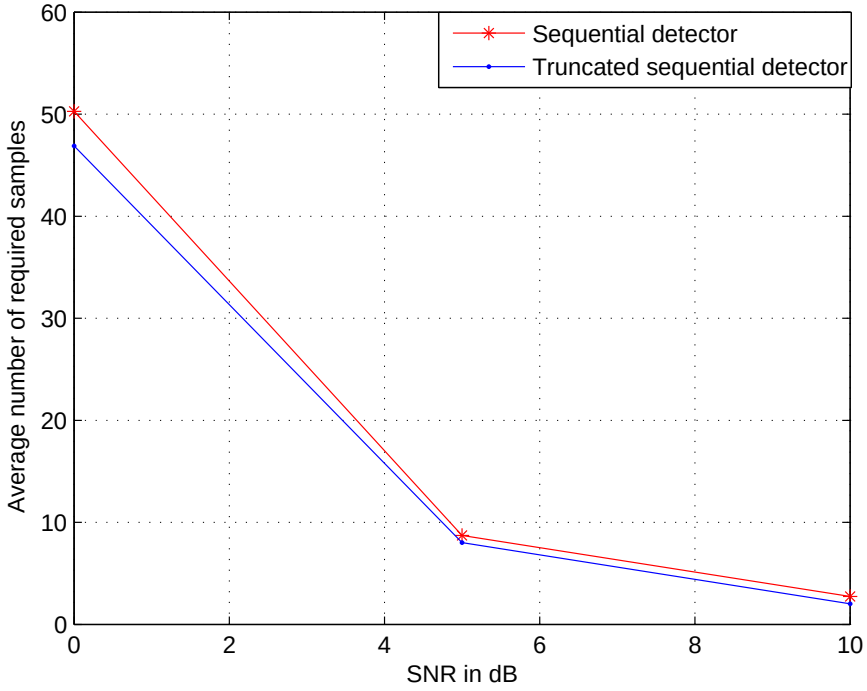

Figure 4.19 Average number of required samples for the truncated sequential detector for a AWGN channel at different received SNR.

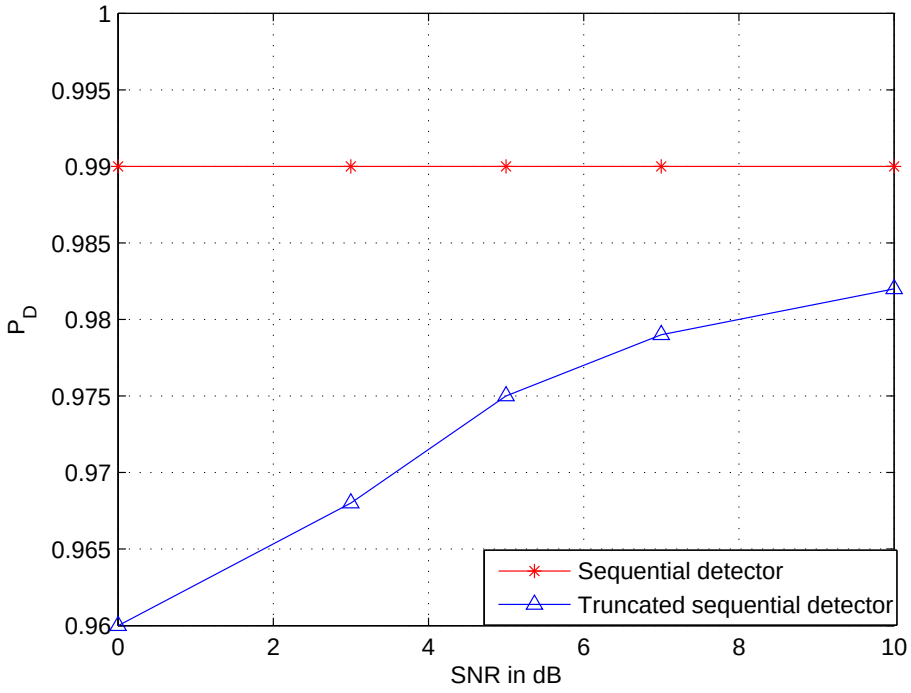

Figure 4.20 Performance degradation of truncated sequential detector compared to sequential detector for a AWGN channel at different received SNR.

4.4.4 Truncated Sequential Detector in Shadowing Channel

In this section, we apply a truncated sequential detector in the log-normal shadowing channel with standard deviation of 6dB. In each simulation loop, we extend the number of transmitted samples to 2000 samples. From Fig. 4.21 we can see that in a shadowing environment a larger number of samples should be taken before any truncation of the process.

Figs. 4.22, 4.23 and 4.24 show the distribution of the number of required samples for the truncated sequential detector in the log-normal shadowing channel. The preset value of the P_D equals 0.99 and P_{FA} equals 0.01. The average received SNR of Figs. 4.22, 4.23 and 4.24 are 5dB, 10dB and 15dB, respectively. The truncation point is set as the number of samples required for a block based energy detector to achieve the same performance as a sequential detector. The truncation point of Figs. 4.22, 4.23 and 4.24 are 99, 28 and 16, respectively. The average number of required samples in Figs. 4.22, 4.23 and 4.24 are 44.26, 11.17 and 4.31, respectively. Fig. 4.25 shows that the average number of samples required is reduced if the average received SNR is increased. Moreover, at moderate to high SNR, the degradation is small.

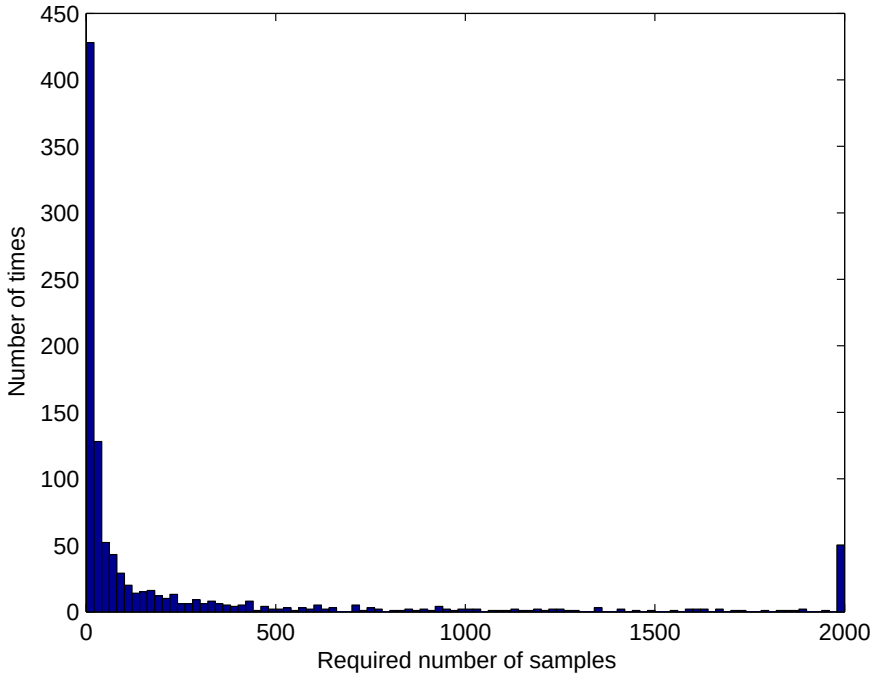

Figure 4.21 Histogram of the required number of samples for the sequential detector for a log-normal shadowing channel at a received SNR of 5dB ($\sigma_{dB} = 6dB$, preset $P_D = 0.99$ and preset $P_{FA} = 0.01$).

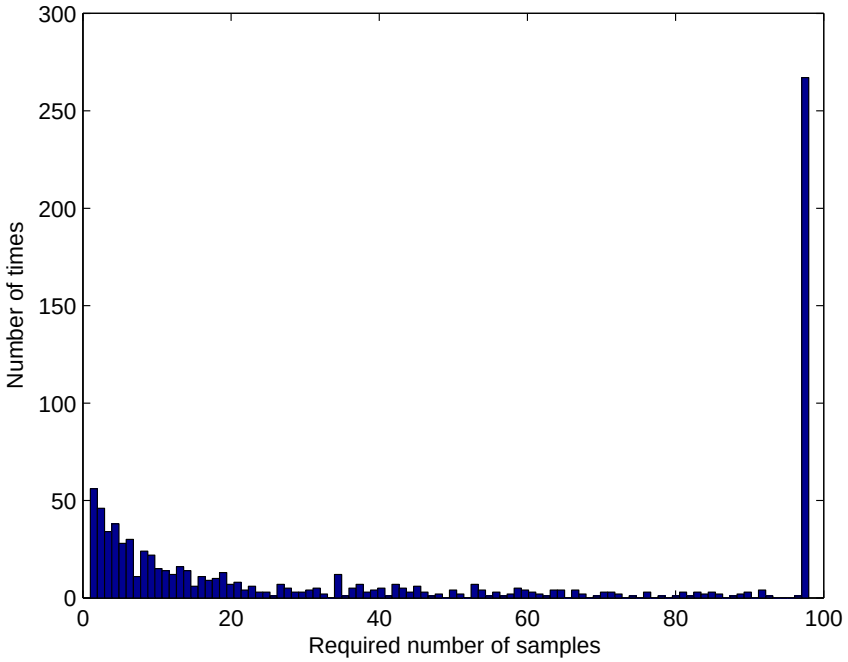

Figure 4.22 Histogram of the required number of samples for the truncated sequential detector for a log-normal shadowing channel at a received SNR of 5dB ($\sigma_{dB} = 6dB$, truncation point=99, preset $P_D = 0.99$, preset $P_{FA} = 0.01$).

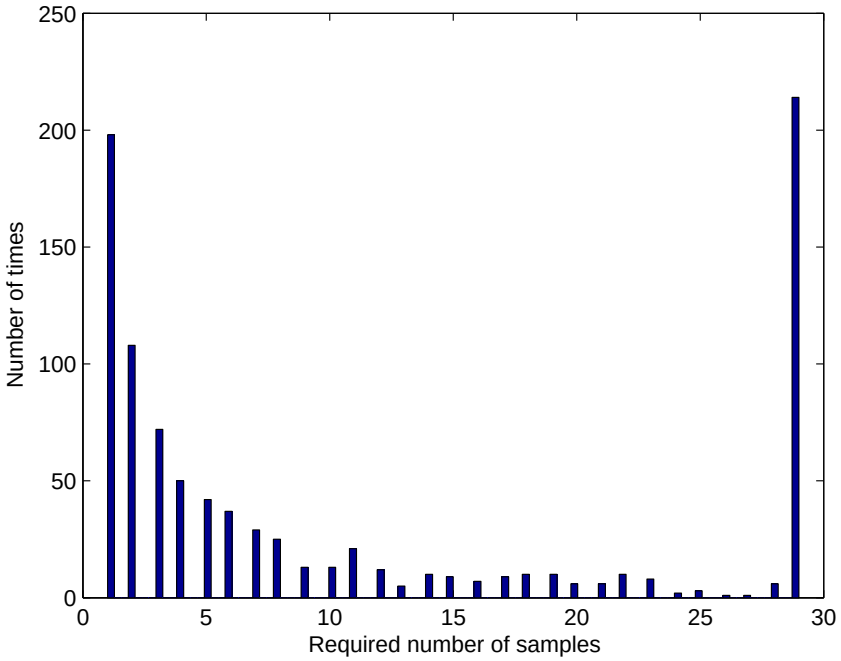

Figure 4.23 Histogram of the required number of samples for the truncated sequential detector for a log-normal shadowing channel at a received SNR of 10dB ($\sigma_{dB} = 6dB$, truncation point=28, preset $P_D = 0.99$, preset $P_{FA} = 0.01$).

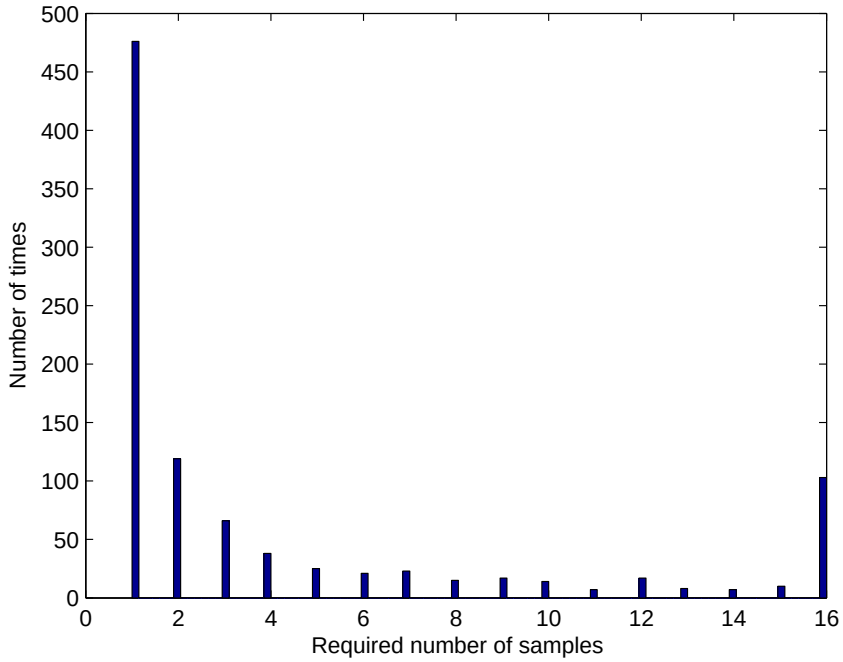

Figure 4.24 Histogram of the required number of samples for the truncated sequential detector for a log-normal shadowing channel at a received SNR of 15dB ($\sigma_{dB} = 6dB$, truncation point=16, preset $P_D = 0.99$, preset $P_{FA} = 0.01$).

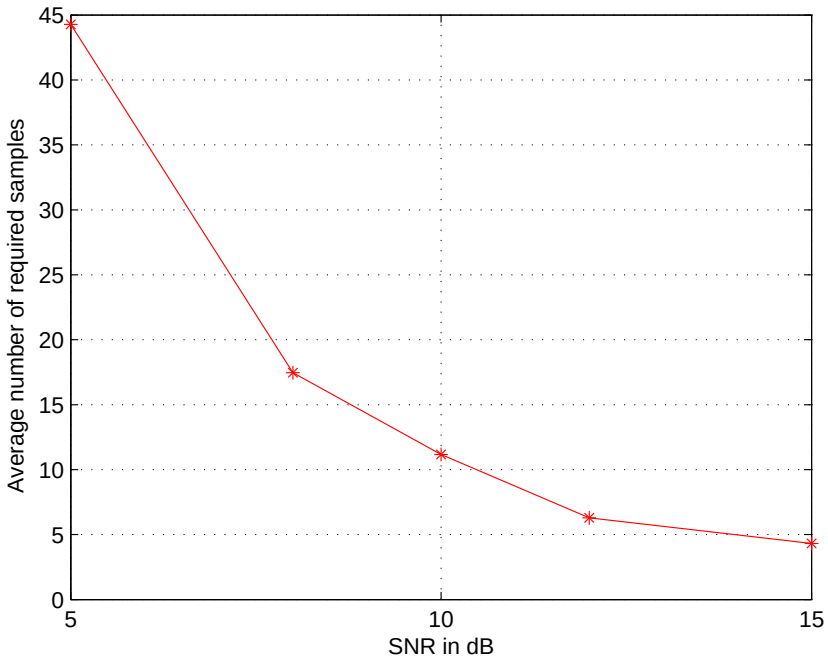

Figure 4.25 Average number of required samples reduction for the truncated sequential detector for a log-normal shadowing channel at different received SNR ($\sigma_{dB} = 6dB$).

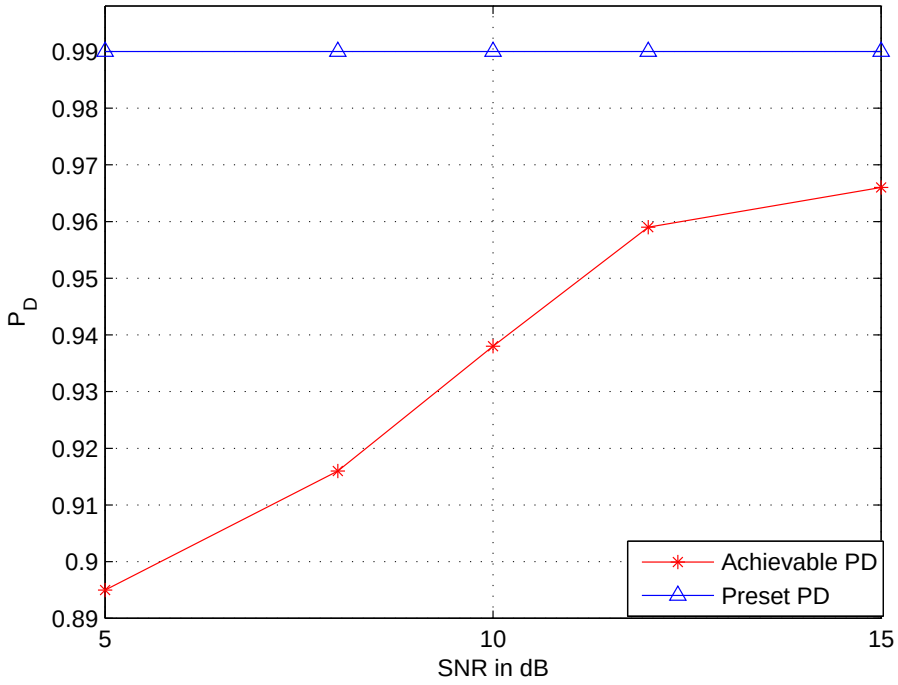

Figure 4.26 Performance degradation for the truncated sequential detector for a log-normal shadowing channel at different received SNR ($\sigma_{dB} = 6dB$).

Now, we need to determine the performance degradation of a truncated sequential detector compared to a sequential detector in the shadowing channel. It is illustrated in Fig. 4.26. The preset value of P_D and P_{FA} are 0.99 and 0.01 in this figure. It is shown that the preset P_D can not be reached if we apply a truncated sequential detector. We also find that the truncated sequential detector loses 10% of its performance at an average SNR of 5dB while it loses 2% of its performance at an average SNR of 15dB. Thus, we can say that the achieved P_D gradually increases from lower SNR to higher SNR.

4.5 COOPERATIVE SENSING PERFORMANCE

In this subsection, we present simulation results of the selection combining rule in the cooperative scheme. We still consider a primary transmitter using QPSK modulation. We still assume the primary transmitter transmits 500 samples in each simulation loop for the cooperative case. Each individual sensor employs a sequential detector. The fusion center applies the selection combining rule which is proposed in chapter 3. In order to model the "hidden terminal" problem, the channel is assumed to be a log-normal shadowing channel with a standard derivation of 6dB.

On employing the selection combining rule described in chapter 3, Figs. 4.27, 4.28, 4.29 and 4.30 demonstrate the distribution of the selected number of required samples at the fusion center for different numbers of individual sensors. The x label represents the selected number of required samples at the fusion center in a given simulation loop. The y label represents the frequency of a certain selected number of samples required in 1000 simulation loops. The average received SNR, preset P_D and P_{FA} are the same for each individual sensor. The average received SNR is 5dB. The preset P_D and P_{FA} are 0.8 and 0.01. The number of individual sensors N_{sensor} in Figs. 4.27, 4.28, 4.29 and 4.30 are 2, 4, 6 and 8, respectively.

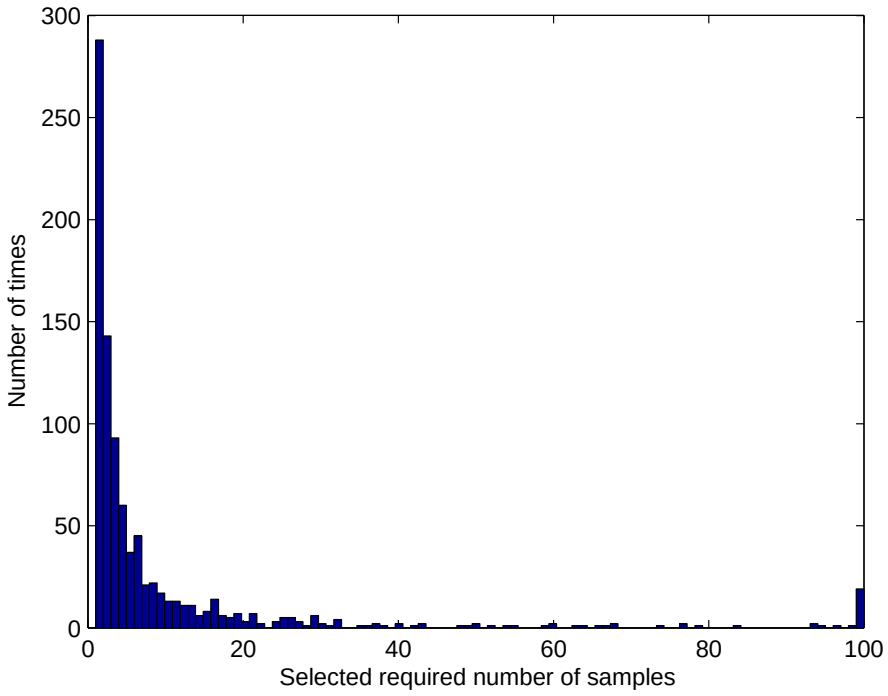

Figure 4.27 Histogram of the required number of samples at the fusion center with $N_{sensor} = 2$ for a log-normal shadowing channel ($\sigma_{dB} = 6dB$, SNR=5dB, preset $P_D = 0.8$ and preset $P_{FA} = 0.01$).

The average number of required samples in Figs. 4.27, 4.28, 4.29 and 4.30 are 9.27, 3.11, 1.92 and 1.53, respectively. Fig. 4.31 plots these four values together and implies that the average number of samples per decision required at the fusion center to make the final decision decreases as the number of individual sensors increases. It implies that as the number of individual sensor increases, the fusion center makes the final decision more quickly. Furthermore, the truncated sequential detector is not used in the cooperative scheme. The fusion center chooses the first coming individual result. Thus, from Fig.

4.31, we find that the average number of required samples at the fusion center can be reduced to a very small value when the number of individual sensor is increased. There is no need to truncate at the individual sensor, thus avoiding performance loss due to truncation.

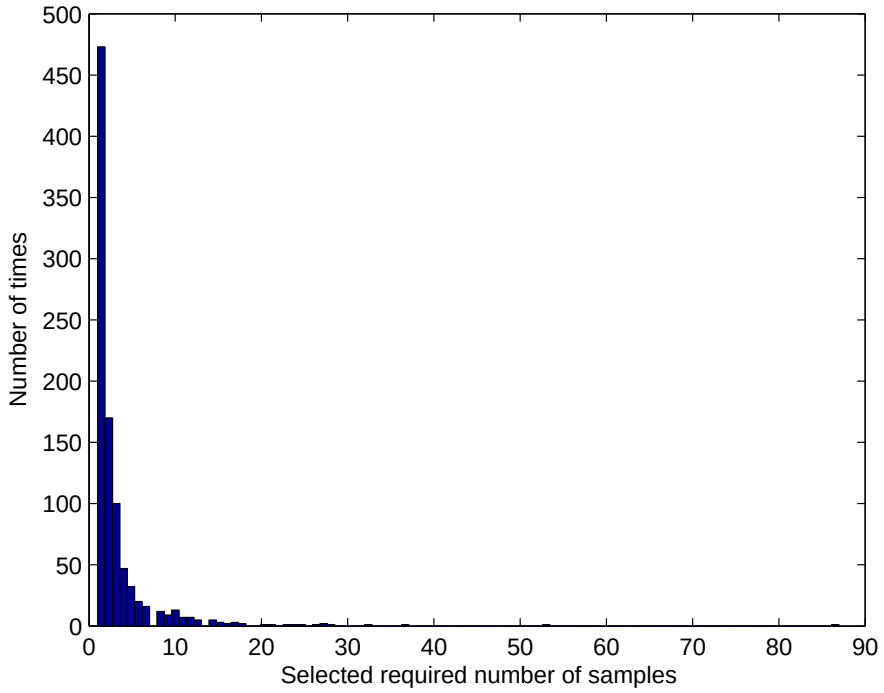

Figure 4.28 Histogram of the required number of samples at the fusion center with $N_{sensor} = 4$ for a log-normal shadowing channel ($\sigma_{dB} = 6dB$, SNR=5dB, preset $P_D = 0.8$ and preset $P_{FA} = 0.01$).

Fig. 4.32 shows the performance of the selection combining rule as the number of sensors increases. The average received SNR, preset P_D and P_{FA} are the same for each individual sensor. The average received SNR is 5dB. The preset P_D and P_{FA} are 0.8 and 0.01 at the individual sensors. From Fig. 4.32 we can see that the overall performance of cooperative sensing is better than that of the individual sensing. The overall performance increases as the number of sensors increases.

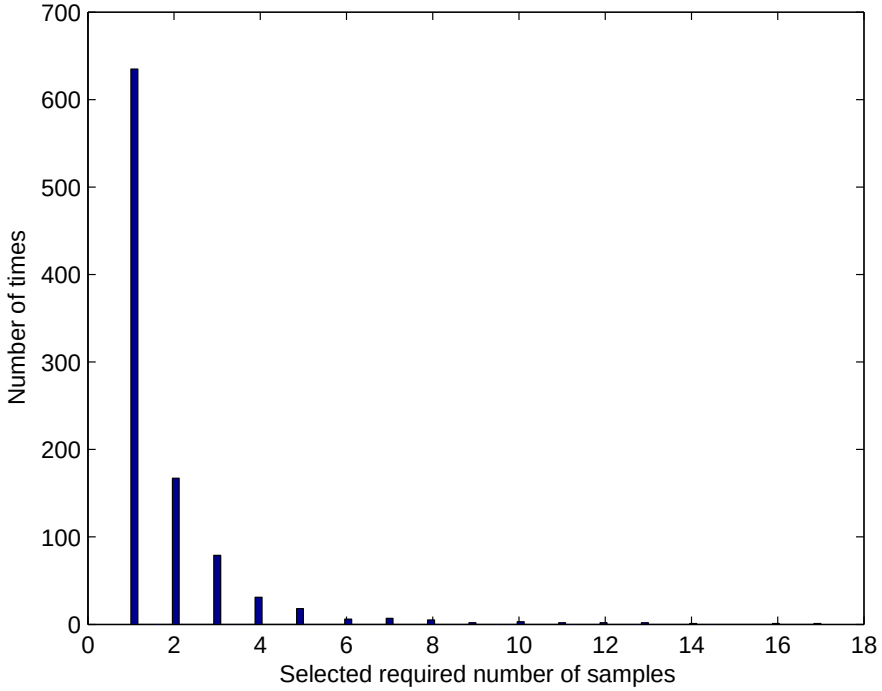

Figure 4.29 Histogram of the required number of samples at the fusion center with $N_{sensor} = 6$ for a log-normal shadowing channel ($\sigma_{dB} = 6dB$, SNR=5dB, preset $P_D = 0.8$ and preset $P_{FA} = 0.01$).

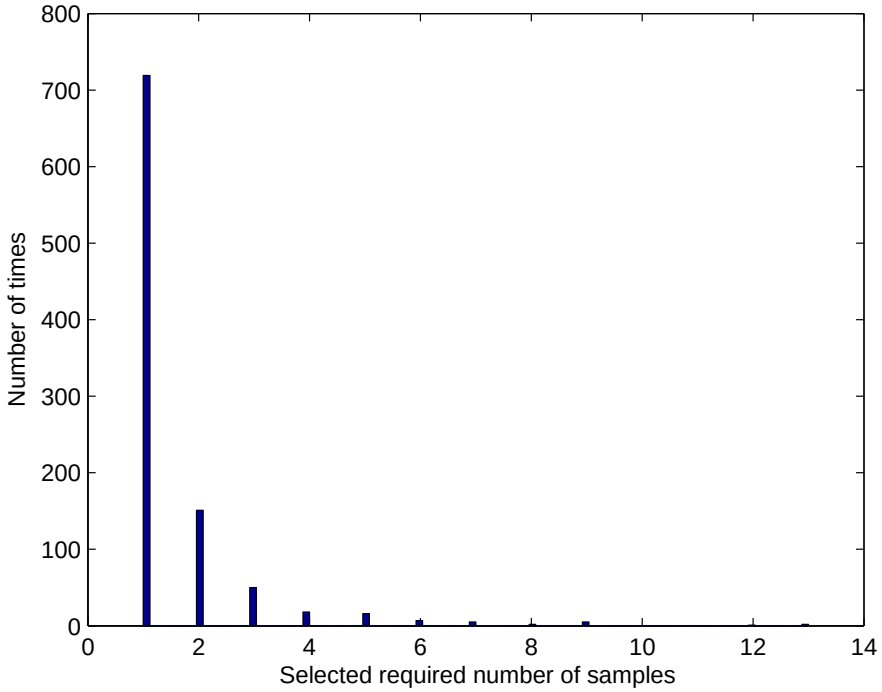

Figure 4.30 Histogram of the required number of samples at the fusion center with $N_{sensor} = 8$ for a log-normal shadowing channel ($\sigma_{dB} = 6dB$, SNR=5dB, preset $P_D = 0.8$ and preset $P_{FA} = 0.01$).

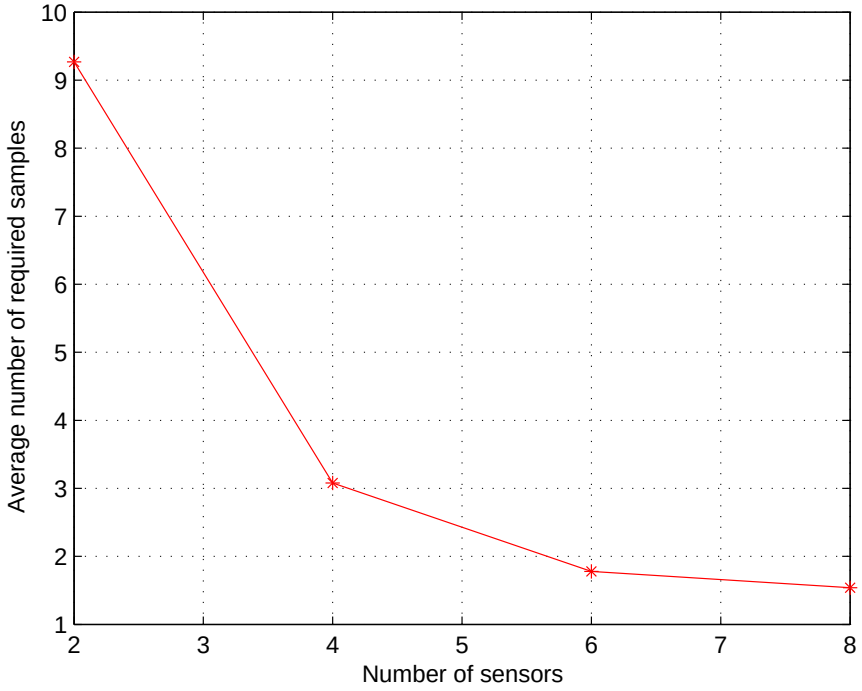

Figure 4.31 Average number of samples required per decision as a function of the number of sensors for a log-normal shadowing channel ($\sigma_{dB} = 6dB$, received SNR=5dB).

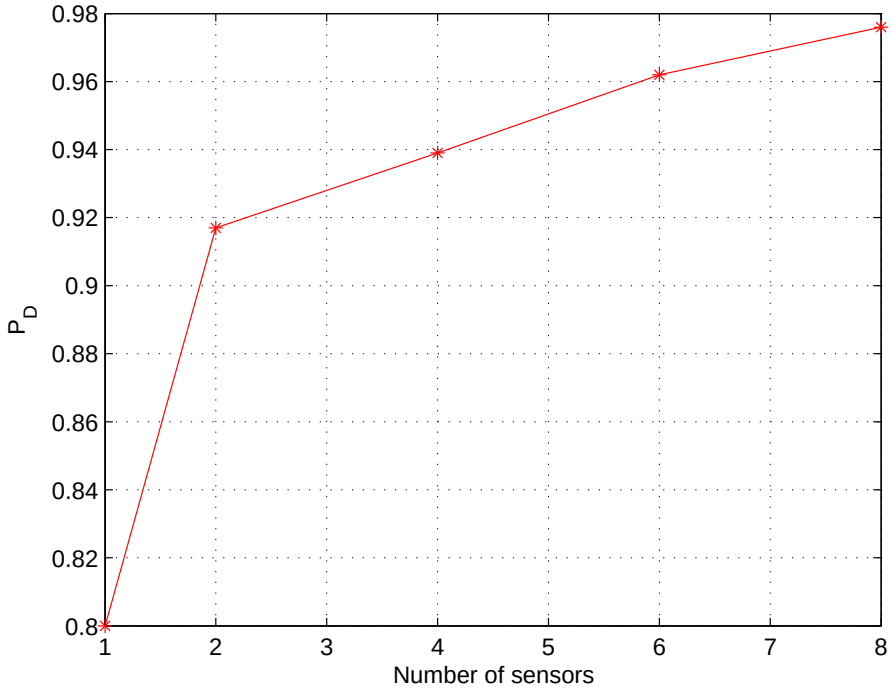

Figure 4.32 Performance improving with different number of sensors for a log-normal shadowing channel ($\sigma_{dB} = 6dB$, received SNR=5dB).

4.6 SUMMARY

In this chapter, computer simulation results for both the proposed individual detectors and a cooperative selection combining rule are presented. First, we investigate the performance of a block based energy detector in a Rayleigh fading channel and in a log-normal shadowing channel for different time-bandwidth products and average received SNR. Secondly, the distribution of the number of samples required for the sequential detector with different received SNR, preset P_{FA} and P_D values are presented. From this we can see that the sequential detector requires fewer samples than the energy detector on average for the same performance. Thirdly, a truncated sequential detector is applied to limit the number of required samples and to avoid allowing an extremely large number of required samples in any decision interval. An extremely large number of required samples is rare in the AWGN channel [27] [36], but is more common in a fading environment. We also demonstrate the performance degradation due to truncation. Fourthly, we find that the average number of required samples can be further reduced by applying a selection combining rule in a cooperative network. Furthermore, the overall detection performance can also be increased by using a selection combining rule.

Chapter 5

CONCLUSION AND FUTURE WORK

5.1 CONCLUSION

In this thesis, we mainly focus on how to reduce sensing time in a CR system by using sequential detection. Both individual detectors and a cooperative scheme are proposed for this purpose.

At the beginning of this thesis, we define a representation of the primary signal considered. We then discuss wireless channels, focusing on the Rayleigh fading channel which is used to model small scale fading and the log-normal shadowing channel, which is used to model large scale fading. They are both used in the following analysis and simulation.

In chapter 2, we first discuss the problem of spectrum scarcity. In order to solve this problem, researchers have proposed a new way to manage spectrum called dynamic spectrum access. Since CR can be viewed as a platform for the realization of dynamic spectrum access, background information on SDR and CR systems was presented. CR is a kind of SDR with several additional abilities. The function of CR is often modelled as a cognition cycle. Our work is the first step of a cognition cycle which is called spectrum sensing. Spectrum sensing is to detect the presence of a primary signal in a noisy environment. It can be viewed as a signal detection problem. For this reason, some fundamentals of signal detection theory are then introduced.

Three popular detectors: matched filter, energy detector and feature detector are also briefly discussed in chapter 2. However, they are all fixed sample-size systems. Their sensing time is fixed and preset. In this case, our interest is to find the P_D we can achieve during the prescribed sensing time.

In the last part of chapter 2, cooperative spectrum sensing is briefly discussed. The purpose of cooperative sensing is to improve detection accuracy, reduce sensing time and

combat the hidden terminal problem. A background literature review of various cooperative sensing schemes was also presented. From the literature review, we find that researchers are more likely to work on how to increase the performance by various cooperative schemes. However, we believe that reducing sensing time is also very important for a CR system and, therefore, focused our research direction on reducing the sensing time.

In chapter 3, fundamental theory and various components of the sequential detector are presented. By using sequential testing, the sensing time is not fixed anymore. P_D and P_{FA} are set before testing. The sequential detector makes a decision whenever it receives a new sample. It needs less sensing time than an energy detector on average. In order to further reduce the sensing time, especially in a shadowing environment, a truncated sequential detector is then introduced. The performance degradation due to truncation is also investigated.

Finally, the selection combining rule at the fusion center is proposed for cooperative sensing. Sensing times of each individual detector are different in a shadowing channel, and therefore, we choose the first decision to arrive as the final decision. By the application of such a selection combining rule, the sensing time can be further reduced.

In chapter 4, we first investigate the performance of an energy detector in Rayleigh fading and shadowing channels for different average received SNR and time-bandwidth product. Secondly, we apply the sequential detector in the AWGN channel and compare it with the energy detector. It is shown that the sequential detector needs less average sensing time than an energy detector for the same performance. The sensing time can be reduced up to 85%. We also find that the average number of required samples for a sequential detector decreases as the received SNR increases. Furthermore, the performance is based on the preset value of P_D and P_{FA}.

Thirdly, we apply a truncated sequential detector in the AWGN channel and find that it can further reduce the sensing time. The effect of truncation on sensing time is not significant when the SNR is large. Then, we apply the sequential detector in the shadowing channel and find that the sensing time may sometimes be extremely long. Thus, we must truncate the sensing time to a reasonable range. The average number of required samples after truncation under different received SNR is then shown. From that we can see that the average number of required samples gradually decreases from lower SNR to higher SNR. The performance degradation due to truncation in the two channel models are also

investigated. We find that the performance of a truncated sequential detector is worse than the sequential detector, but its performance improves as SNR increases.

Fourthly, cooperative sensing using the selection combining rule is applied to further reduce the sensing time in a shadowing channel. From that we can see that the sensing time can be further reduced as the number of individual sensors increases. The overall performance can also be improved as the number of individual sensors increases.

5.2 FUTURE WORK

There are four points that might be useful for further research.

The sequential and truncated sequential detector are only investigated in a log-normal shadowing channel. We also need to investigate the performance of them in the Rayleigh fading channel and in a channel combining log-normal shadowing and Rayleigh fading.

An adaptive sensing time scheme is needed. CR can potentially sense its surroundings environment and change the parameters for itself. The truncation point is preset by the designer in this thesis. In the next step, the selection may be based on the surrounding environment, maximal tolerance sensing time and required performance. By using the new selection rule, the truncation point is not picked by the designer, it is picked by the CR to optimize performance in a certain environment.

A new fusion rule is needed at the fusion center. The proposed selection combining rule is a hard-decision rule. It requires less bandwidth for the control channel, but the performance of it may be relatively low. The performance of soft decision rules are often better than the hard decision rules. In the next step, a soft decision rule may be needed at the fusion center. Each individual sensor would still perform sequential testing and send the likelihood ratio to the fusion center. The fusion center would then perform a sequential test using the first results to arrive. The overall performance may be improved by using this method.

A bandpass filter is employed at the front end of all the detectors in this thesis. The detector can only know the presence of a primary signal over the bandwidth W of the bandpass filter. A wideband spectrum sensing scheme may be proposed which can make W very wide or use some form of FFT to identify the spectrum holes in a larger bandwidth.

As CR can be viewed as a “smart” radio, all the previous work might be extended to

an adaptive approach, in this case, CR can optimize the performance in different environments.

REFERENCES

[1] Q. Zhao and A. Swami, "A decision-theoretic framework for dynamic spectrum access," *IEEE Wireless Commun. Mag: Special Issue on Cognitive Wireless Networks*, 2007.

[2] DRM Website://www.drm.org/fileadmin/media/downloads/drmpresentationv1.6.pdf.

[3] Q. Zhao, L. Tong and A. Swami, "Decentralized cognitive mac for dynamic spectrum access," *Proc. DySPAN*, Nov. 2005.

[4] R. H. Walden, "Analog-to-digital converters survey and analysis," *IEEE J. Select. Areas. Commun.*, vol. 17, Apr. 1999.

[5] C. Cordeiro, K. Challapali, D. Birru and S. Shankar, "IEEE 802.22: the first world wireless standard based on cognitive radios," *Proc. DySPAN*, Nov. 2005.

[6] Z. Quan, S. G. Cui, A. H. Sayed and H. V. Poor, "Wideband spectrum sensing in cognitive radio networks," *Proc. ICC* , 2008.

[7] S. Haykin, *Communication System*. New York: John Wiley and Sons, 2001.

[8] T. Rappaport, *Wireless Communications: Principles and Practice*. New Jersey: Prentice Hall, 2002.

[9] J. Cavers, *Mobile Channel Characteristics*. Kluwer Academic Publishers, 2000.

[10] B. Sklar, *Digital Communications: Fundamentals and Application*. New Jersey: Prentice Hall, 2001.

[11] R. Clark, "A statistical theory of mobile-radio reception," *Bell Syst. Tech. J.*, vol. 47, pp. 957-1000, Dec. 1968.

[12] G. L. Stuber, *Principles of Mobile Communication*. Kluwer Academic Publishers, 1996.

[13] B. Sklar, "Rayleigh fading channels in mobile digital communication systems part 1: characterization," *IEEE Commun. Magazine*, July. 1997.

[14] H. Urkowitz, "Energy detection of unknown deterministic signals," *Proc. IEEE* vol. 55, No. 4, Apr. 1967.

[15] R. Ramanathan, C. Partridge, R. Krishnan, M. Condell, S. Polit, "Opportunistic spectrum access: challenges, architecture, protocols," *Proc. ACM WICON 2006*, Boston, 2006.

[16] F. K. Jondral, "Software defined radio-basics and evolution to cognitive radio," *EURASIP Journal On Wireless Communication And Networking*, 2005.

[17] R. Rubenstein, "Radios get smart," IEEE spectrum, Feb. 2007 .

[18] P. Marshal, "The next generation program," [online]. Avilable at Http: //www. darpa. mil/sto/smalluitops/xg. html.

[19] IEEE 802.22 working group on wireless regional area networks, [online]. Avilable at Http: //www. ieee802. org/22.

[20] R. Price and N. Abramason, "Detection theory," *IEEE Trans. Inform. Theory*, vol. 7, pp135-139, Jul. 1961.

[21] T. Kailath and V. Poor, "Detection of stochastic processes," *IEEE Trans. Inform. Theory*, vol. 44, pp2230-2259, Oct. 1998.

[22] J. Mitola, "Cognitive radio an integrated agent architecture for software defined radio," *Phd Thesis, KTH Royal Institute Of Technology*, Stockholm, Sweden, 2000.

[23] R. W. Broderson, A. Wolisz, D. Cabric, S. M. Mishra and D. Willkomm, "White paper: corvus: a cognitive radio approach for usage of virtual unlicensed spectrum," *Tech. Rep*, 2004.

[24] Q. Zhao and B. M. Sadler, "Survey of dynamic spectrum access," *IEEE Signal Processing Magazine*, May. 2007.

[25] J. Mitola, "The software radio," *IEEE National Telesystems Conference*, 1992.

[26] S. M. Kay, *Fundamentals Of Statistical Signal Processing: Detection Theory*, Prentice Hall PTR, 1998, vol. 2.

[27] A. Wald, *A Sequential Analysis*, John Wiley & Sons, New York, 1947.

[28] W. A. Gardner, "Signal interception: a unifying theoretical framework for feature detection," *IEEE Trans. Commun.*, vol. 36, No. 8, Aug. 1988.

[29] W. A. Gardner, "Signal interception: performance advantages of cyclic-feature detectors," *IEEE Trans. Commun.*, vol. 40, No. 1, Jan. 1992.

[30] N. Han, S. H. Shon, J. H. Chung and J. M. Kim, "Spectral correlation based signal detection method for spectrum sensing in ieee 802.22 wran systems," *Proc. ICACT*, 2006.

[31] R. Tandra, "Fundamental limits on detection in low SNR," *MS Thesis, University of California*, Berkeley, USA, 2005.

[32] C. Cordeiro, "A PHY/MAC proposal for IEEE 802.22 WRAN systems," *IEEE 802.22, doc.no 22-06-0005-05-0000*, Mar. 2006.

[33] M. Nekovee, "Dynamic spectrum access with cognitive radios: future architecture and research challenges," *BT Technology Journal*, vol. 24, Apr. 2006.

[34] R. Viswanthan and P. K. Varshney, "Distributed detection with multiple sensors: part 1-fundamentals," *Proc of IEEE*, vol. 85, No.1, Jan. 1997.

[35] P. K. Varshney, "Multisensor data fusion," *Electronics & Communication Engineering Journal*, Dec. 1997.

[36] J. Hancock and P. Wintz., *Signal Detection Theory*, Mcgraw-Hill Book, New York, 1966.

[37] D. Cabric, A. Tkachenko and R. W. Broderson, "Experimental study of spectrum sensing based on energy detection and network cooperation," *ACM 1st Int. Workshop on Technology and Policy for Accessing Spectrum*, Aug. 2006.

[38] H. Tang, "Some physical issues of wide band cognitive radio," *IEEE DySPAN*, Nov. 2005.

[39] M. Sahin and H. Arslan, "System design for cognitive radio communications," *Proc. CROWN*, 2006.

[40] C. Cordeiro, M. Ghosh, D. Cavalcanti and K. Challapali, "Spectrum sensing for dynamic spectrum access of TV bands," *Proc. CROWN*, 2007.

[41] W. Lehr And J. Crowcroft, "Managing shared access to a spectrum commons," *Proc. DySPAN*, Nov. 2005.

[42] K. Kim, I. A. Akbar, K. Bae, J. S. Um, C. M. Spooner and J. H. Reed, "Cyclostationary approaches to signal detection and classification in cognitive radio," *Proc. DySPAN*, 2007.

[43] B. Wild and K. Ramchandran, "Detecting primary receivers for cognitive radio applications," *Proc. DySPAN*, 2005.

[44] Z. Tian And G. B. Giannakis, "A wavelet approach to wideband spectrum sensing for cognitive radio," *Proc. Crown*, 2006.

[45] A. Pandharipande and J. P. M. G. Linnartz, "Performance analysis of primary user detection in a multiple antenna cognitve radio," *Proc. ICC*, 2007.

[46] N. M. Neihart, S. Roy and D. J. Allstot, "A parallel multi-resolution sensing technique for multiple antenna cognitive radios" *Proc. ISCAS*, 2007.

[47] I. F. Akyildiz, W. Y. Lee, M. C. Vuran and S. Mohanty, "Next generation/dynamic spectrum access/cognitive radio wireless network: a survey," *Science Direct*, May, 2006.

[48] A. Sahai, N. Hoven, S. M. Mishra, and R. Tandra, "Fundamental tradeoffs in robust spectrum sensing for opportunistic frequency reuse," *Technichal report, University of California*, Berkeley, CA, Mar. 2006.

[49] A. S. Margulies and J. Mitola, "Software defined radios: a technical challenge and a migration strategy," *IEEE 5Th International Symposium On Spread Spectrum Techniques and Applications Proceedings*, 1998.

[50] J. Mitola, *Software Radio Architecture: A Mathematical Perspective*, JSCA, IEEE Press, Newyork, April. 1999.

[51] J. Mitola, "The software radio architecture," *IEEE Commun. Mag.*, May. 1995.

[52] Y. Benkler, "Overcoming agoraphobia: building the commons of the digitally networked enviroment," *Harv.J.Law.Tech*, vol. 11, No. 2, 1998.

[53] C. Raman, R. Yates and N. Mandayam, "Scheduling variable rate links via a spectrum server" *Proc. DySPAN*, 2005.

[54] O. Ileri, D. Samardeija and N. Mandayam, "Demand responsive pricing and competitive spectrum allocation via a spectrum server" *Proc. DySPAN*, 2005.

[55] R. Etkin, A. Parekh and D. Tse,"Spectrum sharing for unlicensed bands" *Proc. DySPAN*, 2005.

[56] J. Huang, R. Berry and M. Honig, "Spectrum sharing with distributed interference compensation," *Proc. DySPAN*, 2005.

[57] T. Yucek and H. Arslan, "A survey of spectrum sensing algorithms for cognitive radio applications," *IEEE Communications Surveys & Tutorials*, 2009.

[58] H. V. Poor, *An Introduction To Signal Detection and Estimation*, Birkhuser, 1994.

[59] M. K. Simon and M. S. Alouini, *Digital Communication Over Fading Channels* New York: John Wiley and Sons, 2000.

[60] J. B. Anderson and R. Johannesson, *Understanding Information Transmission*, IEEE press, 2005.

[61] C. Rago, P. Willett and Y. B. Shalom, "Censoring sensors: a low communication rate scheme for distributed detection," *IEEE Trans on AES*, vol. 32, No. 2, Apr. 1996.

[62] W. Wang, W. Zou, Z. Zhou, H. Zhang and Y. Ye, "Decision fusion of cooperative spectrum sensing for cognitive radio under bandwidth constraints," *Proc. ICHIT*, Nov. 2008.

[63] Z. Quan, S. Cui and A. H. Sayed, "Optimal linear cooperation for spectrum sensing in cognitive radio networks," *IEEE J. Select Topics Signal Processing*, vol. 2, No. 1, Feb. 2008.

[64] Munehiro, Hiroyuki, Kazunori and Kazuhiro "A novel cooperative sensing technique for cognitive radio," *Proc. PIMRC*, Sept. 2007.

[65] X. Huang, N. Han, G. Zheng, S. Sohn and J. Kim, "Weighted collaborative spectrum sensing in cognitive radio," *Proc. CHINACOM*, Aug. 2007.

[66] J. Zhu, Z. Xu, F. Wang, B. Huang and B. Zhang, "Double threshold energy detection of cooperative spectrum sensing in cognitive radio," *Proc. CROWN*, May. 2008.

[67] C. Sun, W. Zhang and K. B. Letaief, "Cooperative spectrum sensing for cognitive radios under bandwidth constraints," *Proc. WCNC*, Mar. 2007.

[68] W. Wang, W. Zou, Z. Zhou and Y. Ye, "Detection fusion by hierarchy rule for cognitive radio," *Proc. CROWN*, May. 2008.

[69] C. Sun, W. Zhang and K. B. Letaief, "Cluster-based cooperative spectrum sensing in cognitive radio systems," *Proc. CROWN*, May. 2008.

[70] Z. Han and H. Jiang, "Replacement of spectrum sensing and avoidance of hidden terminal for cognitive radio," *Proc. WCNC*, Mar. 2008.

[71] H. Li, C. Li and H. Dai, "Quickest spectrum sensing in cognitive radio," *Proc. CISS*, Mar. 2008.

[72] A. Parsa, A. A. Gohari and A. Sahai, "Exploiting interference diversity for event-based spectrum sensing," *Proc. DySPAN*, Oct. 2008.

[73] Z. Ye, G. Memik and J. Grosspietsch, "Energy detection using estimated noise variance for spectrum sensing in cognitive radio networks," *Proc. WCNC*, Mar. 2008.

[74] J. Ma and Y. Li, "Soft combination and detection for cooperative spectrum sensing in cognitive radio networks," *Proc. GLOBECOM*, Nov. 2007.

[75] Z. Chair and P. K. Varshney, "Optimal data fusion in multiple sensor detection systems," *IEEE Trans.on AES*, vol. 23, pp98-101, Jan. 1986.

[76] L. Chen, J. Wang and S. Li, "Cooperative spectrum sensing with multi-bits local sensing decisions in cognitive radio context," *Proc. WCNC*, Mar. 2008.

[77] Q. Chen, P. Varshney, K. G. Mehrotra and C. K. Mohan "Bandwidth management in distributed sequential detection," *IEEE Trans. Inform. Theory*, vol. 51, No. 8, Aug. 2005.

[78] E. Visotsy, S. Kuffner and R. Peterson, "On collaborative detection of tv transmissions in support of dynamic spectrum sharing," *Proc. DySPAN*, Nov. 2005.

[79] J. H. Baek and S. H. Hwang, "Cooperative spectrum sensing with multiples of verification-aided energy detector in cognitive radio," *Proc. VTC*, 2008-Fall.

[80] R. Chen, J. Park and K. Bian, "Robust distributed spectrum sensing in cognitive radio networks," *Proc. INFOCOM*, Apr. 2008.

[81] N. Kundargi and A. Tewfik, "Hierarchical sequential detection in the context of dynamic spectrum access for cognitive radios," *Proc. ICECS*, Dec. 2007.

[82] Y. Shei and Y. T. Su, "A sequential test based cooperative spectrum sensing scheme for cognitive radios," *Proc. PIMRC*, Sept. 2008.

[83] J. Unnikrishnan and V. V. Veeravalli, "Cooperative sensing for primary detection in cognitive radio," *IEEE J. Select Topics Signal Processing*, vol. 2, No. 1, Feb. 2008.

[84] W. Zhang, R. K. Mallik and K. B. Letaief, "Cooperative spectrum sensing optimization in cognitive radio networks," *Proc. ICC*, May. 2008.

[85] Y. Chen, "Optimum number of secondary users in collaborative spectrum sensing considering resources usage efficiency," *IEEE Commun. Letters*, vol. 12, No. 12, Dec. 2008.

[86] N. Ansari, E. S. Hou, B. Zhu and J. G. Chen "Adaptive fusion by reinforcement learning for distributed detection systems," *IEEE Trans. AES*, vol. 32, No. 2, Apr. 1996.

[87] H. Uchiyama, K. Umebayashi, T. Fujii, F. Ono, K. Sakaguchi, Y. Kamiya and Y. Suzuki "Study on cooperative sensing in cognitive radio based ad-hoc network," *Proc. PIMRC*, Sept. 2007.

[88] R. Viswanathan and P. Varshney, "Distributed detection with multiple sensors: part 1-fundamentals," *Proceedings of IEEE* , Jan. 1997.

[89] R. S. Blum, S. A. Kassam and H. V. Poor, "Distributed detection with multiple sensors: part 2-advanced topics," *Proceedings of IEEE*, Jan. 1997.

[90] C. R. Stevenson, C. Cordeiro, E. Sofer and G. Chouinard,"Functional requirements for the 802.22 WRAN standard," *IEEE 802.22-05/0007r46*, Sept. 2006.

[91] Y. S. Yeh and S. C. Schwartz, "Outage probability in mobile telephony due to multiple log-normal interferers,"*IEEE Trans. Commun.*, vol. 32, No. 4, Apr. 1984.

[92] Y. C. Liang, Y. Zeng, E. C. Y. Peh and A. T. Hoang,"Sensing throughput tradeoff for cognitive radio networks," *IEEE Trans. Wireless Commun.*, vol. 7, No. 4, Apr. 2008.

[93] M. Abramowitz and I. A. Stegun, *Handbook Of Mathematical Functions*, NewYork: Dover Publications, Inc, 1970.

[94] T. Weiss and F. Jondral, "Spectrum pooling : an innovative strategy for the enhancement of spectrum efficiency," *IEEE Communication Magazine*, vol. 42,pp. S8-S14, Mar. 2004.

[95] W. H. Tranter, K. S. Shanmugan, T. S. Rappaport and K. L. Kosbar, *Principles Of Communication Systems Simulation With Wireless Application*, Prentice Hall PTR, 2004.